X-650-73-10

EARTH RESOURCES TECHNOLOGY SATELLITE-1

Symposium Proceedings

September 29, 1972

NASA TM X: 66193

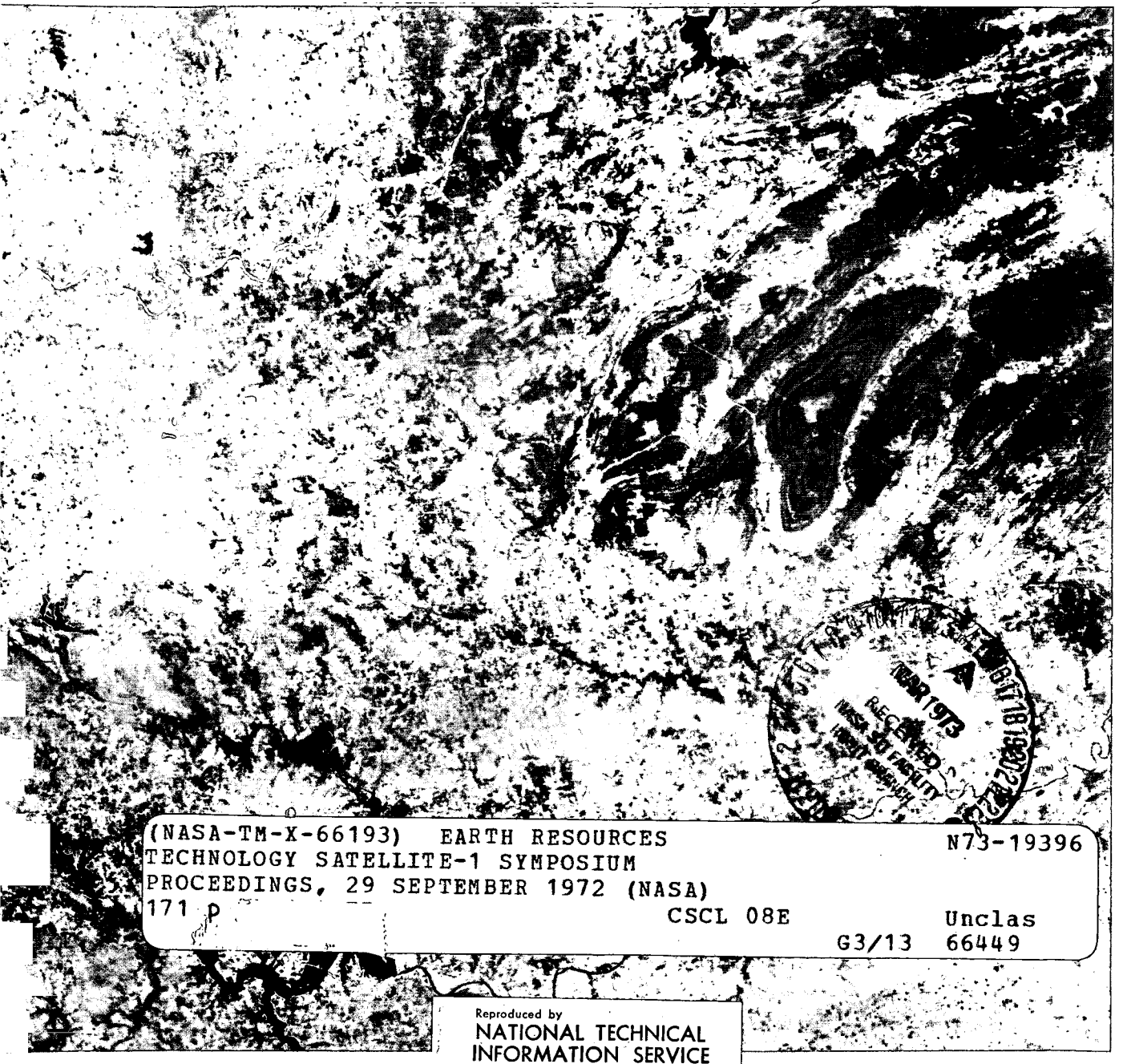

Goddard Space Flight Center, Greenbelt, Maryland
National Aeronautics and Space Administration

Cover Illustration. Color composite of one of the earliest images recorded by ERTS-1, showing Lake Texoma on the Oklahoma-Texas border and the Ouachita Mountains.

X-650-73-10

EARTH RESOURCES TECHNOLOGY SATELLITE-1 SYMPOSIUM PROCEEDINGS

September 29, 1972

Compiled by
William A. Finch, Jr.
Research Associate
Laboratory for Meteorology and Earth Sciences
Goddard Space Flight Center

January 1973

GODDARD SPACE FLIGHT CENTER
Greenbelt, Maryland

PREFACE

The papers included here represent an early "quick look" appraisal of the applications of ERTS-1 imagery. They were presented at a one-day symposium conducted at the Goddard Space Flight Center on September 29, 1972. In order to present a multiplicity of research areas, a series of twenty-minute presentations was followed by several five-minute presentations for a total of twenty-nine participants.

In critiquing the material presented here one must keep in mind that most of the investigators had less than one month, some less than two weeks, after receipt of ERTS-1 data, in which to make their evaluations and prepare material for this symposium.

To take advantage of the timeliness of the material it was necessary to employ procedures to expedite publication. Although all contributors to the symposium were afforded an opportunity to revise their material, the period for response was necessarily short in order to meet publication deadlines.

Considerable editorializing was necessary primarily for the purpose of achieving a somewhat uniform format, particularly in the case of figure references and captions. Care was exercised not to alter an author's context, but where this may have inadvertently occurred the editor assumes full responsibility.

Since there were some 350 graphics used by the participants in the symposium, most of which were in color, cost and time factors made selectivity mandatory. Again this became essentially an editorial function.

William A. Finch, Jr.
Research Associate
Laboratory for Meteorology and Earth Sciences
Goddard Space Flight Center

CONTENTS (Continued)

Page

Preliminary Assessment of the ERTS-1 Data Collection System
James F. Daniel 126

Detection of Ice Conditions in the Queen Elizabeth Islands
E. Paul McClain 127

Analysis of Arctic Ice Features
William I. Campbell 129

Detection of Snow Conditions in Mountainous Terrain
Donald R. Wiesnet 131

Detection of Circulation Features in the Great Lakes
A.E. Strong 133

Delineation of Permafrost Boundaries and Hydrologic Relationships
Duwayne M. Anderson 135

Chlorophyll Structure in the Ocean
Karl-Heinz Szekielda and Robert J. Curran 139

Barge Dumping of Wastes in the New York Bight
C.T. Wezernak and F.J. Thomson 142

Coastal Ocean Observations From ERTS
R. Charnell and G. Maul 146

Interpretation of Wetlands Ecology From ERTS-1
Richard R. Anderson, Virginia Carter, and Bill McGinness 147

Multispectral Scanner Imagery of the Sierra Nevada: Geologic Analysis
Paul D. Lowman, Jr. 148

Quick Look Analysis of Los Angeles Test Site Scene with General Electric Multispectral Information Extractor System (GEMS)
Richard Economy 151

Crop Classification Using ERTS-1 Digital Data
Charles Sheffield and Ralph Bernstein 153

Computer Processing of ERTS-1 MSS Data From the "San Francisco" Frame
F.J. Thomson, M. Gordon, J. Morgenstern, and F. Sadowski 155

CONTENTS

	Page
Preface	iii
Introduction: Performance of Sensors and Systems *Stanley P. Freden*	1
ERTS-1 Applications to California Resource Inventory *Robert N. Colwell*	7
An Early Analysis of ERTS-1 Data *D.A. Langrebe, R.M. Hoffer, and F.E. Goodrick*	21
First Results From the Canadian ERTS Program *L.W. Morley*	39
A First Look at Canadian ERTS Experiments in Forestry *L. Sayn-Wittgenstein*	48
Geologic Interpretation of ERTS Imagery of Western Wyoming – First Look *Robert S. Houston and Nicholas M. Short*	58
Geologic Questions and Significant Results Provided by Early ERTS Data *W.D. Carter*	77
Cartographic Applications of ERTS Imagery *Alden P. Colvocoresses*	88
A Preliminary Appraisal of ERTS-1 Imagery for the Comparative Study of Metropolitan Regions *James R. Wray*	95
Urban-Field Land Use of Southern New England: A First Look *Robert B. Simpson*	100
Use of ERTS-1 in Coastal Studies *Orville T. Magoon*	108
The Estuarine and Coastal Oceanography of Block Island Sound and Adjacent New York Coastal Waters *Edward Yost, Rajender Kalia, Sondra Wenderoth, Robert Anderson, Rudolph Hollman*	117

CONTENTS (Continued)

Page

The Advantages of Side-Lap Stereo Interpretation of ERTS-1 Imagery in Northern Latitudes
Charles E. Poulton 157

Glossary 162

INTRODUCTION: PERFORMANCE OF SENSORS AND SYSTEMS

Stanley C. Freden
Goddard Space Flight Center

The Symposium began with a session titled "Performance of Sensors and Systems." Three papers were given in this session: (1) "Performance of ERTS Spacecraft System," by Mr. Wilfred Scull; (2) "Performance of ERTS Ground Data Handling System," by Mr. Louis Gonzales; and (3) "Performance of ERTS Observing System," by Dr. Stanley C. Freden. This report is a compilation of those three presentations.

ERTS-1 was launched on 23 July, 1972 and placed into a nominal orbit by the Delta launch vehicle. The first orbital adjustment was done in two parts on July 28 and 29, to correct the orbit to the eighteen day repeat cycle.

Data have been acquired almost continuously since two days after the launch. The only interruption occurred between orbits 148 on 3 August and 181 on 5 August, when the sensor system was turned off because the malfunctioning of one of the two video tape recorders produced a serious power transient in the spacecraft. Consequently, this tape recorder was deactivated and the spacecraft returned to its normal status. Thus, one video tape recorder is now eliminated from the ERTS-1 system.

A second malfunction occurred during orbit 198 on 6 August in the power switching circuit which controls the operation of the return beam vidicon (RBV) cameras. This malfunction did not result in any interruption of image acquisition, which was continued with the multispectral scanner (MSS). The RBV cameras have been turned off since that malfunction. It has been determined that the malfunction was strictly associated with the switching circuit and there is no reason to believe that the cameras are not in good working order. The cameras have remained off, however, because only one sensor system can be used in conjunction with the one operating video tape recorder. Because of the importance of the 1-micrometer infrared band and because of the greater photometric accuracy of the MSS, we are, therefore, using the MSS for world-wide data recording. The RBV cameras could be operated simultaneously with the MSS in the direct transmission mode which is possible only

over North America. But, because in this region the RBV images are largely redundant with the MSS images, the cameras have so far remained off.

As of the end of the third eighteen-day cycle, the ground track had drifted about 10 kilometers from its initial starting point; we therefore made a second orbital adjustment on September 28. This correction was made so that the predicted motion of the descending nodes will come back and retrace their earlier drift motion. In this way, we do not anticipate another orbital correction until about the end of the 14th eighteen-day cycle; and the descending nodes will remain within about 13 kilometers of their initial starting points.

In terms of data acquisition, as of the 25th of September, we had acquired approximately 1400 return beam vidicon scenes and approximately 9,000 multispectral scanner scenes. In addition, quite a number of messages from the 33 active data collection platforms have also been received.

We acquire approximately 188 scenes per day, on the average. Images are acquired over the United States during every pass regardless of cloud cover. Outside the United States the 144 scenes available for acquisition per day are programmed on the basis of cloud cover and requirements for repetitive coverage. Sensor programming is functioning well, on that basis. Processing of these images lags about 2000 scenes behind acquisition. Thus, on the average, initial images are produced within approximately 2 weeks after acquisition. The procedures for cataloguing, assessment of the images, quality control, selection of the appropriate images for each investigator's test sites, duplication, and finally shipment to the investigators have, however, proven to be more formidable than anticipated. Thus, the time lapse between data acquisition and shipment to the investigator is considerably longer than the 14 days we had originally specified. Attempts are being made to shorten this time period.

We next looked at the quality of the data products, compared to pre-launch specifications. Three items were considered: resolution; geometric fidelity, or relative mapping accuracy; and radiometry. We want to emphasize that the findings presented here are preliminary. We are working to refine these results.

Considering first the resolution of the film product, not the CCT's (computer compatible tapes), we have taken some of the imagery and selected some typical characteristic targets and looked at the ground resolution versus the contrast for these targets. Figure I-1 shows a plot of this for RBV band 2 and MSS band 5, which have roughly the same spectral characteristics. The shaded areas between the solid lines are what was predicted, based on prelaunch testing, bar chart testing and prelaunch sensor evaluation. The "X"s represent targets which are resolvable; the "O"s represent targets which are not resolvable. Notice that objects larger than 100 meters, or so, are always seen.

In particular, we looked at three sets of piers in Boston Harbor. These piers have about equal width to spacing and a length to width ratio of about 3 to 5 and therefore simulate a bar chart. The spacings on these three sets of piers are 90, 80, and 50 meters. The 90 and 80 meter piers, which subjectively have medium contrast, were resolvable in the imagery,

whereas the 50 meter piers were not. Thus the resolution is somewhere between 50 and 90 meters at this contrast.

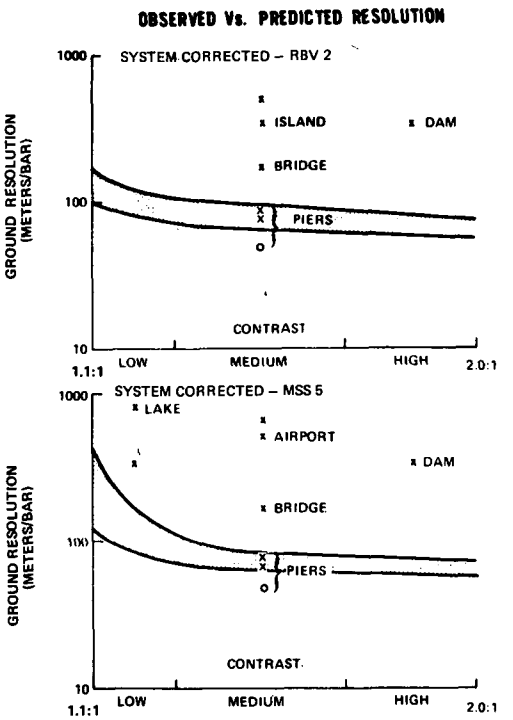

Figure I-1. Observed and predicted resolution of ERTS-1 RBV and MSS sensors.

We have not yet looked in detail at the resolution which can be derived from computer compatible tapes, but there is an indication it is somewhat better than is obtained from film.

We next considered what we might call "geometric fidelity" or "relative mapping accuracy." Thus, if we overlay an image on a map, scale, rotate and translate the images to "best fit" the map, and then determine the relative displacement of points on the image from points on the map, we have a measure of the relative mapping accuracy. A summary of the preliminary results, obtained from one of the earlier images, is shown below.

Film Product	Relative Mapping Accuracy[1]	
	MSS	RBV
70 mm[2]	≈ 400	≈ 150
9.5 inch[3]	≈ 150	50 - 100

[1]Meters, rms
[2]System corrected (bulk)
[3]Scene corrected (precision)

A few words should be said about absolute mapping accuracy. That is, the reported position of the center of the image as compared to the actual position. At the present time, this difference is about 3 km, but with improved data processing techniques which are being implemented, we expect to reduce this error to about 1.5 km.

With regard to registration, this should be as good as, or somewhat better than, the relative mapping accuracy. We have also visibly registered an MSS and RBV image and could not detect any registration error with the unaided eye.

Now, going to what is probably the most difficult thing to evaluate, at least at this point in time, the radiometry; how good is the overall system in terms of radiometric accuracy? We have done several things to try to answer this question. Again, we want to emphasize that the results are preliminary:

We have measured the reflectivity of various targets; that is, we have taken the sensor outputs, and, using an atmospheric model, related these to the reflectivity of the targets on the ground. These have been compared with known or measured reflectivities, and we find that they agree reasonably well.

We have also performed two other tests: (1) we have taken horizontal scans across a particular scene, for both the RBV and MSS, to look at the contrast in the images, and (2) we have taken vertical scans in the MSS image over very uniform parts of an image to look for what we call banding, caused by our inability to completely remove characteristic differences which may occur in the six channels which comprise each sensor band.

Figure I-2 shows the scene where this was done; it is the Pyramid Lake, Honey Lake, Eagle Lake area near the northern California-Nevada border. The horizontal scan lines are shown through Eagle Lake and a sandy area; densitometer traces along the scan lines are shown on the right. These are for MSS band 6 (0.7 – 0.8 μm) and RBV band 3 (0.70 – 0.83 μm). If you look at the digital levels that are marked "CCT" you see that in this scene we are operating between 2.4 and about 50, we are well within the dynamic range of the instruments, which goes up to a digital level of 63. However, if one takes the densitometry off the film, we find a digital level of 63, which indicates that the film is saturated.

Two other things should also be noted here; one is the much greater contrast of the MSS image as compared to the RBV image. This is seen visually as well as on the densitometer traces. The other is the shading of the RBV image at the top and bottom of the image.

We have also taken vertical scans through the Pyramid Lake and Honey Lake areas on the MSS image to look for banding. Figure I-3 shows the vertical densitometer scans for the three regions, the two lakes and the sand. We see the digital levels for the film, and the CCT's; the mean values are plotted at the bottom; the deviations from the mean or noise are plotted at the top. For the Pyramid Lake region we see the periodic noise which we call banding. It has a value of less than one digital bit. If we look at the brighter region, we do not see the banding; indicating that the predominant noise in the system is essentially random at the higher digital steps.

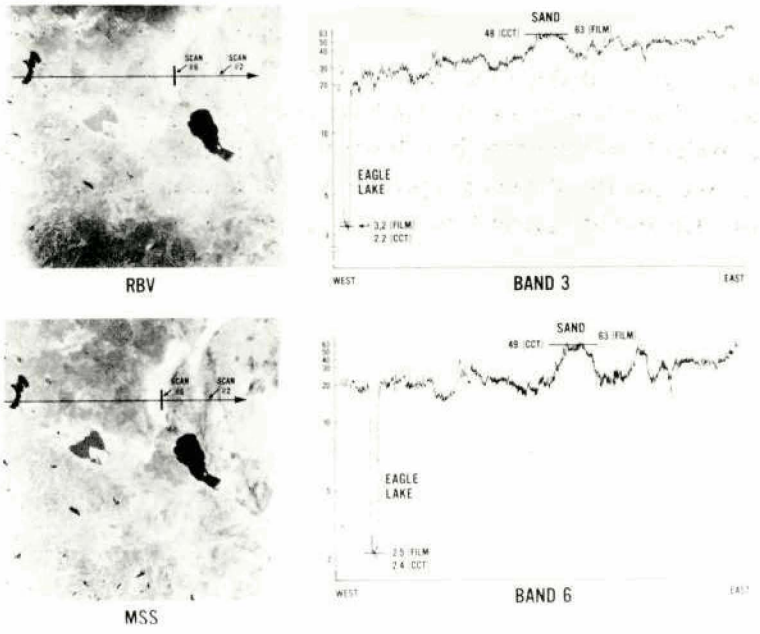

Figure I-2. Horizontal densitometer traces from an RBV and an MSS image of an area near Pyramid Lake, Nevada.

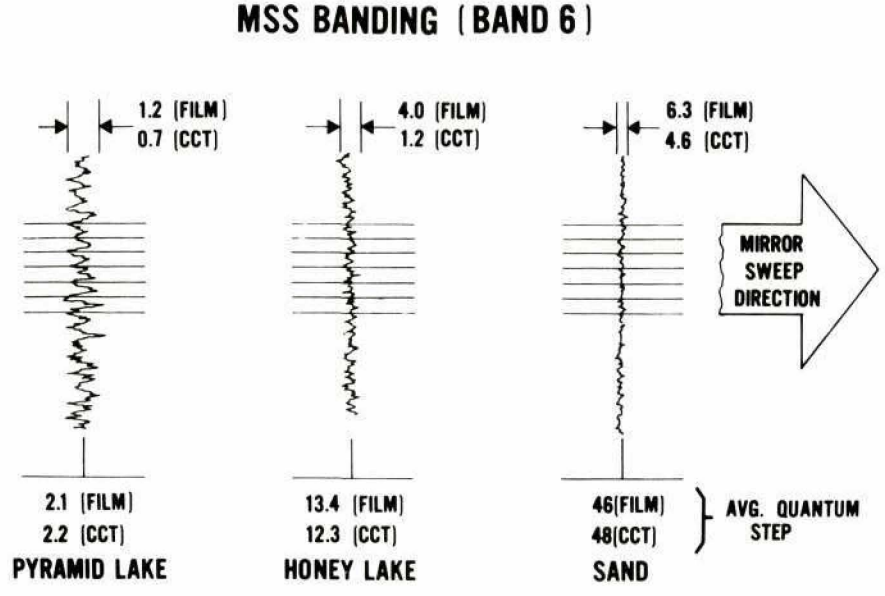

Figure I-3. Vertical densitometer scans from the MSS image shown in Figure I-2.

CONCLUSION

In conclusion, we can state at this time that the ERTS-1 spacecraft is operating satisfactorily, with the exception of one tape recorder. We have been somewhat slower than expected in getting the data products to the users, but this situation is improving. Finally, preliminary tests indicate that the quality of the data products with reference to resolution and geometric and radiometric quality are at least as good as we had expected.

ERTS-1 APPLICATIONS TO CALIFORNIA RESOURCE INVENTORY

Robert N. Colwell
Associate Director
Space Sciences Laboratory
University of California

INTRODUCTION

Several federal, state and private agencies currently are investigating the usefulness of ERTS-1 observations for the making of resource inventories in California. These include the U.S. Forest Service, the Bureau of Land Management, the University of California, several agencies within the Administrative Branch of the State of California (including the California Department of Agriculture and the California Resources Agency), and such private industrial groups as Earth Satellite Corporation, IBM, and Natural Resources Management Corporation. The report given here pertains to work that has been performed to date by personnel of the University of California. Our NASA-funded study involves scientists from five campuses of the University of California and seeks to make an integrated study of earth resources in the state of California using ERTS-1 and supporting aircraft data.

From the outset, those of us who have been involved in the University's integrated study have recognized the possibility that two kinds of benefits might be achieved through our study: (1) some of the ERTS-based resource inventories should prove to be of direct and immediate benefit operationally to the managers of California's earth resources, even though ERTS-1 was intended to serve only as an experimental system, and (2) resource inventory techniques developed and tested in California should prove to be applicable, with only minor modification, to many analogous areas in developing parts of the globe.

By July 25, 1972, less than 48 hours after ERTS-1 had been launched, it was obtaining operationally useful data of vast portions of the state of California. In fact, cloud-free coverage of nearly half of the state was obtained during the three passes made over California by ERTS-1 on July 25, 26 and 27.

Throughout the course of our study we intend to exert a maximum effort to ensure that the analyses which we make of ERTS imagery will be responsive to the expressed needs of the resource managers themselves. Collectively the various "user groups" with which we are working are representative of most of the resource managers of the state of California. Long before the launch of ERTS-1, and in anticipation of its potential usefulness as a resource inventory tool, we were working closely with these groups. This previously established relationship has greatly facilitated our working in a meaningful way with these same groups during the limited period of time that actual ERTS-1 imagery has been available to us. We are confident that our findings to date, as described and illustrated in the remainder of this progress report, are much more than mere pleasing discoveries as to the kinds of features that are discernible on ERTS-1 imagery. Instead they are truly responsive to the

needs of these various groups for timely, accurate information relative to the resources which they seek to manage.

SOME EXAMPLES OF ERTS-1 IMAGERY

One of the first multiband photographs taken by ERTS-1, and the first one that was reconstituted by NASA to form a composite color image, is the one of Central California shown in Figure II-1. The area shown covers more than 10,000 square miles and extends from

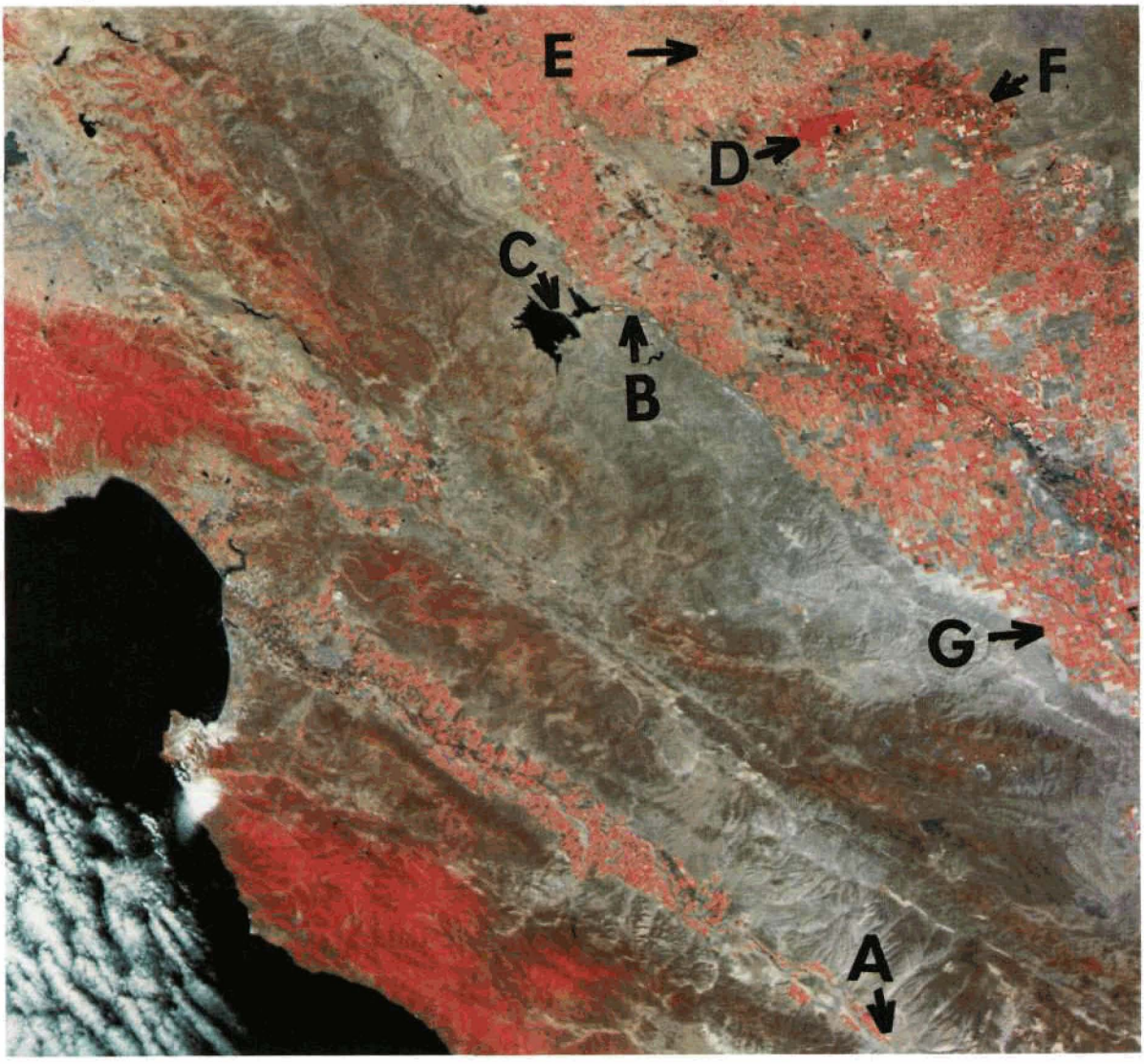

Figure II-1. Shown here is an infrared ektachrome simulation made from one "frame" of imagery that was obtained of an area in central California by the ERTS-1 satellite on July 25, 1972. Bands 4, 5 and 7 as recorded by the MSS were used in making this color composite. The area shown encompasses more than 10,000 square miles. For a discussion of the usefulness of such imagery in the making of earth resources surveys, see text.

Monterey Bay and the Pacific Ocean on the left, across several ranges of mountains, and also across the Great Central Valley of California to the foothills of the Sierra Nevada Mountains, which appear in the extreme upper right of the photo.

Figure II-1 was formed by combining images from bands 4, 5, and 7 of the ERTS-1 multispectral scanner (i.e., the bands which expose for green, red, and near-infrared energy, respectively) in such a way as to form a simulation of the color scheme that is provided by an infrared Ektachrome false color photo. Consequently, the intensity of red coloration in Figure II-1 is an indication of the degree of vigor of the green vegetation, area-by-area. Once this fact is realized, the value becomes apparent of using ERTS-type imagery to illustrate certain broad ecological relationships. For example, a study of the figure shows that the intensity of red is great throughout the mountain ranges nearest the coast, because the moist, cool sea breezes engulf these mountains much of the time and prevent the vegetation from becoming dry, even in mid-summer, as this July 25 photo clearly indicates. However, the mountain ranges that are progressively further inland exhibit progressively less red coloration because they have been influenced less by the coastal environment and more by the hot summer conditions characteristic of inland areas.

As a corollary to the foregoing, the Salinas Valley (the bright red strip of cultivated fields paralleling the coast and just a few miles inland) is used almost all year around to grow such cool weather vegetable crops as lettuce and cabbage. These crops would "bolt" (i.e., produce undesired seed stalks instead of edible heads of leaves) if grown during the summer in the hot Great Central Valley, which is the area of bright red cropland that occupies most of the upper right quarter of the figure.

During the daytime a strong updraft of warm air is created over the Great Central Valley. Since "nature abhors a vacuum," there is a strong tendency for cool air from the ocean to be drawn inland to replace this rising warm air. However, it is clearly seen in the figure that this air will be partly blocked by the mountain ranges. Hence it tends to enter at Monterey Bay and sweep down the Salinas Valley before finding its way inland. Once the interpreter of space photography is able to infer this fact, he can correctly conclude that the Salinas Valley is largely unsuitable to the growing of orchard crops which are not sufficiently wind firm. He also could correctly infer that the winds will be especially strong most of the time in the King City area (labeled A on Figure II-1) because they are funneled in from both sides as the valley becomes narrower. Consequently the soils near King City are correctly inferred as being rich in wind-derived sand. Also the air temperatures are likely to be somewhat warmer at King City than at the upper end of the Salinas Valley (near Monterey Bay) but still somewhat cooler than in the Great Central Valley, especially during the summer growing season.

This combination of soil and climate is ideal for the production of certain varieties of cool-weather grapes. Consistent with this fact, approximately 12,000 acres of vineyards are at this time in the process of being planted near area A of Figure II-1.

Crops that prefer a more "continental" type of climate do especially well in the broad flat Great Central Valley, except in areas where the soil suffers from high salinity, boron

toxicity, or poor drainage. Such unsuitable areas for crop growth are clearly seen in the upper right quarter of the figure, surrounded on all sides by highly productive cropland which is irrigated with the aid of water from the Sierras, far to the north and east. This water is made available for use here by a system of canals (such as the Delta-Mendota Canal at B) and storage reservoirs (such as the large San Luis Reservoir at C). Some areas which are occupied by fertile but relatively impervious clay soils can be located on ERTS-type photography by the uniquely dark red color signature of the rice crops associated with them (as at D), since rice is ideally suited to such soils. Other areas, such as at E, which are occupied by fertile but much sandier soils, also can be located on ERTS-1 photography by virtue of the finely mottled red-gray coloration produced by hot-weather vineyards (such as Thompson seedless grapes) associated with them.

The presence of deep fertile soils and the absence of strong winds can be inferred in area F once the interpreter, with only limited field checking, learns to recognize that a reddish-brown coloration, of the type shown here, almost invariably indicates orchard crops. The fact that these orchard areas are separated by many miles from the rice-growing areas at D highlights another conclusion of significance from the agricultural standpoint: Various herbicides can be applied to the rice fields at D (in order to kill a weed known as water grass and thus increase rice yields by approximately 25 percent) with little likelihood that these herbicides will drift to and damage the orchards, which are highly susceptible to injury by the same herbicides. In an area elsewhere in California's Great Central valley, but not shown in Figure II-1, damage in the amount of approximately $12 million allegedly was done by such herbicides to orchards which, as discernible on the ERTS-1 photography, were in much closer proximity to rice fields.

Finally, with respect to the area labelled G on the figure, the interpreter of space photography can correctly infer that soil, climatic, and irrigation factors are favorable in this area for the production of still other crops exhibiting much different color signatures than any of those previously mentioned. By way of documenting this fact, an enlargement of that portion of Figure II-1 in the immediate vicinity of point G is shown in Figure II-2. Prompt field checking here by the writer, of a contiguous area of more than 50 square miles, showed a very strong correlation between crop type and its color as imaged on both figures. Specifically the photo-interpreter could identify crop types with an accuracy exceeding 90 percent merely by using the following five-color code: (1) all *brown* fields contain mature safflower; (2) all *light yellow* fields contain mature barley; (3) all *black* fields contain the recently-burned stubble of barley or other "small grains;" (4) all *blue-gray* fields are fallow, and (5) all other fields are *red* or *pink* and are occupied by healthy green crops, mostly alfalfa and sugar beets.

At the time of this writing we are in the process of documenting on ERTS-1 photography of this same area taken 36 days later, and similarly color-combined that: (1) nearly all brown fields contain mature "seed alfalfa;" (2) all black fields contain recently burned stubble, and correspond almost exactly to the fields which appeared yellow in Figure II-2; and

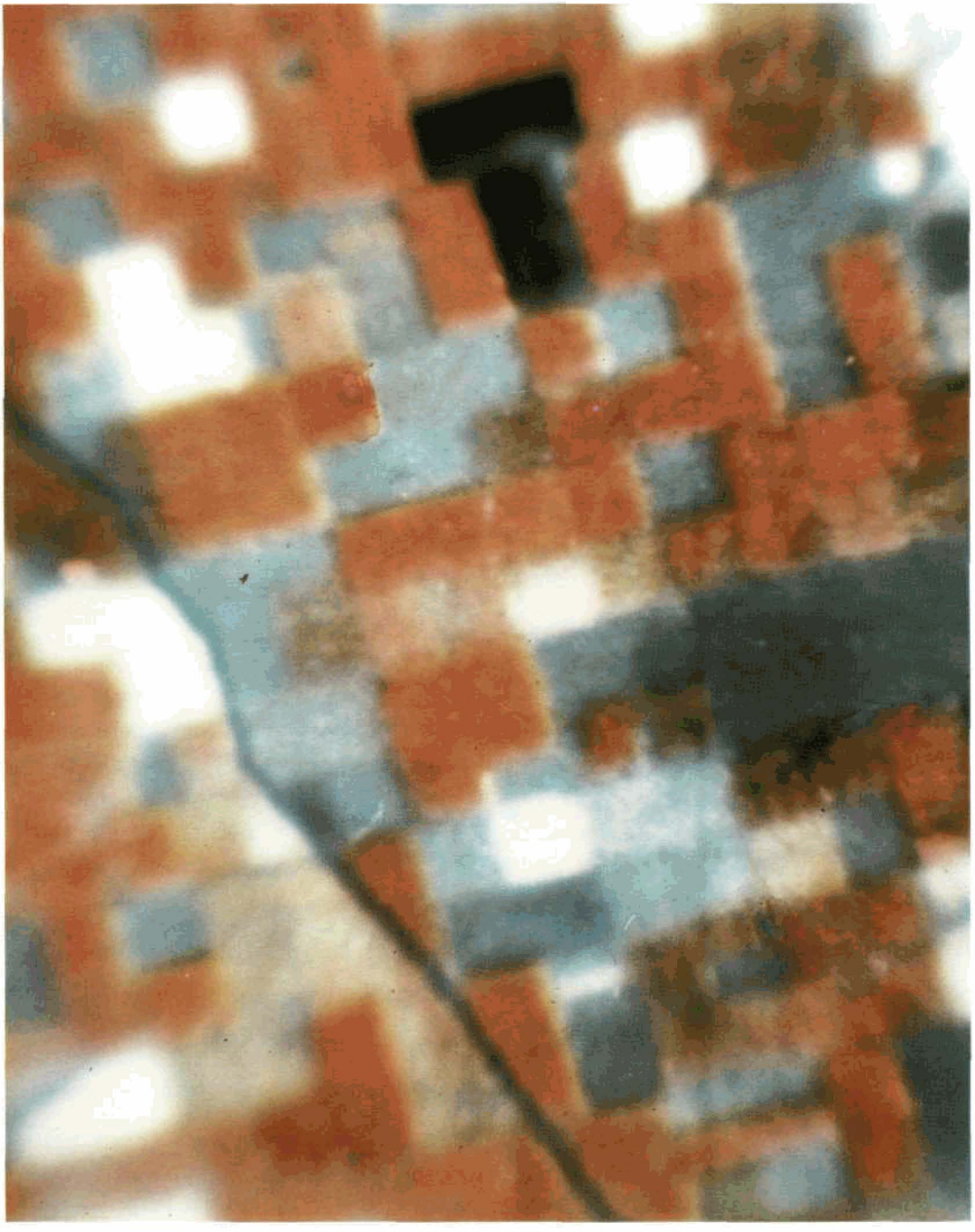

Figure II-2. This is a greatly enlarged view of that portion of the ERTS-1 frame of Figure 1 that is in the immediate vicinity of the area labelled "G." A very close correlation was found to exist here between crop type and image color of the corresponding agricultural field, thereby facilitating the use of automatic data processing techniques of the type shown for a portion of this area in Figure II-7.

(3) many fields which formerly were blue-gray have changed to red, indicative of a late-growing crop – mainly cotton.

In summary of what we have said thus far:

1. The tremendous synoptic view afforded by a single "frame" of MSS imagery, as obtained from ERTS-1, portrays certain ecological relationships very clearly – perhaps more clearly than they could be portrayed by any other means presently available. As suggested earlier, our ability to discern and understand such ecological relationships as imaged on Figure II-1 may be of value not only to resource managers in California, but also to those in many other analogous but lesser developed parts of the world. It is quite probable that similar ecological signatures can be discerned on similar ERTS imagery of these lesser developed areas. If so then perhaps much can be inferred from the area-by-area resource development that already has occurred in California, as to the optimum development of resources that should be undertaken in analogous parts of these lesser developed areas.

2. Within agricultural areas, many individual crop types and associated soil conditions can be identified through interpretation of a color-composite ERTS image of the type shown in Figure II-1.

3. The capability of ERTS to provide sequential coverage of any given area every 18 days (weather permitting) already is showing great promise as a further aid to crop identification. However, in this application as in the previously-mentioned ones, vigorous and timely field checking of representative calibration areas must be resorted to. In this instance, the field checking is required not only to identify the crops that are growing at any given time, field-by-field throughout the calibration area, but also to develop by this means an accurate crop calendar that can be applied intelligently throughout a vast extended area.

At this point we should find it instructive to examine at least one other frame of ERTS-1 imagery, the better to determine whether the success achieved in interpreting Figure II-1 was merely a random success. In so doing, we may be able not only to verify or refute certain generalizations that we tentatively drew from our interpretation of the figure, but we may also discover additional noteworthy uses and limitations of such imagery from the standpoint of the ecologist and resource manager.

The area shown in Figure II-3, like that shown in Figure II-1, is a simulated infrared Ektachrome color composite made from MSS bands 4, 5 and 7 of ERTS-1. Figure II-3 was taken approximately 24 hours after Figure II-1 and covers an area that is mostly north and west of it. (The lower right corner of Figure II-3 will be seen to overlap only slightly the upper left corner of Figure II-1.)

From a study of the broad area labeled I in Figure II-3, the experienced photo-interpreter could readily conclude that the topography is too rugged and the soils too shallow through out most of this area to permit the production of agricultural crops. On this enhanced

Figure II-3. This frame of ERTS-1 imagery also was made from MSS bands 4, 5, and 7 and was obtained on July 26, 1972 of an area in north-central California. As described in the accompanying text, many of the relationships between terrain condition and image appearance that were found to exist for the area shown in Figure II-1 were also found to exist in this area.

false-color imagery, the reddish coloration of certain features is indicative of the presence of trees and shrubs which have remained green even during the dry summer period when this space photo was taken. Such coloration contrasts sharply with the lighter toned areas, also seen in area I, most of which are covered with various annual grasses which have turned brown by this season of the year.

The healthier and more succulent the vegetation, the brighter red it appears to be on a false-color presentation of the type shown in Figure II-3. As we realize this fact we see, in Figure II-3 as in Figure II-1, an excellent example of the usefulness of a broad synoptic view such as ERTS provides in highlighting certain significant ecological relationships. Specifically, within area I we see a succession of four or five ranges of mountains which generally parallel the fog-enshrouded Pacific coast (lower left corner of the photo). With each range further inland the coastal influences which would tend to keep the vegetation from drying up during the hot California summer become progressively less pronounced and hence the mountain ranges appear progressively less red, as seen on the space photo. Throughout area I there are numerous dark blue features, most of which are either natural lakes and man-made reservoirs (such as those labeled L) or areas in which the wildland vegetation recently has been burned and the dark-toned ash is exposed (such as the area labeled F).

Progressing now to area II, as annotated on Figure II-3, we see the characteristic mid-summer signature of dry-land agriculture as practiced on this typical rolling foothill topography and on the upper slopes of the valley floor. Most of the individual fields are seen to be relatively large as compared with those in the central part of the valley (area III). Furthermore most of the fields in area II exhibit on this July 26 imagery the characteristic light tone distinctive to mature crops, but interspersed with fields that are dark in tone due to the recent burning of stubble from the annual cereal crops (wheat, oats, and barley) that comprise the dominant dry-land agricultural production of such areas.

Area III shows a portion of the Great Central Valley of California which has been termed "the largest and most fertile flat land area in the world." Near the center of the photo the southern limits of the Sacramento Valley and the northern limits of the San Joaquin Valley are defined by the confluence of the south-flowing Sacramento River with the north-flowing San Joaquin River, forming the so-called "delta" region. Much of this delta region was flooded in the spring of 1972 when one of the levees of the Sacramento River gave way. The portion that still remained flooded as of July 26 is clearly delimited as area X on this space photo. On sequential space photography of this type, obtained from ERTS-1 imagery of this area every 18 days, a determination is now being made of the rate at which the flood waters are receding (partly as a result of repairing levees and pumping flood waters back into normal channels). Ground observations combined with an interpretation of these photos is providing a valuable measure of the effects of various periods of inundation (2 weeks, 4 weeks, 6 weeks, etc.) on reductions in crop yield and on the mortality of orchard trees resulting from various known lengths of time that the crops have been inundated.

Within area III, several soil types and associate crop types can be accurately delineated by virtue of this synoptic view, only a few of which have been annotated on Figure II-1. For example, area IIIA (like area D of Figure II-1) consists mainly of heavy clay soils devoted primarily to the production of rice. Since this irrigated rice was by far the most succulent crop on July 26, it is readily definable field-by-field by its very red color on the ERTS-1 image of Figure II-3. In marked contrast, area IIIB (like E of Figure II-1) is a sandy-soiled area in which virtually all the crops grown are vineyards; area IIIC (like F of Figure II-1) contains deep well-drained soils in which fruit and nut orchards predominate; area IIID contains peaty-muck soils in which sugar beets and asparagus predominate, and area IIIE contains soils of intermediate fertility, depth, and irrigability within which safflower, corn, and small grains are among the predominant crops grown.

Large urban areas assume a characteristic blue-gray appearance on space photographs that have been color-enhanced as in Figure II-3. An example within this area is Stockton (labeled IIIF).

In the March, 1964 issue of *American Scientist,* this writer presented a simulated space photo of part of the area shown in Figure II-3 and gave an analysis indicating where the optimum site would be for the construction of a large dam and reservoir that would facilitate agricultural production and other aspects of regional development. Now that the dam has been built and the reservoir constructed (labeled L on Figure II-3), the reader may find it instructive to compare Figure II-3 of the present article with Figure 14 of the article just referenced, and with the analysis that was made of that figure.

Area IV, as outlined on Figure II-3, includes two smaller reservoirs, the necessity of which can best be appreciated on a broad synoptic view of the type provided by this single ERTS-1 frame of imagery. These two reservoirs, and several nearby ones that are similar to them, are primarily used to provide temporary storage of water that is transported to them by pipelines from the main fresh-water source, viz., the Sierra Nevada Mountains (upper right corner of Figure II-3), for use in the very large centers of population that fringe San Francisco Bay. Without such a temporary storage capability, the pipelines used to transport this water would have to be of far greater size and number to obviate water shortages in the Bay Area cities during periods of peak use, such as the 3- to 5-day hot spells that occasionally are experienced there during summertime periods.

For several reasons area IV is one for which far more detailed resource information is needed than the broad reconnaissance type which we have been describing thus far as we referred to Figure II-3. But perhaps if we were to greatly enlarge only that portion of the ERTS-1 space photo that is outlined in area IV of Figure II-3, the additional detail could be seen.

The result of making such an enlargement is shown in Figure II-4. A scientist from the Forestry Remote Sensing Laboratory of the University of California is shown viewing an enlarged portion of the ERTS-1 image covering essentially the same test site that is portrayed in area IV of Figure II-3. She is in the process of attempting to determine by image analysis the vegetation and terrain category at each of 100 marked and numbered points. She will

Figure II-4. In this scene an image analyst is shown in the process of determining the interpretability of earth resource features on that portion of the ERTS-1 image that is centered on San Pablo Reservoir. For each of 100 spots that are marked on this imagery, a separate crew of investigators has determined the type of vegetation present. This has been done by direct on-the-ground observation. A comparison of this "ground truth" with the image analyst's interpretation point-by-point provides a measure of the accuracy with which each type of vegetation can be identified on this kind of imagery, as summarized in Figure II-5.

later attempt to classify the same numbered points using not space photography, but higher resolution *aerial* photography of this same area. Under NASA sponsorship, a large amount of testing similar to this is done at the Forestry Remote Sensing Laboratory using many image analysts whose backgrounds, degrees of motivation and degrees of visual and mental acuity are known to encompass the full range likely to be exhibited by the population from which remote sensing image analysts of the future are likely to be drawn. Furthermore these individuals are tested not only at the beginning of the day when their visual and mental acuity may be highest, but also at various times throughout the day, and under a variety of working conditions and corresponding degrees of fatigue. The kinds of viewing and interpreting equipment also are varied in some tests, to determine the effects of these factors.

By proper experimental design, highly quantitative and statistically significant results of the type shown in Figure II-5 can thus be obtained relative to the accuracy of image analysis that is achievable as a function of:

- Image quality, in terms of film, filter, scale, dynamic range, time of day, and season of the year
- Image analyst characteristics, as described above
- Equipment and techniques used by the image analyst.

PHOTO-INTERPRETER'S RESULTS	GROUND DATA							TOT. SEEN BY P.I.	COMMISSION ERROR	PERCENT CORRECT
	MP	E	MH	C	G	W	N			
MP	21	6	15	10	2		1	55	34	61.8
E	2	3	5	6				16	13	81.3
MH	2		43	7	3			55	12	21.8
C			13	14	18		6	51	37	72.5
G		3	8	10	49	3	12	85	36	42.4
W	1					27	1	29	2	6.9
N	1			1	3		4	9	5	55.6
TOTAL PLOTS	27	12	84	48	75	30	24			
OMISSIONS	6	9	41	34	26	3	20			
PERCENT CORRECT	77.8	25.0	51.2	29.2	65.3	90.0	16.7			

Figure II-5. Cumulative interpretation results for three interpreters are shown here, based on their attempts to identify four vegetation/terrain categories from ERTS-1 imagery, using the techniques and equipment shown in Figure II-4. The numbers in the body of the box array of results indicate the total number of points identified by all interpreters. The numbers in the bold-faced diagonal row indicate the number of points identified correctly. The number and types of "omission errors" appear in each vertical row, and of "commission errors" in each horizontal row. Symbols appearing in this figure have the following significance: G = grassland, W = water, and N = non-vegetated. A comparison of interpretation time and costs to make similar interpretations, not of this area but of another of our northern California test areas will be found in Figure II-6.

TASK	HIGH ALTITUDE CIR TRANSPARENCY (9 x 9 in.)	ERTS-1 COLOR ENHANCED FALSE - COLOR ENLARGED PRINT (16 x 16 in.)
DELINEATION OF WATERSHED BOUNDARY (2.5 MILLION ACRES)	3.0 HOURS	0.5 HOURS
PLOTTING EFFECTIVE AREAS	5.0 HOURS	0.0 HOURS
DELINEATION OF HOMOGENEOUS AREAS	48.0 HOURS	3.0 HOURS
PHOTO INTERPRETATION TRAINING & TESTING	6.0 HOURS	2.0 HOURS
RESOURCE TYPE CLASSIFICATION	210.0 HOURS	30.0 HOURS
TOTAL INTERPRETATION TIME REQUIRED	272.0 HOURS	35.5 HOURS
HOURLY WAGE	$7.00/HOUR	$7.00/HOUR
TOTAL INTERPRETATION COSTS (TIME)	$1,904.00	$248.50
TOTAL COST/ACRE	0.07	0.0098
COST RATIO	7	1

Figure II-6. Projected interpretation time and costs of regional Feather River Watershed image analysis on ERTS-1 imagery, compared with infrared ektachrome aerial photography of the same area as obtained from an altitude of 70,000 feet.

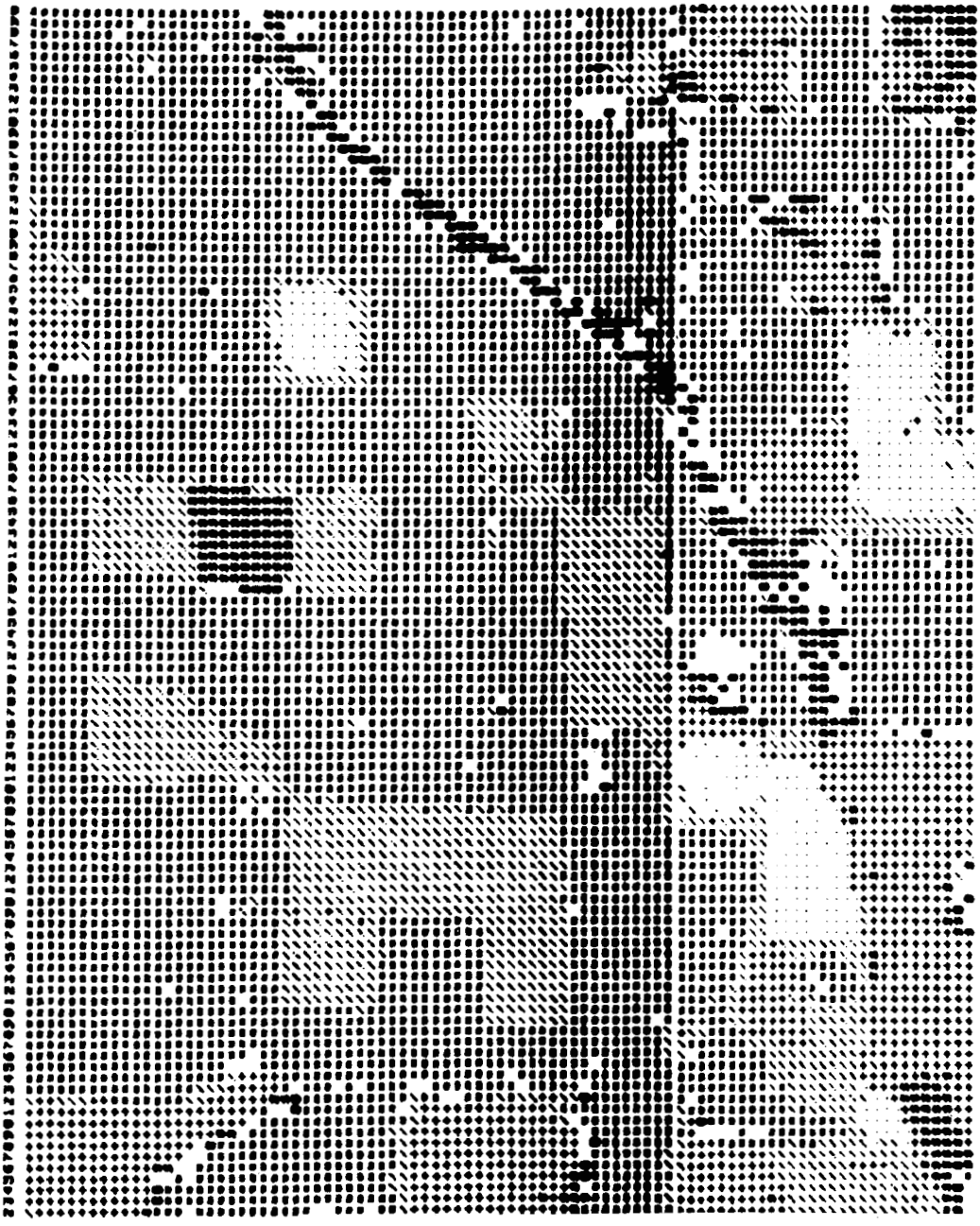

Figure II-7. Shown here is the "computer printout" of part of the area shown in Figure II-2 which was made by scanning the corresponding black-and-white images and programming the computer to print out a unique symbol for each of the five categories, plus water (total of six). Preliminary evaluation of this printout indicates that correct classification exceeds 95 percent in all six categories. Once the MSS magnetic tape records become available to our group, this type of printout can be produced directly from the tape records, thereby obviating the necessity of scanning photos that have been made from the tape records.

A PRELIMINARY APPRAISAL OF TIME AND COST FACTORS

As of now our group has had only one opportunity to make an appraisal of time and cost factors associated with the interpretation of ERTS-1 imagery. The area which we have studied for this purpose is the Feather River Watershed in the northern Sierra Nevada Mountains of California, within which our NASA Bucks Lake Forestry Test Site is located. The projected interpretation time and cost required for producing vegetation/terrain resource maps from both high altitude and ERTS-1 imagery of this are presented in Figure II-6. Approximately sixty high altitude images are needed to compile the complete regional map compared with one ERTS-1 image. The total time and costs required for imagery interpretation, including resource type classification, has been estimated to be seven times greater on high altitude than on ERTS-1 imagery. The amount of resource information loss (when ERTS-1 imagery is compared to high flight imagery) is also an important consideration and is now in the process of being determined by our group for this same area.

A PRELIMINARY APPRAISAL OF POSSIBILITIES FOR AUTOMATIC DATA PROCESSING

As previously indicated, we have attempted to classify agricultural crop types by means of computer techniques for that portion of Figure II-1 that is located in the immediate vicinity of area G. Our results in this regard are very promising, as evidenced by an examination of the computer printout for that area seen in Figure II-7. Some of our earlier studies, based on simulated ERTS-1 imagery as obtained with high altitude aircraft, indicate that even higher accuracies can be obtained if multidate imagery as well as multiband imagery is used. As the number of frames of imagery (or corresponding tape records) required for analysis increases, there is a corresponding increase in the attractiveness of automatic data processing techniques as compared with human image analysis techniques.

SUMMARY AND CONCLUSION

At various times during the past several years my associates and I, at the University of California, have proclaimed that the launching of ERTS-1 would usher in the most important photographic experiment in history. With the successful launch of ERTS-1 last July, and the satisfactory operation of its sensor systems since then, we are fast approaching the time when the validity of that assertion can be assessed. However, in attempting to judge the importance of this capability, we must continue to realize that ERTS-1 imagery is of value primarily as an aid to making accurate, timely inventories of earth resources. Only if man exploits this *inventory* information as an aid to more intelligent *management* of earth resources (many of which are rapidly dwindling in quantity or rapidly deteriorating in quality) will the true potential importance of ERTS-1 be realized.

AN EARLY ANALYSIS OF ERTS-1 DATA*

D.A. Landgrebe, R.M. Hoffer, F.E. Goodrick and Staff
Laboratory for Applications of Remote Sensing
Purdue University

INTRODUCTION

ERTS-A was successfully launched to become ERTS-1 on July 23, 1972. The sensors on board were utilized to collect image data over the U.S. for the first time two days later on Tuesday, July 25. An early analysis of a data set was conducted at Purdue/LARS in order to arrive at preliminary indications as quickly as possible about the operating characteristics and potential value of this satellite as a data gathering device.

To this end a black and white image of channel 5 data together with tapes from the multispectral scanner was made available to Purdue on July 26. Based upon a preliminary inspection of this data in image form, plans were made for four sub-projects. These involved the analysis by multispectral pattern recognition techniques of the full frame and two particular subframes and a study of the data quality as discussed below.

The frame made available for analysis (Frame E1002-16312) was taken from the first pass of the satellite across the U.S. and was of the Red River Valley area of Texas and Oklahoma. The frame is centered on a point fifteen miles southeast of Durant, Oklahoma and approximately five miles north of the Red River.

A first look at this data in image form suggested that the area might be rather barren; however, the analysis later showed this to be entirely incorrect. This frame contained important and interesting examples of geology, agriculture, range land, and water resources features.

THE STUDY PLAN

As previously indicated, the data were analyzed in four sub-projects:

1. Sub-project 1 was to be a classification and a general analysis of the full frame in order to make apparent any diversity (see above).
2. A predominant and important feature in the frame is Lake Texoma and associated portions of the Red River. Accordingly, it was decided to choose for study as sub-project 2 a subframe encompassing this area.
3. The northeast corner of the frame contained a portion of the Ouachita Mountains, some of the oldest geologic features of the U.S. Accordingly, a sub-frame in this region was selected by geologists and foresters for analysis.

*Work described in the report was carried out under NASA Grant NGL 15-005-112, and NASA contracts CR 128122 and CR 127475.

4. Finally, it was decided that it would be helpful both to the analysts at LARS and to the ERTS ground station operators to derive as much information as possible regarding various aspects of the quality of this early data. The data processing staff was to work on this task.

The results of this latter sub-project were transmitted back directly to the ERTS ground station operators. These results will not be discussed further in this report beyond the general statement that the data quality, aside from some minor and no doubt correctable flaws, appeared to be very good.

Two passes were made through the analysis of these data. The first was carried out on July 27 and 28. This preliminary analysis was completed without the use of ground observations or even without much general knowledge of the area. On July 30 and 31 two staff members from the Laboratory traveled to the site for ground and low-altitude aircraft observation of portions of the area covered by the frame. Based on their observations and observations and opinions expressed by local officials who accompanied them in the area, a second series of classifications was done on the full frame and the two subframes. Both the preliminary and the second pass results will be discussed presently.

The results of this report are contained primarily in eight images included below (Figures III-1 through III-6, III-9, and III-10). Understanding and interpretation of the results will be aided by a small amount of background on how they are generated. These images are generated on a digital image display system consisting of a television-like screen upon which either data or classification results can be displayed. Facing this screen is a camera capable of exposing either polaroid or normal 35mm film. Provisions are made to interpose color filters between the black and white screen and the photographic camera. In this way color presentations of data and results can be obtained by multiple exposure.

The display system displays approximately 600 lines down the screen face with approximately 800 addressable locations in each line. In addition, the software driving the display system is written to accept commands for displaying only every mth sample of every nth scan line of the data set for arbitrary m and n. Thus, a full ERTS frame can be displayed at lesser resolution or a smaller portion of the subframe can be displayed at full resolution. In addition, an image can be displayed such that a single resolution element in the data can be shown as a contiguous group of four (or up to 16) points when it is desirable to look in detail at a small area of a frame or small features.

In order to carry out the sub-projects described above, it was first helpful to derive presentations of the data in simulated color infrared photography form. The results are shown in Figures III-1, III-2, and III-3.* The remainder of the images are referred to as color-coded

*In the interest of economy and because color is not essential to this report, these three figures are reproduced in black and white.

Figure III-1. Black and white photo of simulated color infrared imagery of the Texoma Full Frame data. Approximately 85% of the area shown in this image.

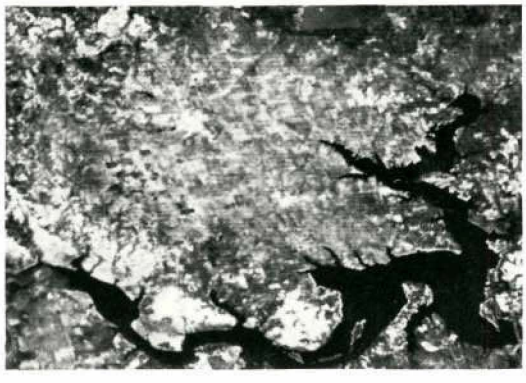

Figure III-2. Black and white photo of simulated color infrared imagery of a portion of the Lake Texoma Subframe.

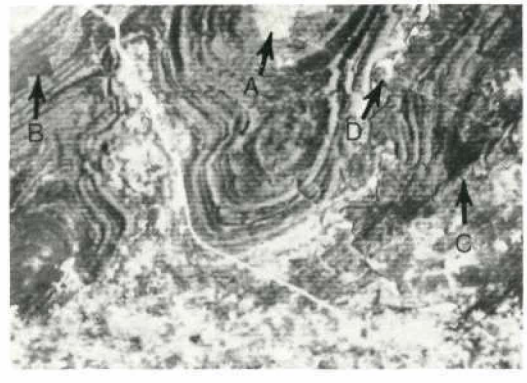

Figure III-3. Black and white photo of simulated color infrared imagery of the Ouachita Mountain Subframe.

classification results (CCR). They are derived by classifying the data into categories, then choosing colors to associate with these categories. As such CCR's cannot accurately be called enhanced images; more properly, they are a means for displaying a large volume of quantitative results in (qualitative) image form. Typically, the number of categories is twenty or less but since the human eye cannot readily differentiate between that many colors, several of the categories are usually grouped together and presented as a single color. Next is a description of the analysis procedure, followed by a description of the two-day observation mission and a description of the results.

ANALYSIS PROCEDURES

When the first analysis of this data was attempted no ground information was available except that which could be deduced from comparing the data imagery to existing maps. By this process water bodies, rivers, major highways, large geologic features, and some forested areas, particularly those which occurred in drainages, could be determined. Agricultural areas and range lands could be identified from their rectangular shape in the data, but it was not possible at this point to estimate what the ground cover was. The first set of training classes was produced with the non-supervised (or clustering) classification processor by using a large sampling interval and allowing the program to automatically pick classes. At this point the program was instructed to find 15 spectrally different classes. Because of the large sampling interval several of these classes typically contained very few points and were either deleted from the analysis or combined with what appeared to be similar classes.

The estimated identification of ground cover classes represented by the non-supervised classification classes was made using information provided by the program about each class. A table of numbers representing the separability of each class is given as part of the output of this program.

Examination of these values allows the analyst to group those classes which appear similar. Another piece of information provided is the mean response of each non-supervised class within each spectral band. The ratios of the visible channels to the infrared channels provides some information as to the nature of the actual cover type. Ratio values less than one tend to indicate soils and dry vegetation while values in the vicinity of one usually represent green vegetation cover. Values much greater than one will almost invariably represent water. Tentative evaluation of cover classes can then be made from examination and comparison of the groupings and ratios provided by the non-supervised classification program. While this procedure is not rigorous it is soundly based on the spectral signature concept. It depends very heavily upon adequate band-to-band calibration.

The classes identified in this manner are necessarily broad and were typically as follows: 1) bright range land areas, 2) medium range land areas, 3) dark agricultural areas, 4) forest cover areas, 5) water. Each of these may have several subclasses. Using these estimated classes a classification was produced using the computer program. This classification was

then compared with the channel 5 imagery for accuracy and several discrepancies were noted to be checked during the ground observation mission.

Following the surface observation mission it was generally possible to increase the detail of analysis both by further detailing the classes delineated by the clustering algorithm and by manually selecting points as training samples for additional classes. In the case of each sub-project the details of these steps are indicated.

THE SURFACE OBSERVATION MISSIONS

After examining the initial analysis, several areas were designated to be examined in greater detail during the two-day surface observation mission. Points of interest were designated in the Ouachita Mountain subframe and in the Texoma subframe. These included several areas in the forested regions of the Ouachita Mountains which had apparently been treated in some unknown manner, two extremely bright areas were also noted, and two lakes south of the Red River were suspected to be of highly different water qualities. In the Texoma subframe the primary interest was different types of water being classified within the lake, possibly associated with silting and water depth. Several bright areas were being classified primarily on the north shore of the lake. In addition, any items of interest which might be seen during the mission would be noted and photographed.

A team of two LARS staff members flew to Oklahoma City on July 30 where they were met by the Oklahoma State Soils Extension Specialist who had scheduled a light plane and pilot from the University to fly the team over the areas of interest. Thus, the ground observation team was airborne over the site on the fifth day after the data had been acquired. The team had with them the channel 5 imagery, reconsituted color infrared photographs made at LARS (color versions of Figures III-1, III-2, and III-3), a black and white photograph of the initial classification, a sectional air navigation chart with many of the points of interest designated, two 35mm cameras with black and white, color negative, and color positive films, and a portable tape recorder to be used for verbal comments.

The area covered by the data was entered north of the Ardmore Mountains and an eastward course was flown to the Atoka Reservoir and the Ouachita Mountain subframe. In this area the banding effect in the Ouachita Mountains (Figure III-3) was observed and photographed and determined to be the result of drought-stressed vegetation in combination with rock outcroppings. The cleared area (Figure III-3, top center at A) was found to be range land which had been converted from forest cover. Other forested areas were in the process of being converted to range land through aerial application of herbicides. In particular, one area which had been noted in the first classification had been sprayed this season and showed the hardwood forest to be brown to the naked eye (Area B near top left center of Figure III-3). One area which had been noted in the reconstituted color infrared picture could not be seen from the air (Figure III-3, dark areas at C). Several small bright areas were determined to be recently harvested hayfields (Figure III-3, at location D).

Approximately one and one-half hours were spent flying over this area observing visually and photographing these various points of interest. During this time the team landed at Hugo, Oklahoma and picked up an Extension Forester who was intimately familiar with the forest and agricultural practices of this local area. He was present in the aircraft during part of the flight over this area. After completing observations in this area, the team proceeded south to observe and photograph the two lakes south of the Red River. The flight continued westward to Lake Texoma and several points of interest were noted and photographed.

At Lake Texoma considerable time was spent in observing the visual changes in water quality and the agricultural uses of the land, particularly that on the north shore of the lake. The team then flew north to the Tishomingo Game Preserve which includes a large natural lake. It had shown differences in water classification and was surrounded by a dense, apparently natural, forested area. From this point the flight continued westward and was terminated at Ardmore, Oklahoma at the end of the day. That evening a tape recorded review of the flight was produced.

The following day the team met with a representative from the Noble Institute at Ardmore who escorted them to the area on the north shore of the lake for examination of agricultural areas and soil types. Several distinctive fields were examined and photographed on the ground for later indentification in the data. Much of the land-use in this part of Oklahoma has been for range land and woodland with the intensive agriculture being cotton, grain sorghum and peanuts in sandy soils, particularly those near the lake. Several stops were made in various fields and also at several points along the north shore of the lake to examine the water quality, width of beaches, and other features near the lake. This second day of the ground observation mission was terminated in the late afternoon and the team returned to Oklahoma City by car and flew back to Lafayette that night.

FULL FRAME ANALYSIS*

In the first iteration analysis (i.e. prior to surface observations) eleven classes were defined from the results of the clustering algorithm output. Using the procedures described above an estimate of ground cover represented in the eleven classes was made. The color-coded classification of a sizable portion of the frame was generated for preliminary evaluation.

The features identifiable in this classification were the areas of water, forested areas along streams and in larger blocks in the eastern portion of the frame, and a part of the Ouachita Mountains evident as the heavily forested area in the northeast (top right) corner. The influence of man was apparent by the angular fields with their north-south and east-west boundary lines. Some larger highways were discernible, but they were not too evident due

*Classification Serial Numbers: 1st Iteration 727294701 (July 27, 1972)
2nd Iteration 809207201 (August 9, 1972)
Run Number: 72001400
Reformatted at line interval of 2 and sample interval of 3.

to the large interval between data points used in this set of data. Some differences in soils were apparent, especially in the very bright areas on the north shore of Lake Texoma.

A puzzling discrepancy was found when several bodies of water indicated on maps were classified into one of the bright range land classes. The Atoka Reservoir was entirely in this class as were small portions of Lakes Texoma and Tishomingo. This error was the result of the large sample intervals which in turn meant that too few points were available to the clustering algorithm from these areas to adequately represent them. It also alerted the analysts to the possibility that significant differences in water quality would be seen in the data.

It was also felt that range land and pasture lands were not separated as distinctly as they might be.

With the knowledge gained from the ground information mission and resource people contacted in Oklahoma, a second iteration of the analysis was produced.

The original classes were retained and additional classes were added, based on the ground information, to correct the known errors and improve the separation of classes. Training samples were taken from the Atoka Reservoir, Lakes Texoma and Tishomingo, and several pasture areas visited by the ground information team. The new set of classes thus was a combination of automatically selected classes from the clustering algorithm and hand-picked classes defined by the analyst.

The color coded classification using the second set of classes is shown in Figure III-4. Seventeen classes were used and they are presented here in eleven colors. The colors and their corresponding estimated cover types are listed in Table III-1.

Table III-1

Category	Spectral Class	Color Code	Cover Type
1	2, 3, 4, 5, 6, 7, 8, 12, 13,	Yellow, Tan, Light Green, Brown	Range lands and pastures
2	1, 17	White, Light Gray	Sandy, or Bare Soils, Light Vegetation, Agricultural fields with sparse canopy
3	9, 10	Dark Green	Forests and woodlots
4	14, 15, 16,	Dark Blue, Blue Gray, Aqua	Water (3 subclasses)
5	11	Dark Purple	Atoka Reservoir

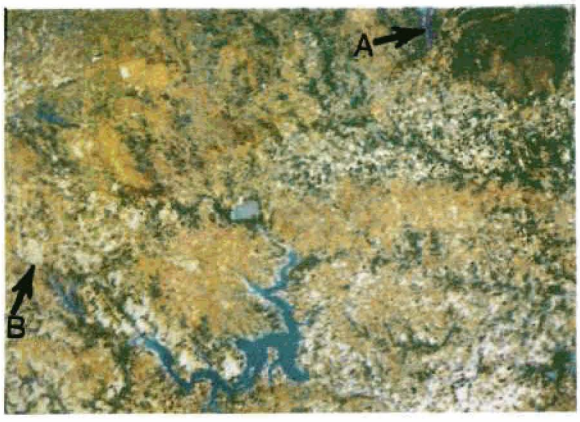

Figure III-4. Color coded classification results (CCR) of a portion of the Texoma Full Frame data.

Figure III-5. Color coded classification results (CCR) of Lake Texoma data.

Figure III-6. Enlargement of area shown in Figure III-5.

The second classification shows more classes and detail than could be seen in the first. The Atoka Reservoir (only southern tip shown, Figure III-4 at location A) is now not only correctly classified but is shown to be a class of water distinct from all others in the picture. The Atoka Reservoir is of relatively uniform depth of about 20 to 30 feet over much of its area and it is a source of water for Oklahoma City. Three other water classes appear in the various lakes. Patterns of yellow, tan and brown pasture and range land are seen forming generally broad east-west lines separated by valleys with green, light gray, and white areas. A large brown area in the Ouachita Mountain (top right corner) is a pasture area which has been converted from the surrounding forest. The boundary lines of a large range are also apparent near the top left. The ranch land has been classified into a range land class indicated by yellow.

Highways are seen again as faint white lines. For example, at the extreme left Interstate Highway 35 enters the picture about half way from the top and continues to the bottom. It passes through the west (left) edge of Ardmore, Oklahoma (Figure III-4 at location B) which appears as a white, almost circular area near the left edge and slightly below the center point. The Red River is a sinuous, light blue line entering Lake Texoma from the West and continuing from the Texoma Dam (North-South straight line at the Southeast corner of Lake Texoma in Figure III-4) to the right edge of the picture.

Figure III-4 covers slightly less than 2/3 of the total frame and represents an area of approximately 75 by 50 statute miles in size. Because of the large amount of data present in this image, it is difficult to fully evaluate and discuss the results. Our objective in this study, to obtain a preliminary indication of the utility of ERTS-1 data, will be more fully approached by a more detailed look at the smaller subframe areas.

TEXOMA RESERVOIR SUBFRAME ANALYSIS*

Thirteen classes were defined by the clustering algorithm in the first analysis of this data. The cover types represented by these classes were estimated as before and a classification was produced.

Although more detail was observed in the field structure of the range land and pasture lands it was still suspected that even more could be produced. Forested areas appeared too extensive when the classification was compared to data imagery. Two water classes were defined in this classification and one appeared to be associated with muddy water in Lakes Texoma and Tishomingo. In Lake Texoma the "shallow/muddy" class was located at the head of the lake and at the heads of each small inlet suggesting that this class could be subdivided to make a greater distinction between shallow clear water and muddy, silted water.

*Classification Serial No: 1st Iteration, 0728294702 (July 28, 1972)
2nd Iteration, 0808207101 (August 8, 1972)
Run Number: 72001401
Maximum Resolution, Line and sample interval of 1

As in the full frame classification the information gathered during the ground mission was used to define additional classes which were added to those selected by the automatic clustering algorithm. Classes were added to improve separation in water quality, agricultural crops, and range land. The second classification contains 18 classes which are subdivided into 4 broad land use categories. The color coded classification is shown in two figures. Figure III-5 shows about half of the subframe (approximately 27 by 25 statute miles) and Figure III-6 is an enlargement of the west end of Lake Texoma (approximately 14 by 12 statute miles). The colors and estimated cover classes for both figures are listed in Table III-2.

Table III-2

Category	Spectral Class	Color Code	Cover Type
1	12, 13, 16, 17, 18	Light Blue, Dark Blue, Blue Gray, Med. Blue	Water (5 classes)
2	1	White	Sandy and Light bare soil, light colored dry vegetation, agricultural fields with low crop coverage
3	7, 14	Red	Agricultural fields with high coverage
4	2, 3, 4, 5, 6, 15	Yellow, Light Brown, Light Tan	Pasture, Range land
5	8, 9	Light Green	Forest, sparse canopy
6	10, 11	Dark Green	Forest, more dense canopy

Features of particular interest in these photographs are the various classes of water which appear in Lake Texoma and Tishomingo. The west (left) end of Lake Texoma shows the delta where the Red River enters the lake as a white hook-shaped feature which is the dry portion of the delta. The aqua blue adjacent to the dry delta is a portion of the delta which is barely covered with water. It is less than three feet in depth in much of the delta area and is visibly muddy to the boundary of the light and medium blue. Figure III-7 shows a photo of the area taken from the north looking south.

There is a very narrow band of blue-gray between the aqua and light blue which may be associated with the edge of the delta. The medium blue and dark blue represent relatively clear water with the dark blue tending to be in the deeper areas. This association is not always true and may have been affected by surface wave action. There is a recurring gradation in color in the small inlets from dark blue, medium blue to light blue which must be related to decreasing depth in these locations.

Figure III-7. Aerial view of the delta in Lake Texoma showing edge of visibly muddy water. View is to the south (Texas) side of the lake.

Figure III-8. Ground view of highway bridge over Lake Texoma. The picture was taken about 1 kilometer north of the lake. View is to the south.

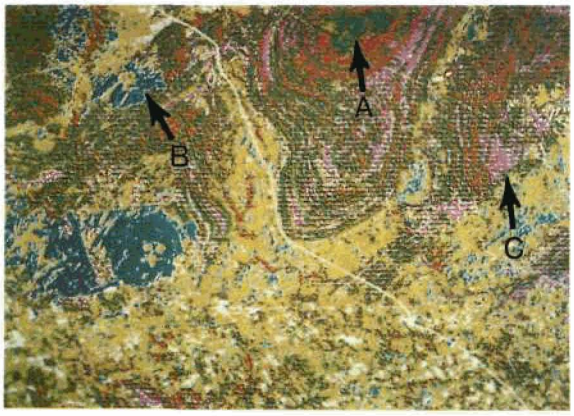

Figure III-9. Color coded classification results (CCR) of the Ouachita Mountain Subframe analysis. (First iteration)

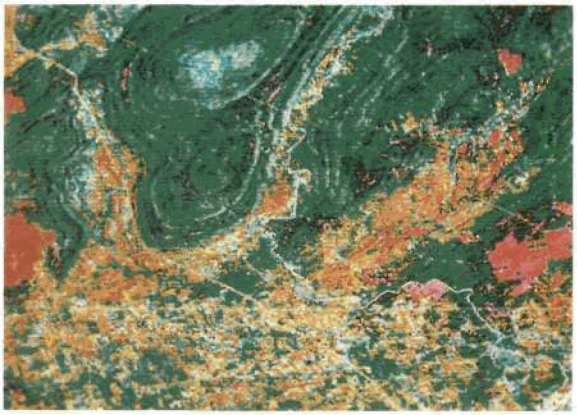

Figure III-10. Color coded classification results (CCR) of the final Ouachita Mountain Subframe analysis.

Lake Tishomingo near the top edge of Figure III-5 was classified into three classes indicated by aqua, light blue and blue-gray, all indicating shallow and muddy or silty water similar to that in the west end of Lake Texoma. Three small lakes may be seen in the light blue class between Lake Tishomingo and Lake Texoma. The yellow line through the green area immediately below Lake Tishomingo is a narrow stream through a very heavily forested area. The stream width is well below the resolution of the scanner and therefore could not be classified into a water class. The rectangular red area at the top right of Figure III-6 is a field of cotton and grain sorghum which was visited on the ground. In addition to occurrence for cases of cropland this red class may be seen occurring frequently near green forested areas particularly near the head of Lake Texoma. In this latter case it probably represents a misclassification of ground cover similar to cropland, possibly heavy weeds and grassland. The white areas near the lake, and in particular just north of the bridge (Figure III-6), were found to be fields of light, sandy soils usually containing peanuts which in most cases showed a very low ground cover, usually between 20 and 50%. It is unlikely that ground areas of this type could be detected as agricultural vegetation at this stage in the growing season due to the very bright soil background. In this area there were also many pastures containing flowering weeds and dry grasses which presented a very bright target. Many of these pastures showed evidence of overgrazing. This exposes greater amounts of soil, appearing brighter in the data.

The yellow, light brown, and light tan fields represent the many varied pasture and grassland cover types which occurred in this area. Ground information was not adequate to define specific cover types in these classes. The dark and light green areas represent woodlands which typically occur in drainage areas. The white classes are seen far more frequently on the north or Oklahoma side of the lake. This is due to the occurrence of deep sands north of the Red River in contrast to relatively shallow loams on the Texas side. Peanuts are grown on the Texas side but the fields are smaller (10-15 acres) compared to 80-500 acres on the Oklahoma side. The large fields provided a bright target since the crop cover was very low at the time data was collected.

There are instances of surprising detail in this classification as, for example, in the case of two highway bridges visible across Lake Texoma and some north-south roads visible in the green forest class. These features are not as wide as the resolution of the scanner; they are visible because of high contrast in the response between the features and their background thus creating enough change in the data point to cause it to be placed in a class different from that of the background. Figure III-8 is a view of the road and bridge across Lake Texoma (see Figure III-6). This photo was taken about 1 km. north of the bridge looking south.

OUACHITA MOUNTAINS SUBFRAME ANALYSIS*

Preliminary classification was carried out using the clustering technique for the entire Ouachita Mountains area in which 15 spectral classes were designated. Detailed analysis of the statistics from this data indicated that several of these spectral classes should be combined, since they were not significantly different. This was carried out, resulting in a set of 10 spectral classes which were used to make the preliminary classification. This classification showed a number of interesting features being spectrally defined and classified. The CCR is shown in Figure III-9. Table III-3 shows the color assignment.

Table III-3

Category	Spectral Class	Color Code	Cover Type
1	1	White	Interstate 75 and other highly reflecting objects.
2	2, 3, 8	Yellow	Soil areas.
3	4	Green	Non-dense vegetation, predominant on the top of the plateau.
4	10	Blue	Areas having low infrared response and caused by the activities of man. These areas do not exhibit the spectral characteristics of green vegetation although they appear to be located in an area which normally would have been forested.
5	9	Magenta	Forested areas having relatively low response in the infrared channels, perhaps due to topographic influences.
6	5, 7	Red	Forested areas with relatively high infrared response.

An extremely straight line which was later verified to be a power line location showed up very clearly in the classification results, as did Interstate 75. (Of course, these were also evident on the individual wavelength bands of ERTS imagery.) Forested areas in the mountains appeared to be well-classified although there was some question concerning the interrelationships between spectral response variations caused by differences in the vegetative cover.

*Classification Serial Number: 1st Iteration, 0727206801 (July 27, 1972)
2nd Iteration, 09082-6908 (Sept. 8, 1972)
Run Number: 72001402
Maximum Resolution, Line and sample interval of 1

Several large blocks of land had a very low spectral response in the infrared channels of the MSS data. The borders of these areas appeared to be very straight, with some rectangular corners, indicating that they were not natural features (note Figure III-3, area B). Another area on top of the plateau (area A, Figure III-3) had similar straight boundary lines with corner features, again indicating human activity, but this area did not have such low infrared response. The initial classification showed that both of these features were identified spectrally and mapped on the classification results. Some other similar areas which had not been previously noted were also identified as having the same spectral characteristics.

Reservoirs in this region demonstrated at least two spectral characteristics which could not be explained in interpretation of the imagery. The differences in spectral characteristics were particularly striking in Channels 4 and 5 (visible wavelengths) of the MSS data, where one reservoir had a relatively high response while the other reservoir had a relatively low response.

In general, the preliminary classification allowed spectral definition of a number of interesting and perhaps significant features, but the significance of these results could not be accurately judged because of a lack of information concerning the actual cover types in these areas. A number of rather specific questions arose concerning the cause of variations in spectral response and the cover type present in several of these locations. A number of these unexplained features were given to the surface observation team as specific target points on which to obtain information regarding the causes of the particular responses which had been observed. General information concerning the cover types and condition was also requested.

Following the return of the surface observation team, we found that the visual and photographic data which had been collected by them proved to be of great interest and of considerable value in interpreting the results of our data analysis sequence. A number of oblique aerial photos of certain areas indicated that the areas having the straight boundaries and rectangular corner features were indeed caused by human activity, but there was a number of different factors involved. In the area on top of the plateau (Figure III-9, location A) a clearing operation had taken place in which the forest cover had been removed and windrowed, allowing native grasses to dominate the scene. This was one type of range land improvement project. Rectangular boundaries observed in these areas on the oblique photography corresponded very well to the ERTS imagery. In another region (Figure III-9, area B) the rectangular boundaries were caused by aerial spray operations of the forest cover. This spray (2,3,5-T) had caused the trees to die, resulting in the tree crowns having a medium brown tone to the eye, and a very low response in the infrared channels of the ERTS imagery. This was another type of range improvement program.

The surface observation team also determined that the powerline area had a grass cover over most of the right-of-way. A third area in the imagery (Figure III-9, area C) which had an extremely low spectral response in Channels 6 and 7 could not be verified by the surface observation team because of a lack of visual difference in the area being investigated. They

flew around the region indicated on the ERTS imagery for some time but were not able at low altitude to identify any apparent differences between this area and the surrounding materials that had a more normal response. Correspondence with the local Extension Forester has indicated that this area was sprayed with 2, 4, 5-T last year but that the spray application was not adequate to completely kill the trees. Consequently, this year the vegetation has developed its normal green appearance (to the eye), but either it is still under a serious stress condition or the vegetation under the forest canopy has been affected or the vegetative density has decreased, resulting in a distinct decrease in infrared reflectance. This situation explains the difficulty that the surface observation team had in locating that particular area on the ground.

Following the return of the surface observation team, a more detailed analysis sequence was undertaken for this area. Particular attention was paid to the mapping of the different forest cover areas and the water resources in this region. A number of small areas were designated for use in clustering analysis and from these it was determined that at least 20 significant spectral categories were present in the data. A set of training samples was developed and the Ouachita Mountain subframe was again classified, using a maximum likelihood algorithm. Further refinements on this classification are still being carried out. It appears that all 20 of the spectral response patterns are of significance for their potential differentiation of the various features in this imagery. However, there do not appear to be 20 categories of cover types which are significant. One of the tasks most in need of further study in this type of analysis is that of grouping the various spectral categories into the surface features of significance.

The final classification results are shown in Figure III-10, and the color code scheme is shown in Table III-4.

This presentation of the final classification results show the power line very distinctly, and I-75 has a fairly distinct spectral characteristic. The areas where the forest cover had been sprayed also were defined as a distinct spectral category. A number of spectral classes were grouped into the various range land areas, including the area on top of the plateau.

One of the most interesting features defined by the final classification involved the distinct banding effect related to the geologic structure of the Ouachita Mountains. Surface observations and aerial photos of this area indicated that the spectral differences causing this banding were the result of a number of different features. In some cases limestone outcroppings caused a very distinct spectral response (Figure III-10, area A) and in other cases the banding was caused by a combination of topography and vegetation effects. Distinct differences in slope and aspect were observable and these seem to be closely related to differences in vegetative density. The surface observation team also indicated that very distinct, observable moisture stress in the forest cover along some of these geologic structures was observed. At the present time, the relationships between spectral response, moisture stress conditions, vegetative density, and the characteristics of the

Table III-4			
Category	Spectral Class	Color Code	Cover Type
1	13, 14	Dark Green	Forested areas
2	12, 15	Light Green	Forested areas having high response due to topographic position.
3	16	Black	Forested areas having low infrared response due to stress conditions and topographic position.
4	17, 19	Dark Red	Forest area that has been spread with 2, 4, 5-T for a range control project. Vegetation has been killed.
5	18, 20, 21	Magenta	Forested areas with low infrared response due to 2, 4, 5-T application last year. (Area could not be distinguished from surrounding vegetation when flying over in a light aircraft).
6	1	White	River Area—water and surrounding vegetation.
7	4	Very Pale Yellow	Highly reflecting objects including I-75, limestone outcrops, and scattered points of highly reflective material (particularly soils).
8	3	Yellow	Agricultural areas having large amounts of highly reflective soil exposed.
9	5, 6, 7, 8	Orange	Agricultural areas with moderately reflective soils.
10	9, 10	Brown	Agricultural areas with relatively low reflecting soils.
11	2, 11	Blue	Range land

underlying geologic features and their moisture holding capacities are not known, but we do believe that the results here indicate that the vegetation is reflecting accurately the underlying geologic and soil characteristics of this area.

Differences in the water quality were cited by local contact personnel as the cause for the spectral differences observed in the reservoirs in this area. These water quality differences were not particularly obvious to the eye from light aircraft, but did show up distinctly on the ERTS imagery. At least three distinct spectral responses have been observed in the reservoirs in this area with a fourth spectral category representing small rivers and their surrounding cover types. A small river north of Antlers, Oklahoma (Figure III-10, location B) showed up clearly in the classification results, although it is believed that this spectral class represents a combination of water and other vegetation and soils materials rather than only the water. This belief is based upon the analysis of the spectral characteristics of the data for that particular class of material as well as knowledge of the size of the river and resolution of the scanner.

SUMMARY AND CONCLUSION

Results of the analysis of this area thus far indicate a great deal of potential in the analysis and interpretation of this ERTS imagery. The analysis discussed in this report, which is only a preliminary one, concentrated on the geologic, forest, range, cropland and water resources of the area. It appears that more than 20 significant spectral classes are present in the data, but a fewer number of categories of informational value are present.

One analysis step most in need of study at the present state of the remote sensing art appears to be the refinement of a straight-forward technique to relate the spectral classes present to the significant categories of interest defined by the users. The work here required analysis of ERTS data in an area where local conditions were not known by the analysts. The analysis sequence tested involved (1) preliminary analysis based solely upon the spectral characteristics of the data, followed by (2) a surface observation mission to obtain detailed information from local resource people, as well as visual observations and oblique color photography of particular points of interest in the test site area. This appears to provide an efficient technique for obtaining particularly meaningful surface observation data. Following such a procedure allows one to concentrate on particular points of interest in the entire ERTS frame and thereby makes the surface observation data obtained particularly meaningful. The final step (3) involved more detailed and refined analysis sequences which can then be pursued in a much more definitive manner. The development of a procedure for utilizing a clustering algorithm in an analysis technique involving small geographic areas for initial clustering also appears to have great potential for further analysis of large scale areas using ERTS data.

We believe this particular analysis sequence has been significant from the standpoint of demonstrating a fast turn-around (and therefore low-cost) analysis capability, a capability to show the complexity of natural resource and man-made features that can be identified and the potential of mapping these using ERTS data, and in the development of better analysis techniques for further ERTS work. Whether CCR's of the type produced here can indeed become accurate and useful land-use maps of an area remains to be seen but promise has clearly been indicated. Multitemporal imagery should provide even greater promise.

ACKNOWLEDGMENTS

The work reported herein was the result of a team effort involving a considerable number of LARS Staff. Particularly notable in addition to the authors were the contributions made by Dr. Philip Swain (first iteration data analysis), Dr. D. Levandowski (geologic feature interpretation), T. A. Martin (results presentation), C. J. Johannsen (ground observation team), L. Bartolucci (hydrological features), and M. Coggeshall (Ouachita sub-frame analysis).

Acknowledgment with special thanks is extended to the following from the Oklahoma area who were generous with their time and resources in assisting in the ground observation task:

W. Elmo Baumann, Oklahoma State Extension Soils Specialist (Emeritus) Stillwater, Oklahoma

C. L. Clymer, Oklahoma Extension Forester, Antlers, Oklahoma

G. D. Simmons, Director, Agricultural Division, Noble Foundation Inc., Ardmore, Oklahoma

M. E. Degeer, Army Corps of Engineers, Tulsa, Oklahoma

FIRST RESULTS FROM THE CANADIAN ERTS PROGRAM

L. W. Morley
Director, Canada Centre for Remote Sensing

By agreement with NASA, the Canadian Department of Energy, Mines and Resources is reading out, processing and distributing all the directly transmitted imagery data from ERTS of Canadian terrain. The receiving station is located at Prince Albert, Saskatchewan which is in Central Canada. It is dedicated to ERTS having no other function. It has a remarkable hi-resolution CRT Quick Look facility enabling images to be viewed 10 minutes after a pass. The magnetic tapes containing the video data from the RBV's and the P.C.M. tapes containing the MSS data are air-expressed daily to the Ground Data Handling Centre operated by the Canada Centre for Remote Sensing in Ottawa. Here they are transformed to uncorrected and map-corrected hard copy.

The imagery is then reproduced in quantity by the National Air Photo Library and is marketed, at the cost of reproduction to the user community—both national and international. We only have one category of users. Copies are obtained by writing The National Air Photo Library, Department of Energy, Mines and Resources, Ottawa, Canada. The price is $1.00 for a 9-by-9 inch black and white print; $2.00 for a black and white transparency; $3.00 for a colour transparency. Enlargements can be made to order at a price dependent on the specifications. Standing order forms are available from the National Air Photo Library.

To date 225 orbits over Canada have been recorded up to and including September 26th. About 120 orbits have been processed.

The software on the map-corrected imagery was recently de-bugged and has started on the colour precision-corrected imagery.

About 200 standing orders for imagery have been received by the National Air Photo Library and we expect this to be multiplied several times as the high quality of the imagery becomes better known.

There are usually 4 orbits a day over Canada but as the orbits progress westerly, the 4th orbit misses Canada before another one appears at the east. The orbits average about 18 minutes covering about 60-65 scenes per day over Canada—that is, about 15 scenes per orbit. About 3,000 scenes have been recorded over Canada as of September 26.

The following scenes are representative of the various types of terrain imaged by ERTS in Canada. With the exception of Figure IV-1, they are all taken from band 6 of the MSS.

Figure IV-1 is a simulated IR ektachrome colour print of the city of Vancouver, Canada, and the snow-covered mountains to the north. This is one of the first precision-corrected

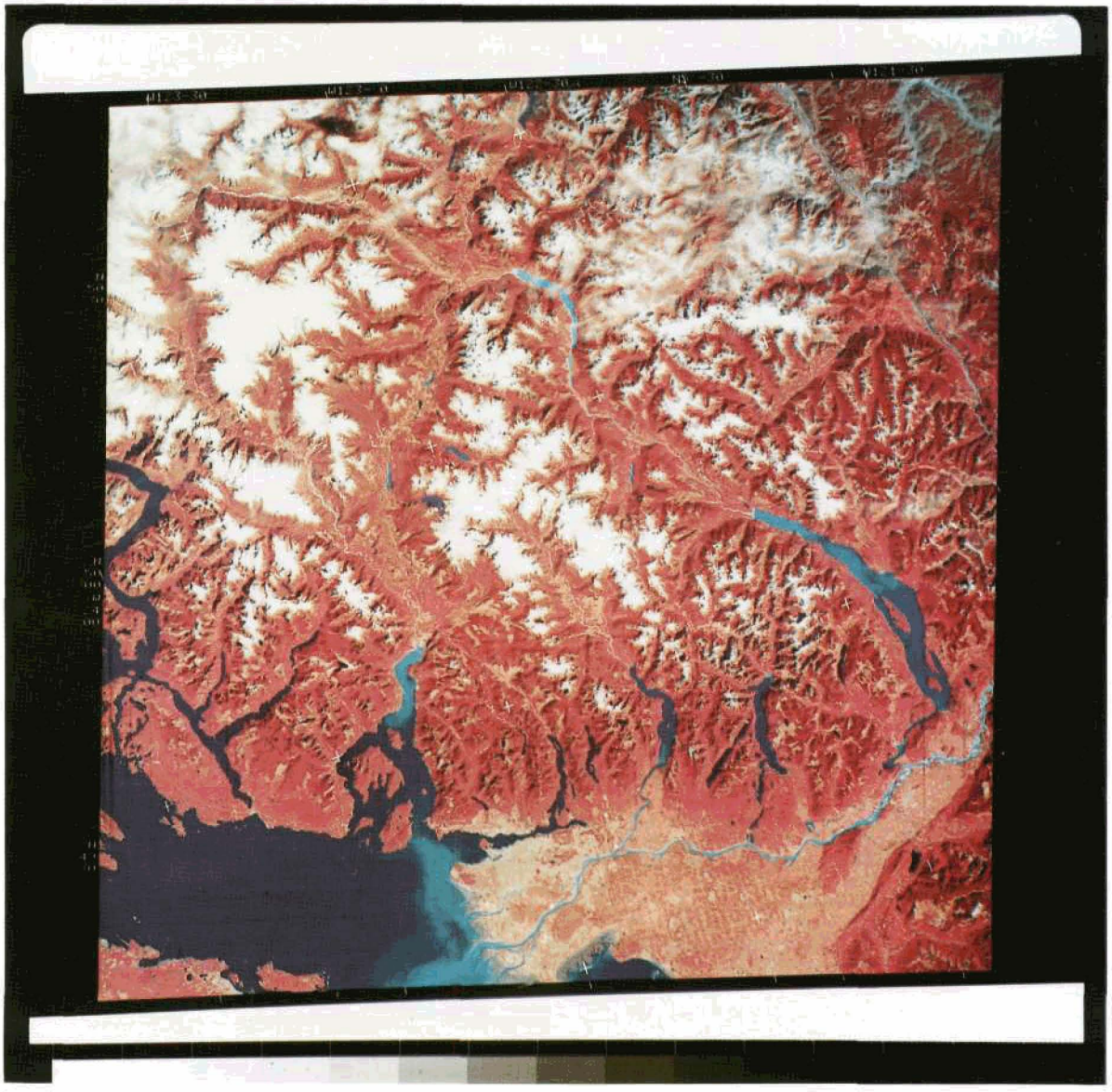

Figure IV-1. Vancouver, Canada, first colour precision-corrected image from the Canadian ERTS GDHC, Ottawa.

images which has been produced by the Canadian ground data handling centre in Ottawa. The silt-laden Fraser River runs through the city of Vancouver and discharges into the Strait of Georgia, producing a large light-plume against the dark-blue, relatively clear water. The picture was taken on September 2nd and shows the extent of the snow cover in the mountains to the north of Vancouver. Some of the applications of this image will be as follows:

- To construct a land-use and potential land use map of the area. It is fairly obvious that the available useful land in this area is limited because of the presence of the mountains.
- To measure the acreage of forested area and the amount of cutting that has already been done.
- From the relative sizes of the snow covered areas in the different bands, it would be possible to estimate the area of melting snow and correlate this with the run-off. Once this correlation had been done it would be possible in the future to predict the run-off from melting snow.
- Geological Structure: it is quite possible that some major faults and folds visible on this image have not previously been observed on aerial photos or mapped in the field.

Figures IV-2, IV-3 and IV-4 are three images in bands 4, 5, and 6 of the MSS centering on Winnipeg, Canada. Winnipeg is the centre of a wheat and cereal crop area in the Province of Manitoba. The cultural features and roads show up best in band 4 and it is possible to see most of the major roads in the area as well as the Winnipeg floodway which bypasses the city to the east. Individual fields can be clearly distinguished and from an examination of the various bands with some knowledge of the area, it should be possible to determine the type of crop in a given field, or whether it has already been harvested or was put out to summer fallow. The central part of the picture shows the fields in a darker colour, reflecting the clay till soil of the area while the generally lighter area in the southwest corner reflects the sandy loam. The east and north east portion of the scene shows the forest and swamp area underlain by the Precambrian shield.

Figure IV-5 covers the Bathurst Inlet in the Coronation Gulf in the region of the Arctic Circle. This is Precambrian barren land country. Repetitive ERTS data in this area will be used to study the sea ice conditions in order to evaluate the area for future shipping lanes and for potential harbours. ERTS imagery in areas such as this can be used to map major geological structural features, some of which may not have been observed by ground geological mapping or on aerial photos of the region. It will be useful for mineral exploration companies to observe the time of break-up and freeze-up in the rivers and lakes to tell when float planes could be landed. This is an area where the arctic ecology is very fragile and can be permanently damaged by careless bulldozer activity. Repetitive ERTS coverage will enable managers to assess and monitor such damage.

Figure IV-6 shows Cornwallis and part of Devon Island in the Canadian Arctic. Such Arctic Island pictures will be most useful in assessing and understanding the sea ice conditions in

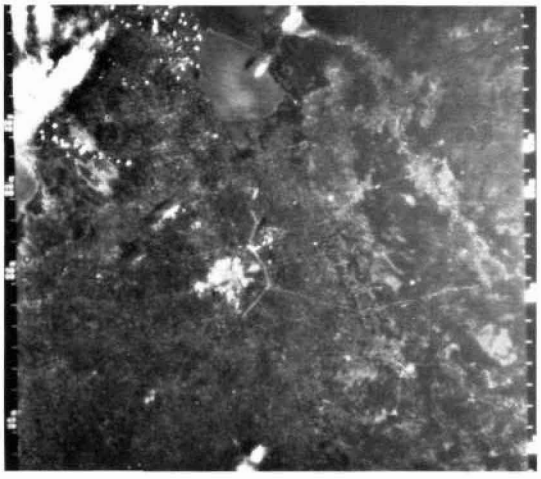

Figure IV-2. Winnipeg, Canada, MSS Band 4.

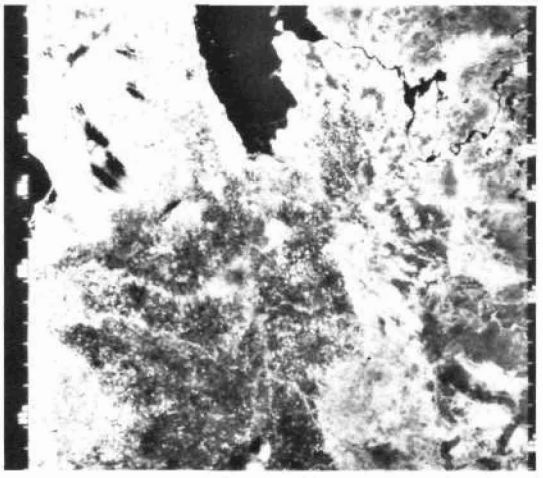

Figure IV-3. Winnipeg, Canada, MSS Band 5.

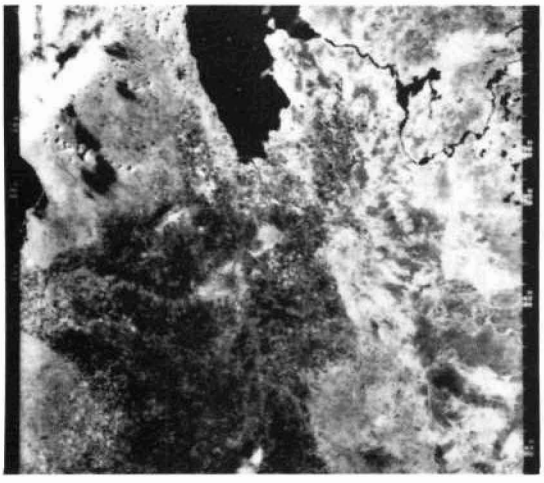

Figure IV-4. Winnipeg, Canada, MSS Band 6.

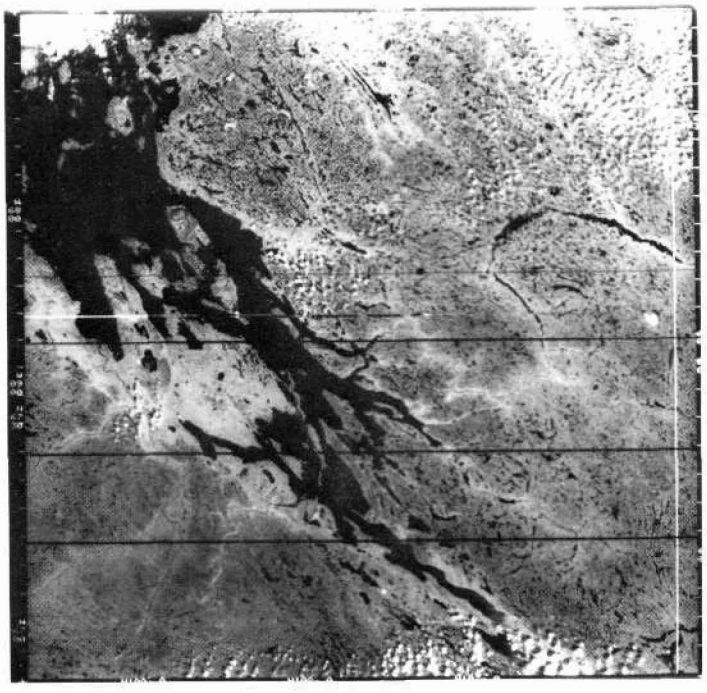

Figure IV-5. Coronation Gulf, Arctic Circle.

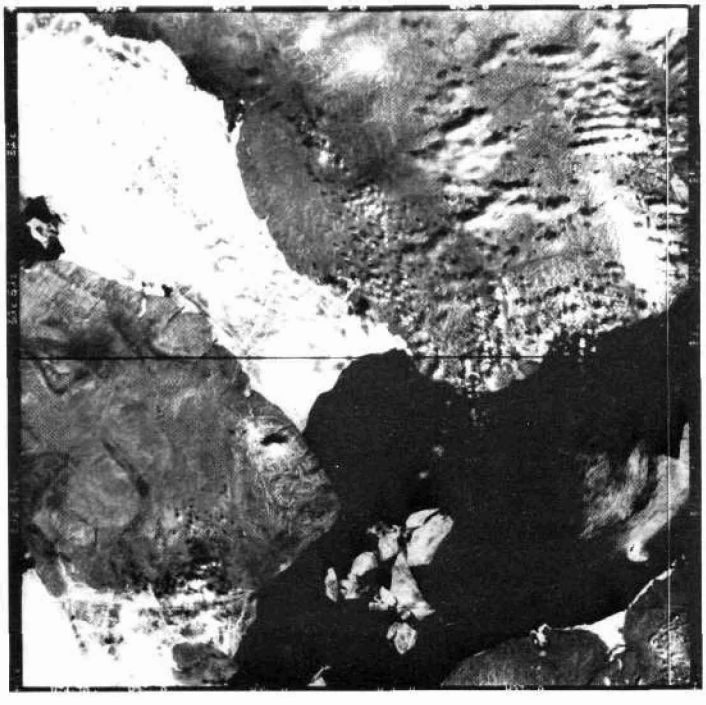

Figure IV-6. Cornwallis Island, Arctic Canada.

the Northwest Passage for the further development of Arctic shipping lanes. Because there is about 90 percent overlap between corresponding orbits on successive days, it is also possible to chart ice movement over a 24-hour period which will yield information on currents in the area. There are only about 7 weeks which are snow-free in this area. This particular picture captured the scene during a snow-free period. Such imagery will be useful for studying the hydrology of the region.

Figure IV-7 of Southern Ellesmere Island shows the iced-in condition of Norwegian Bay at this time (July 29th) and the snow-capped mountains feeding the glaciers. Several glaciers can be observed in the image. Repetitive ERTS images will allow the gross monitoring of glaciers and it should be possible to determine the major sources of icebergs and to monitor glacier surges.

Figure IV-8 shows the St. Lawrence River, Montreal Island, and Lake St. Joseph in Quebec. Lake St. Joseph is the delta of the St. Lawrence River, since it is at this point that the River reaches sea-level. The area is known as the St. Lawrence Lowlands and is between the Laurentian highlands to the northwest underlain by the Precambrian shield and the Appalachian highlands to the southeast. The Monteregion hills which are old volcanic pipes piercing the lowlands are clearly visible. Main application in this area will be for hydrological studies, land use patterns and for ice conditions for shipping purposes.

Figure IV-9 is an image of the Strait of Juan de Fuca, the Olympic Mountains in Washington, and the Southern part of Vancouver Island. The major geological faulting is clearly visible on Vancouver Island. The areas of timber harvesting on the skirts of the Olympic Mountains can be seen in the original image.

Figure IV-10 is in the area of the northern part of the Fraser River in British Columbia. The prediction of run-off from melting snow is an important application in this area. Geological structure and land use patterns are also two important applications.

Figure IV-11 is the first ERTS view of the famous Rocky Mountain Trench in British Columbia. This trench continues right up to Alaska. Its geological significance and origin has long remained one of the world's geological enigmas.

Figure IV-12 was taken over Northeast Labrador, and is the first ERTS scene ever recorded over Canada. Of interest is the so-called snow-enhancement where the structure of the snow-covered rugged terrain stands up in sharp relief. Were it not for the snow, the relief would be difficult to see and interpret.

In conclusion, we may say that the first ERTS imagery of Canada is exciting to see and contemplate. Its resolution, clarity, and image content are really better than expected. The present difficulty we have in Canada is to make people aware of its existence and value. Within a few months, the big problem will be to get the data promptly into the hands of those who can get most advantage from it. Finally there will be an enormous educational job to train people how to use it quantitatively.

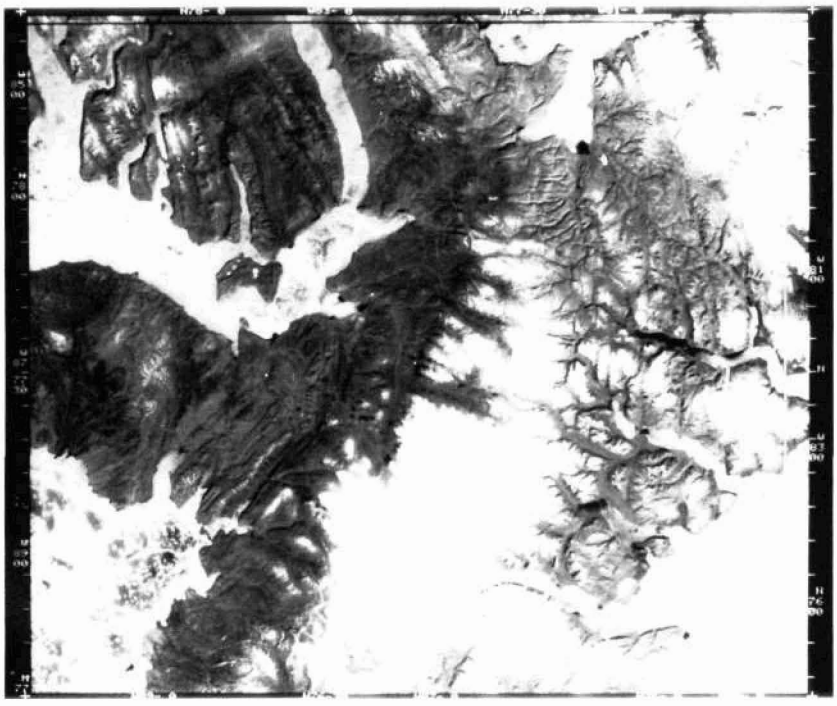

Figure IV-7. Central Ellesmere Island.

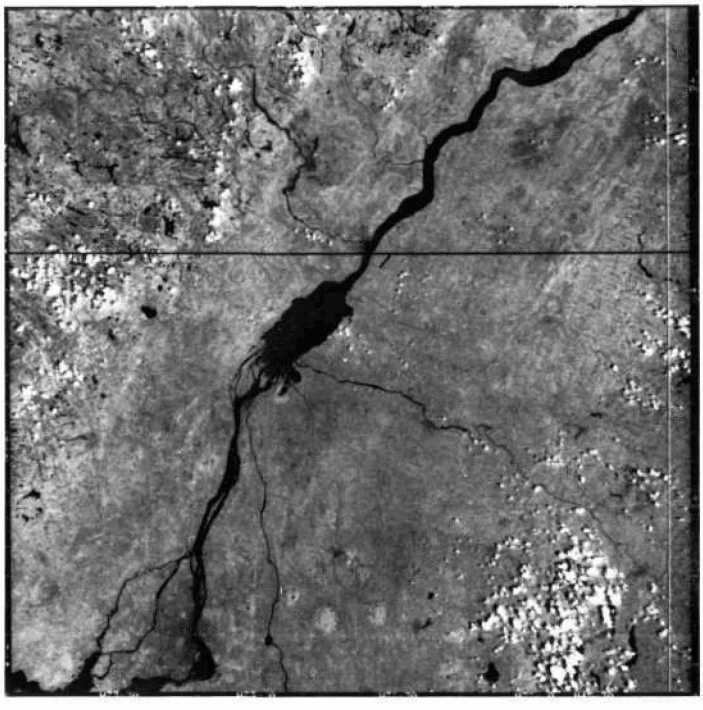

Figure IV-8. Montreal-St. Lawrence Lowlands.

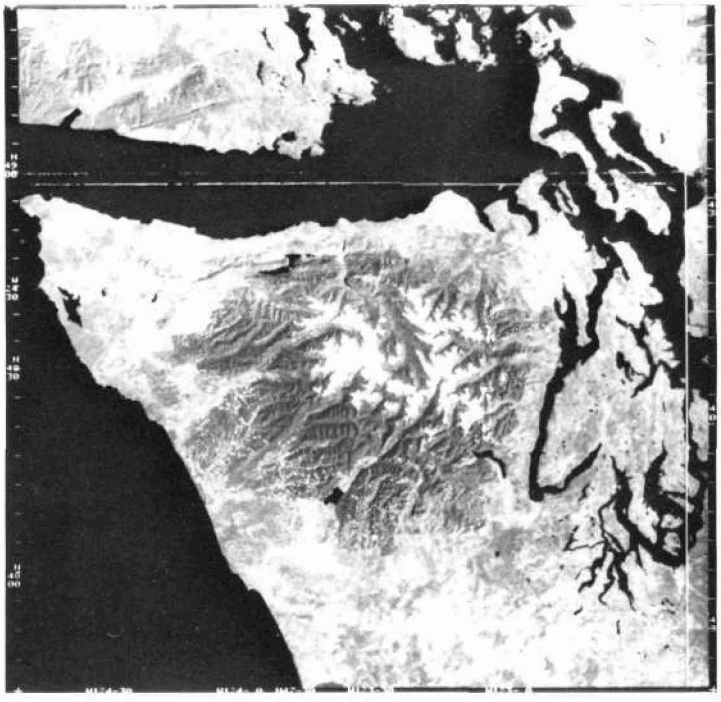

Figure IV-9. Olympic Mountains, State of Washington, USA.

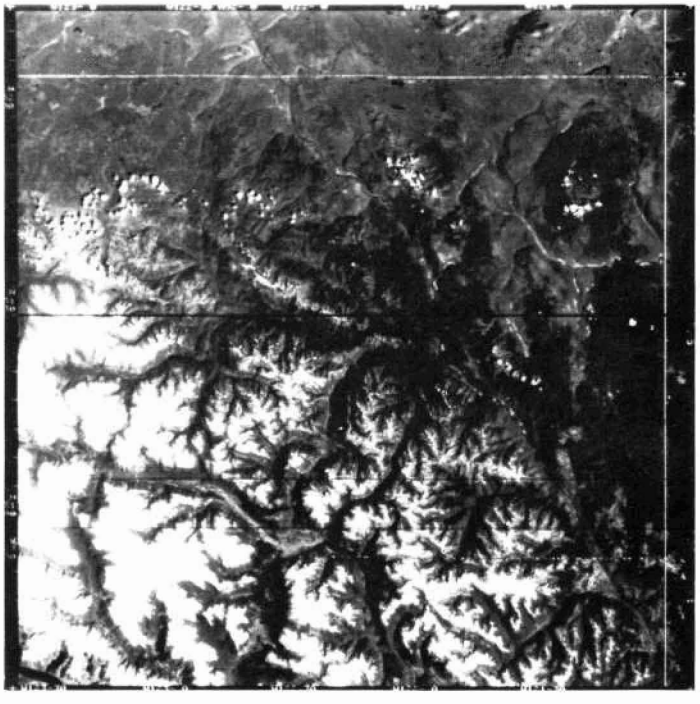

Figure IV-10. Northern Fraser River, British Columbia.

Figure IV-11. Rocky Mountain Trench, British Columbia.

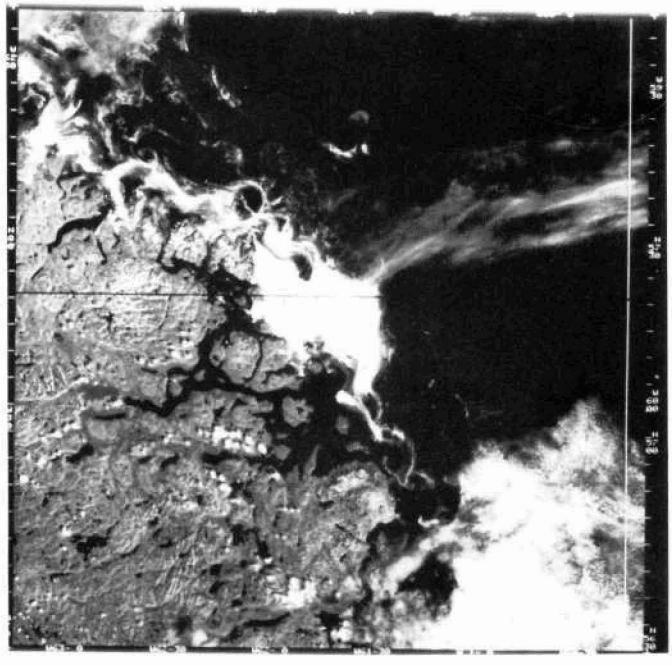

Figure IV-12. Northeast Labrador; The first ERTS image taken of Canada.

A FIRST LOOK AT CANADIAN ERTS EXPERIMENTS IN FORESTRY

L. Sayn-Wittgenstein*

The Canadian Forestry Service has 25 ERTS experiments. A detailed (although now slightly outdated) listing, with names of investigators is given in a paper by Sayn-Wittgenstein and Moore, published in the Proceedings of the First Canadian Remote Sensing Symposium.

Preliminary, often sketchy results have been received from about half the experiments. The first impressions follow.

IDENTIFICATION OF VEGETATION TYPES

We are optimistic about the possibilities of identifying and mapping forests and other vegetation types. The most encouraging results have been received from experiments in the boreal forest and in the Arctic:

- A colour composite using MSS Bands 4, 5 and 6 produced strikingly clear separations between coniferous forest (mostly spruce), hardwoods (mostly poplars) and areas covered by willow and alder (not shown). The test area is in Wood Buffalo National Park at the Alberta-NWT border. (Investigators are C.L. Kirby and P. van Eck).
- MSS imagery of the Mackenzie River Delta allowed the separation of spruce forest, willow and alder flats, and mud banks. Tundra could also be distinguished and several interesting but still unexplained vegetation differences are visible in the tundra. The interpretation methods used were entirely conventional: magnification of a single image, e.g. of Band 6 (Figures V-1 and V-2).
- Forest, range land, orchards, agricultural areas and cities could be identified on MSS imagery of the Okanagan valley in B.C. Conventional methods as well as electronic image slicing equipment (Digicol) were used.
- Results obtained by image slicing and enhancement, using purely photographic techniques (Agfacontour film), are impressive. A test using such enhancements (U. Nielsen responsible) of MSS imagery of northern Labrador led to a striking display of several vegetation types (Figures V-3, V-4 and V-5). Subsequent investigations (by W.C. Wilton and J. Bouzane) confirmed that spruce forests, recently burned areas and scrubby transition forests with a ground cover of lichen had been delineated. A wealth of geologic features, unexplained differences between bodies of water, clouds and smoke from burning fires can also be seen.

*Program Coordinator, Canadian Forestry Service, Department of the Environment, Ottawa.

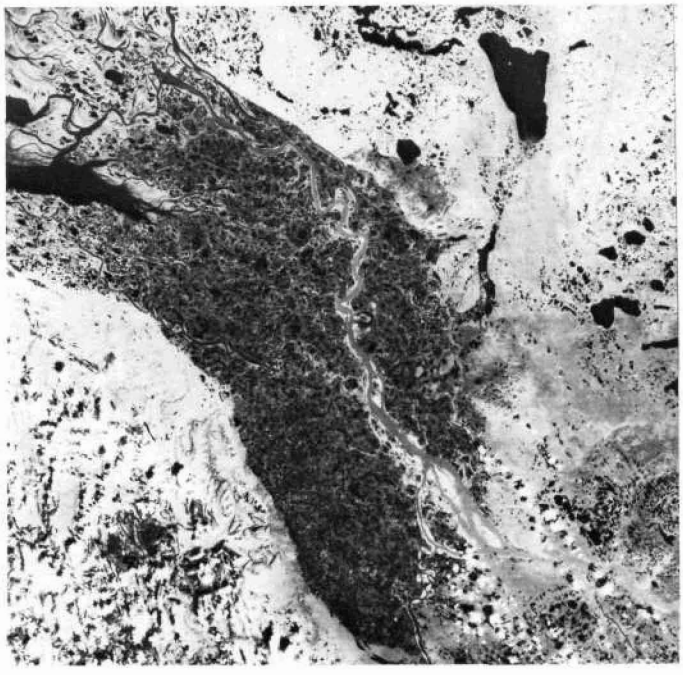

Figure V-1. Mackenzie River delta near 68° N, 134° W. ERTS-1, MSS Band 6.

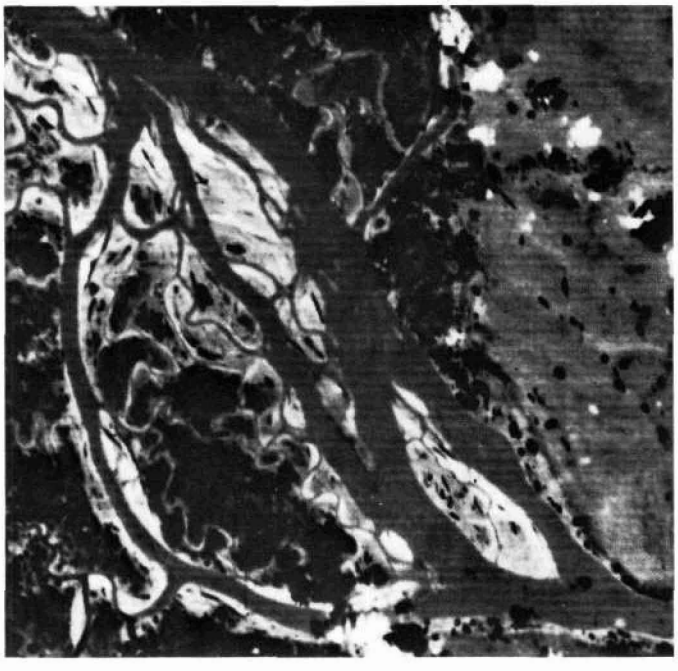

Figure V-2. Enlargement of a portion of Figure V-1.

Figure V-3. Harp Lake area in Labrador in the vicinity of 55° N, 62° W. ERTS-1 MSS Band 6.

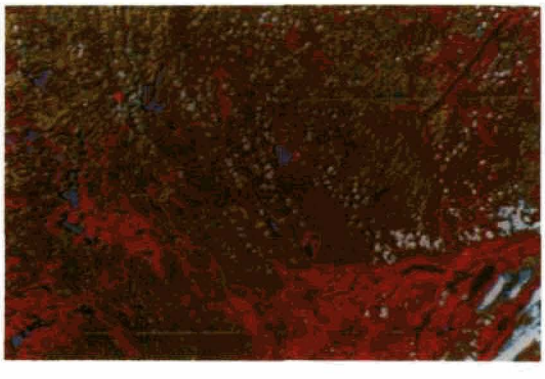

Figure V-4. Color enhanced MSS Band 5 of the same area shown in Figure V-3, using Agfacontour film.

Figure V-5. Color enhanced MSS Band 6 of the same area shown in Figure V-3, using Agfacontour film.

FIRE

ERTS will make it possible to assess the distribution and extent of fires in the northern forest and the tundra.

- A recent (1972) fire was clearly recognized on MSS and RBV imagery from Labrador. Similar observations were received from other areas (Peace River, Okanagan).
- The patterns left by fires from previous years are clearly visible on ERTS MSS imagery (Labrador).
- In 1968 a fire burned several hundred square miles near Inuvik, NWT. The burn was clearly visible in the MSS Band 6 (shown in Figure V-1). Electronic enhancement also showed the burn pattern, but this procedure also introduced difficulties as it was impossible to separate certain muddy water bodies from the burn (W.L. Wallace and J.P. Peaker).

Relying upon both tone and visible erosion and drainage patterns we suspect that in the Inuvik burn it is possible to recognize areas of scrub spruce with low shrubs, strongly eroded slopes and areas of fireweed and dead and fallen birch. The flowering of fireweed is at its peak at the end of July, when the ERTS image in question was obtained; this must have been a major influence on the imagery.

LAND ANALYSIS

One investigator, P. Gimbarzevsky, has met considerable success in delineating broad physiographic units on MSS imagery of the Lake Claire area of northern Alberta. He brought to his task a general knowledge of the area and considerable experience with the photo-interpretation methods of the Canada Land Inventory. His preferred method was to use a standard stereoscope, with each eye looking at a different band.

The detailed observations (with reference to Figure V-6) are as follows:

- *Unit A* is a deltaic plain dissected by the Birch River.
  1. The winding channel of the Birch River is well defined on Bands 6 and 7, visible but less pronounced on Bands 4 and 5.
  2. The Birch River discharging into Lake Claire and a fairly sharp outline of current deposition are visible on Bands 4, 5 and 6.
  3. The outline of a typical delta is pronounced on all four bands.
  4. Wet areas, probably subject to periodic flooding, are well defined by a dark grey tone on Bands 6 and 7.
  5. The present beach is best defined on Band 6 by its light tone.

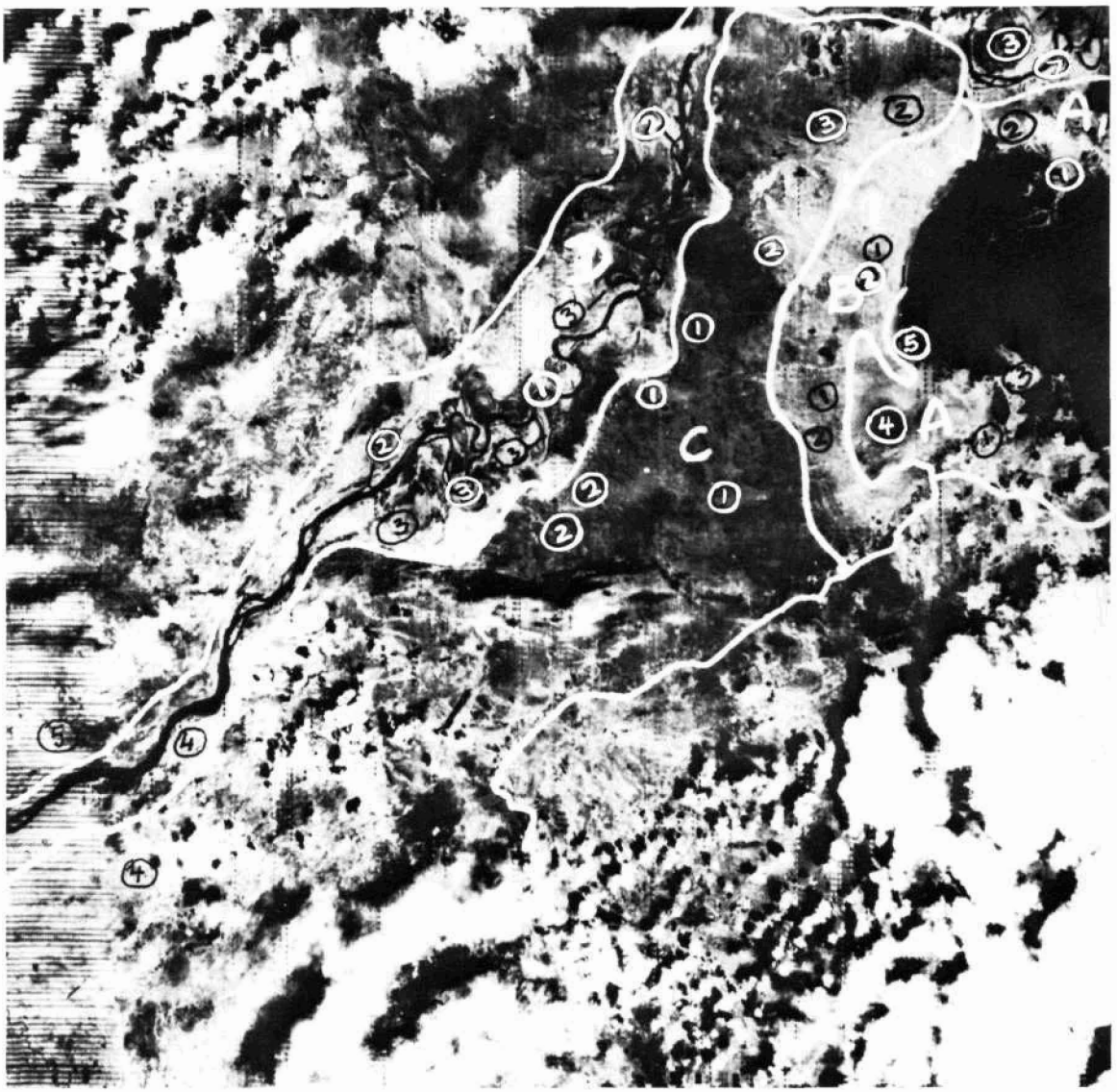

Figure V-6. Lake Claire area in Northern Alberta near 58° 30′N, 112°W. Picture clarity is hindered by the presence of clouds and system noise.

- *Unit* A_1 is a deltaic plain north of Lake Claire dissected by the Claire River.
  1. Delta channels of the Claire River are best defined on Bands 6 and 7.
  2. Wet, near-shore alluvial deposits (forested) are visible on all four bands: very light on Bands 6 and 7, light grey on Bands 4 and 5.
  3. Well-drained alluvial deposits (forested) are visible on all four bands.
- *Unit B* is a series of old beach lines which mark the past extent of Lake Claire.
  1. Discontinuous curvilinear beach ridges – quite pronounced on Band 5; less pronounced, but visible on Bands 6 and 7.
  2. Parallel depressions between the beaches and shore lines can be seen on Bands 5, 6 and 7.
- *Unit C* is an organic-mineral complex.
  1. Poor drainage is indicated by a mottled pattern on Bands 6 and 7.
  2. Well drained areas – probably aeolian sand, are distributed throughout the Unit C as fine ridges which are visible on all bands.
  3. A sharp difference in tone on Bands 6 and 7 is probably a fire boundary.
- *Unit D* – the Peace River flood plain.
  1. River channel is well defined on all four bands.
  2. Islands are visible on all bands.
  3. Meanders, meander lakes and meander scars are best defined on Bands 6 and 7, visible on Bands 4 and 5.
  4. Two main tributaries of the Peace River from the south the Wabaskaw and Mikkwa Rivers are quite pronounced on Bands 6 and 7, barely recognizable on Band 5, not visible on Band 4.
  5. The eroded channel of the Caribou River, north tributary of the Peace River, is recognizable on Bands 6 and 7.
  6. A series of rapids and falls (Vermillion Chutes) are visible on Bands 4, 5 and 6 as two distinct lines, but are not visible on Band 7.
  7. Man-made clearing on the south bank of Peace River (Sweet Grass Landing) visible on Bands 4 and 5, they are not visible on Bands 6 and 7.
  8. A road, north of Sweet Grass Landing, is visible on Bands 4 and 5.

Among the many landforms seen on ERTS imagery one should mention the pingos, those low hills along the Arctic coast, which are caused by frost heaving. One ERTS investigator

(W.C. Moore) has located several known pingos on MSS Band 6 imagery. Perhaps the well drained often bare soil at the top of the pingos has produced a contrast with the surrounding wet tundra.

INSECT DAMAGE AND POLLUTION

ERTS imagery was unavailable for several important experiments in central and eastern Canada. Insect infestations in British Columbia were not visible on MSS and RBV imagery, but it must be added that only black and white imagery was available and that enhancement techniques have not yet been used in this experiment (J.W.E. Harris). We also have no ERTS imagery for areas on which wind damage and SO_2 damage to vegetation have been documented.

WATER

- Clear water can be readily distinguished from muddy and sediment-laden water. The Mackenzie River Delta (Figure V-1) with its turbid channels and clear stagnant ponds offers good examples. The difference is obvious on all bands. In the Arrow Lakes area of B.C., lakes with colloidal glacial clays were best detected on Band 4 (A.H. Aldred).
- River rapids show up clearly; excellent examples were seen on Band 6.
- Approximately circular Arctic lakes with a maximum diameter of less than 350 feet were not visible on MSS Band 6, those over 400 feet were.
- A 70-acre landslide along a river was visible. In general mud banks, sand bars and eroded river banks show up well in Band 6.

HUMAN ACTIVITY

- The Canadian Forestry Service has a series of test areas on which logging operations have been documented. For some, ERTS imagery has not yet been obtained. But, judging by the ease with which strip-logging has been recognized in British Columbia (esp. MSS Band 5), there is good reason to be optimistic about the value of ERTS for monitoring and classifying logging operations which involve clear-cutting.
- The Canadian north is criss-crossed by seismic lines–straight, bulldozed paths made during oil explorations. So far we have been disappointed because little evidence of seismic line activity could not be detected. But there is hope that imagery at other times of the year (perhaps after the first snow) will produce better results.
- Miscellaneous examples of human activity observed on ERTS imagery are: roads and power lines; a bridge across Lake Okanagan; ski-slopes; a power dam on a lake (identified by an interpreter who did not expect to see a dam in that portion of northern Labrador).

PATTERN RECOGNITION

Parallel to the work in photographic and electronic enhancement there is an experiment (L. Sayn-Wittgenstein and Z. Kalensky) to test mathematical approaches to pattern recognition. Initial tests concentrate on those key parameters and statistics which can be used to identify objects on ERTS imagery by textures and spatial variations on imagery.

We have some preliminary results based on analyses of digital data obtained by scanning ERTS imagery (Figure V-7) with a microdensitometer. An example of the density profiles subjected to analysis is given in Figure V-8; Figure V-9 shows some of the statistics calculated. It is nothing new that there are significant differences between the mean densities of various classes. But we find it encouraging that there are also significant differences in standard deviations; standard deviation is one of the simplest expressions of texture.

There appear to be basic differences in the patterns of serial correlation calculated for treed muskeg, open muskeg, coniferous forest, ice, and water. For example the correlograms (Figure V-10) show possibly significant differences: the curve for muskeg displays the downward convex, exponentially decaying shape claimed by Matérn to be characteristic of many natural populations. The line calculated for "Arctic Ocean" does not appear to differ significantly from a straight line; a scan from Lake Claire suggests a possibly significant periodicity, etc. Spectral (*not* spectrum!) analyses of the same data have been completed (Figure V-11) and suggest patterns that have previously been documented using aerial photographs and forest survey data. Much remains to be done in testing the significance of these preliminary results, but we are confident that the analysis of spatial variation will produce some interesting results.

Figure V-7. ERTS image used for microdensitometer analysis.

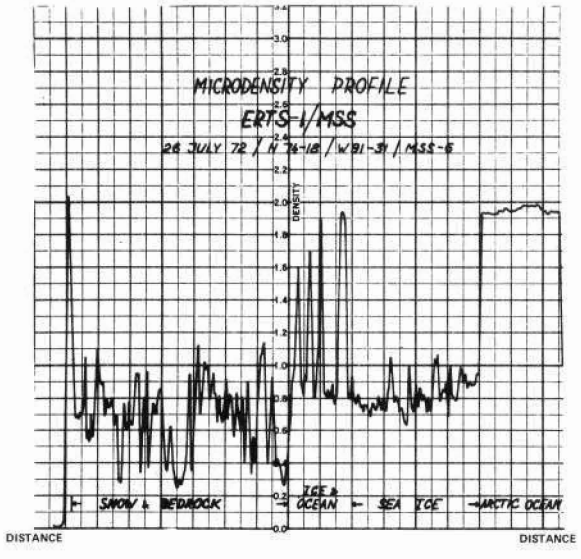

Figure V-8. Microdensity profile.

IMAGE Date Latitude Longitude Spectral Band	Object Class	STATISTICAL MEASURES The Arithmetic Mean $\bar{x}$	The Standard Deviation σ	 $100\sigma/\bar{x}$	The First Serial Correlation Coefficient r_1
		(D)	(D)	(%)	
A 27 July 1972 M56-54 W114-27 MSS-6	Lake	1.20	0.03	2.2	0.72
	Forest	0.98	0.05	5.4	0.71
	Treed Muskeg	0.87	0.04	4.7	0.64
	Muskeg	0.71	0.05	7.6	0.67
B 26 July 1972 N74-18 W91-31 MSS-6	Arctic Ocean	1.93	0.02	0.9	0.64
	Sea Ice	0.80	0.10	12.0	0.62
	Snow and Bedrock	0.66	0.20	30.9	0.58

Figure V-9. Statistical analysis of a microdensity profile.

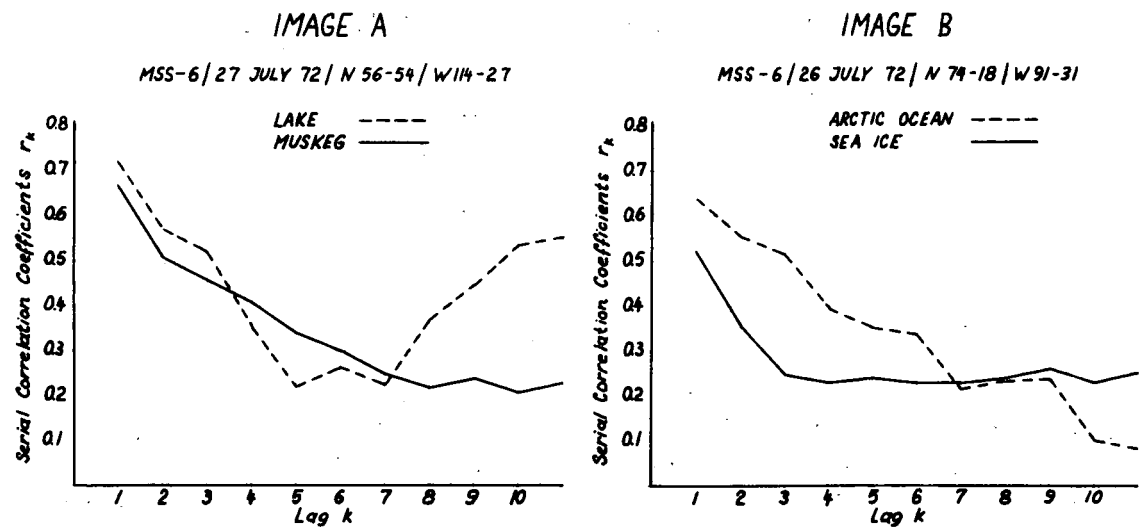

Figure V-10. Correlogram of ERTS-1 imagery.

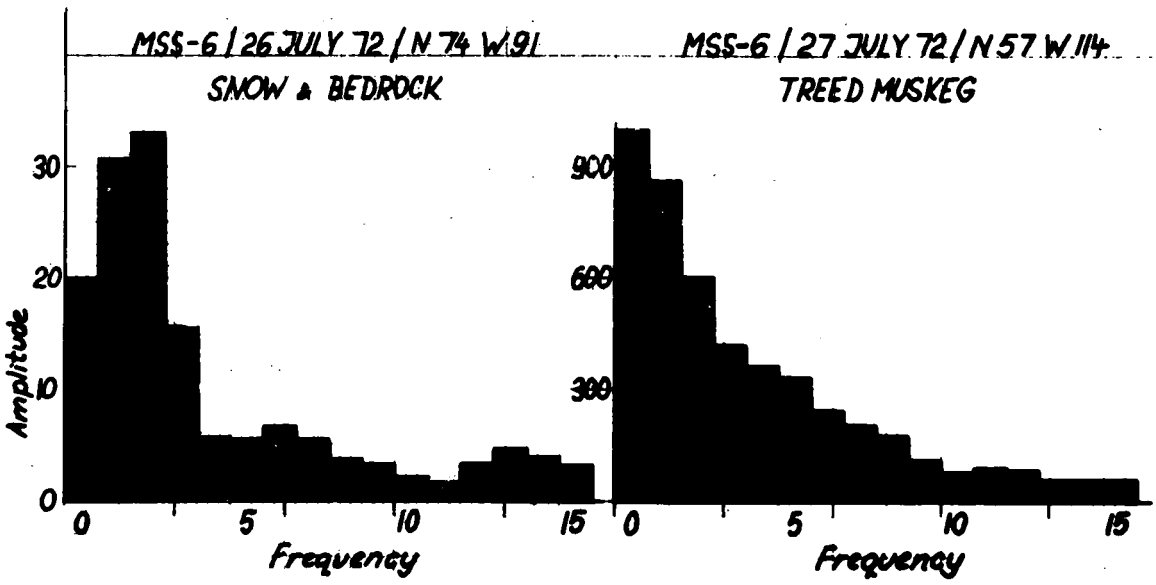

Figure V-11. Spectral analysis of data shown in Figure V-10.

GEOLOGIC INTERPRETATION OF ERTS IMAGERY OF WESTERN WYOMING–FIRST LOOK*

Robert S. Houston
University of Wyoming

Nicholas M. Short
Goddard Space Flight Center

INTRODUCTION

At the time of this study (late September, 1972) ERTS imagery was available from passes on the 5th and 6th of August. The images were from MSS-5 only and covered most of western Wyoming (Figure VI-1a). These images have been joined in a 6-frame uncontrolled photomosaic reproduced in Figure VI-1b. The area was largely cloud-free during these passes and the 9.5-inch positive transparencies used for this study show excellent detail. Single object resolution was not determined, but in areas of favorable contrast roads 10 meters wide can be recognized and some formations with a thickness of ten meters can be traced in outcrop.

We were concerned with the following questions:

- Can good ERTS imagery be used for regional geologic mapping?
- Can regional facies changes in major sedimentary units be recognized?
- Do major structural features show well at ERTS resolution?
- Is it possible to distinguish major lithologic units such as metasedimentary versus granite-gneiss terrain in rocks of Precambrian age?
- Can igneous intrusive bodies, such as stocks and plugs, be distinguished?
- Are major geomorphic features readily recognizable at ERTS resolution?

The answer to all of these questions proved to be "yes" in much of the area, if the interpretation is made by individuals who have a general familiarity with the geology of the region studied.

We will consider the topics mentioned above by referring to individual ERTS images, and by pointing out key features of the terrain.

ROCK SPRINGS AREA

Figure VI-2 is an image of the Rock Springs area of southwestern Wyoming. The vertical edge of the image is approximately 15 degrees east of north so that true north is roughly

*Contributions by Donald L. Blackstone, Jr., Roy M. Breckenridge, Ronald W. Marrs, and Ronald B. Parker.

parallel to the long dimension of the large elliptical-shaped anticline that trends roughly north-south in the center of the image. The river in the southwest is the Green River ponded behind Flaming Gorge Reservoir. The dark patches in the northwest are irrigated fields of the Farson agricultural district. The image area is not heavily vegetated and bare rock exposures are common in the sage-grassland terrain. Dark timbered areas can be noted in the extreme northwest and northeast where the southern margin of the Wind River Mountains and the Green Mountain uplift are exposed.

The most noticeable cultural features are the main line of the Union Pacific Railroad that can be traced as a dark sinuous line across the center of the photograph and three major trona mines that can be seen along the Green River and its tributary, Blacks Fork, in the west-central part of the image. The trona mines resemble small clouds with an adjacent dark shadow, but the dark areas are ponds and the light areas are waste piles. Note that these pseudo clouds (trona mines) have shadows to the southeast whereas true clouds found in the south center of the image have shadows to the northwest.

Major geologic features of this image are the Rock Springs uplift, the north-trending elliptical-shaped structure in the center of the image and the Washakie Basin, another circular form, that covers most of the southeast quarter of the image. The Rock Springs uplift is an anticline with rocks of Cretaceous age exposed in the core and rocks of Tertiary age exposed at the margin. The Washakie Basin is a syncline with topographically high rocks of Tertiary age forming concentric rims.

Perhaps the most striking single geologic feature of this image is the Killpecker Dune Field that trends roughly east-west across the northern margin of the Rock Springs uplift (Figure VI-3a). This is the largest cold weather sand dune field in North America and is made up of inactive or stabilized dunes that are grass covered and show as a dark band on the image and active dunes (moving today) that are vegetation free and show as white areas on the image.

On this figure the inactive dune area is outlined in solid line and the active in dashed line. A number of other areas that are probably unmapped dunes are also shown, illustrating the value of the images in mapping major geomorphic features of this type.

At the western margin of the Rock Springs uplift, beds of the Wilkins Peak Formation of Tertiary age are exposed. The middle member of the Wilkins Peak Formation is a thin (approximately 10 meters thick at its northernmost outcrop) light colored unit probably deposited in a great playa lake (Eugster and Surdam, 1972). This unit is the host for the evaporite mineral trona (hydrated sodium bicarbonate) that is mined in the subsurface, west of the outcrop area. These trona beds of western Wyoming are the world's major source of soda-ash for the chemical industry. This playa facies or middle member of the Wilkins Peak Formation can be traced over its entire exposed limit on the image (Figure VI-3b).

The trona beds serve as an excellent illustration of mapping of regional facies in sedimentary rocks with ERTS imagery. If the unit were exposed in another area along a line trending

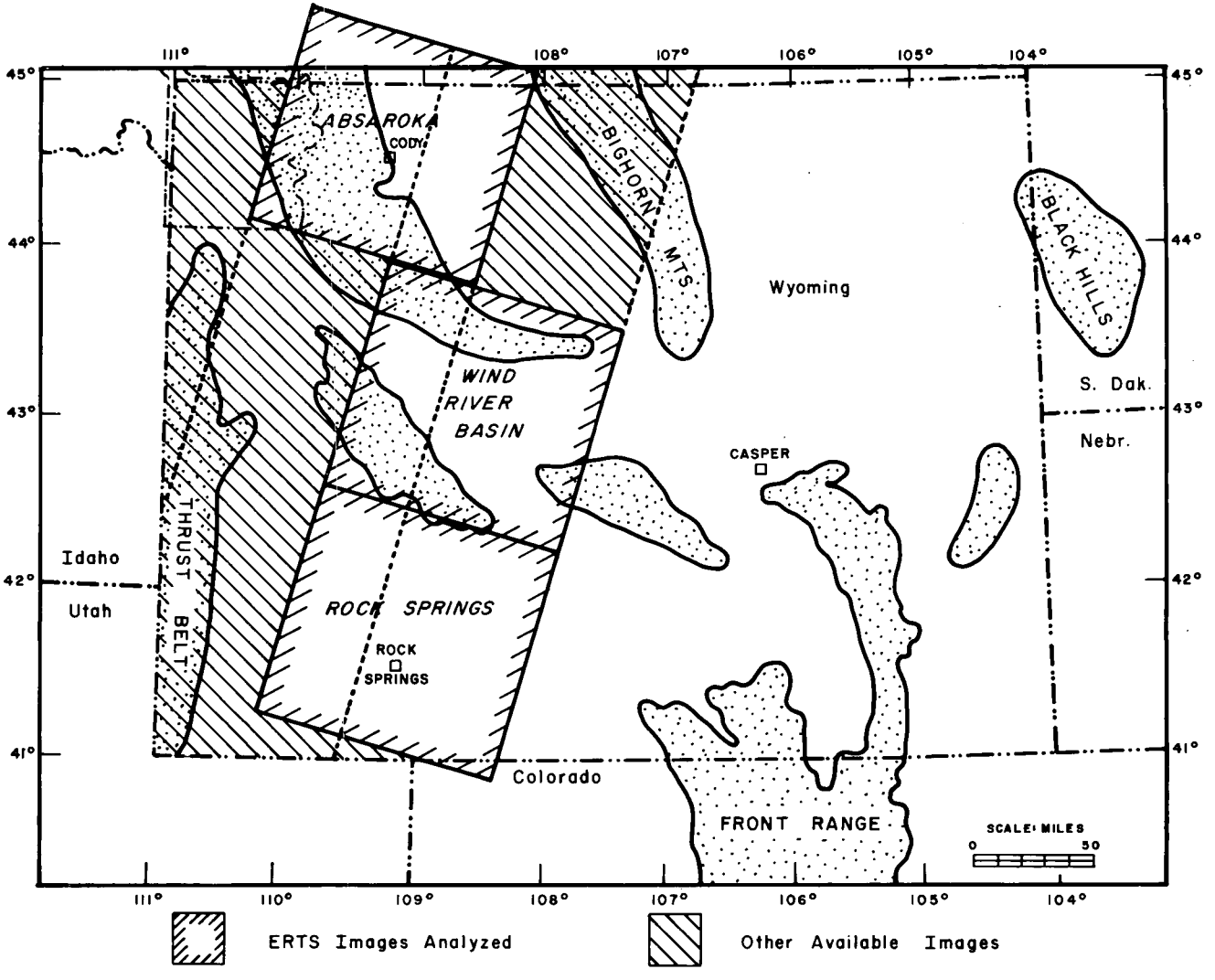

Figure VI-1a. Index map of Wyoming showing location of ERTS images.

Figure VI-1b. Photomosaic of index map area produced from six ERTS images.

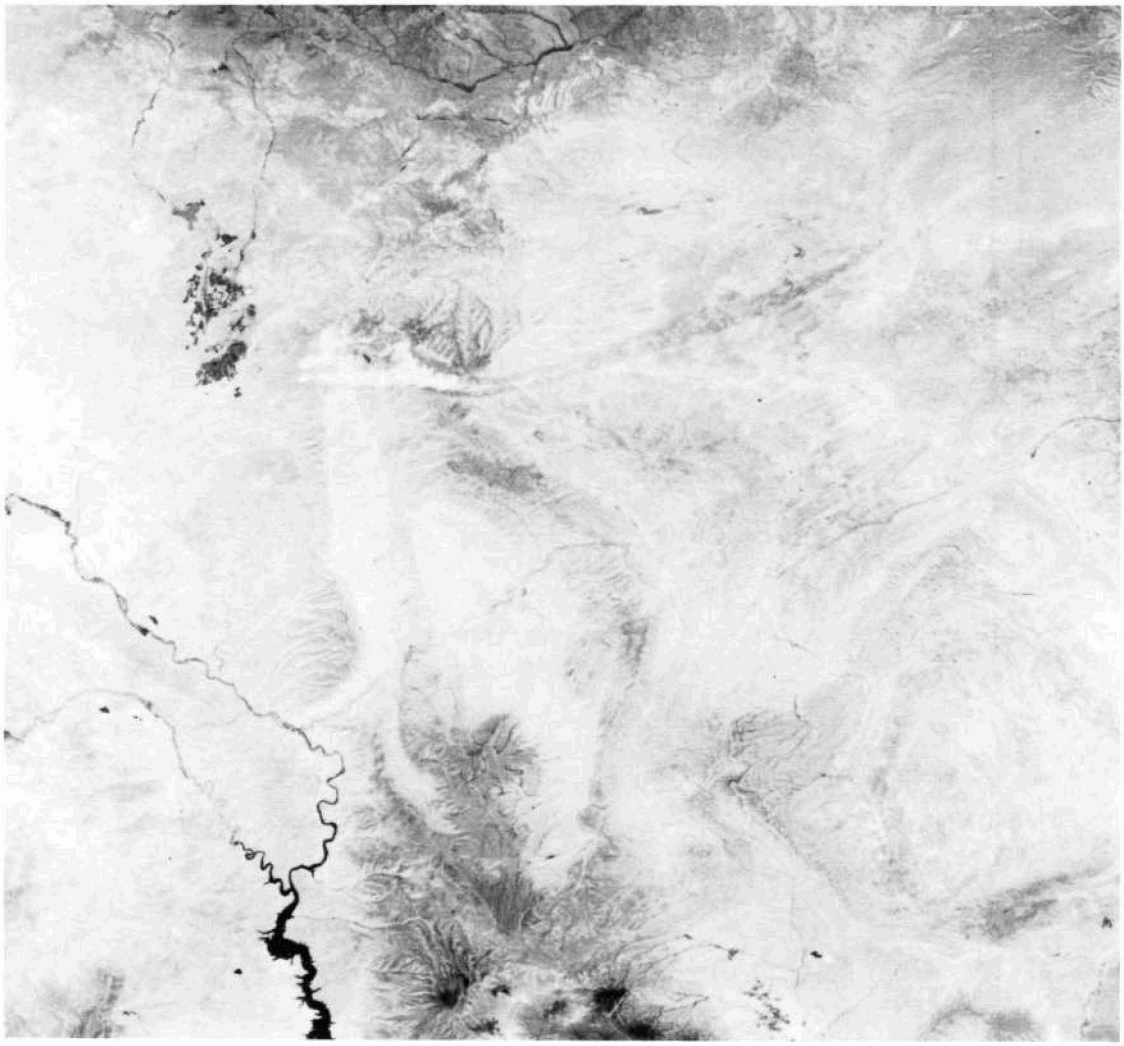

Figure VI-2. ERTS (MSS-5) image of the Rock Springs area of southwestern Wyoming.

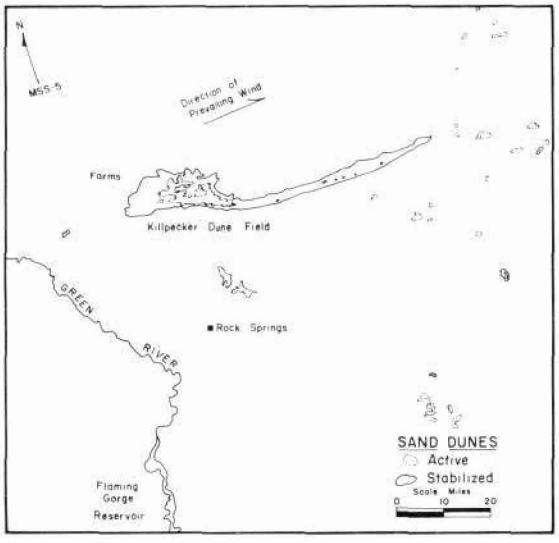

A.

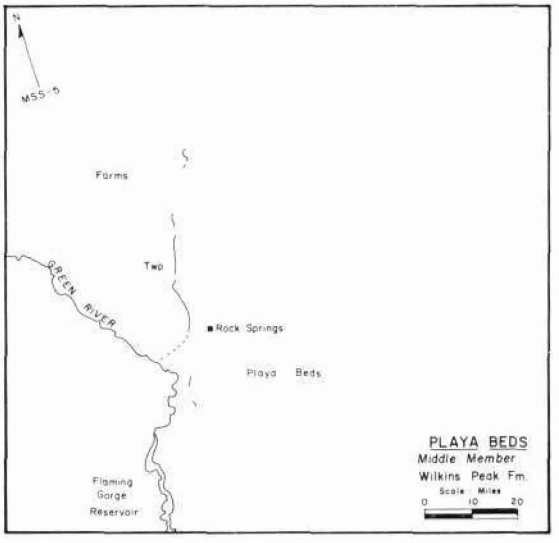

B.

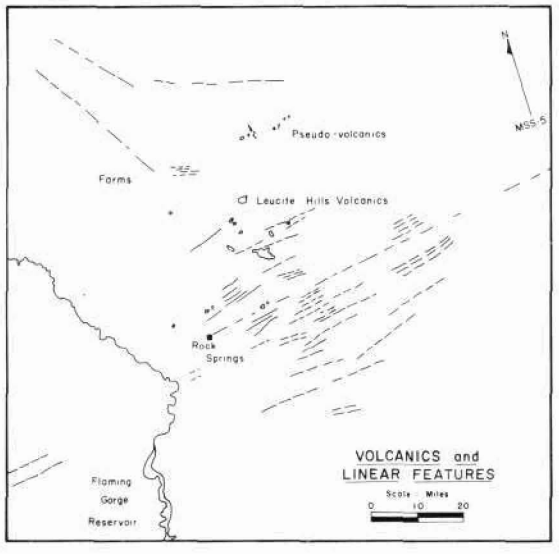

C.

D.

Figure VI-3. Geologic interpretation of Rock Springs area MSS-5 image. A. Map of major dune fields. B. Map showing outcrop limit of middle member of the Wilkins Peak Formation. C. Map of Major lineaments (faults?) and volcanic plugs and flows. D. Photograph showing middle member of Wilkins Peak Formation (Photo by R. C. Surdam)

east-west it might be possible to estimate the extent of this facies, but if we assume that it continues in the subsurface to the west of the outcrop area we might guess that the best place to prospect for trona would be near the center of the outcrop area, and, of course, the three trona mines noted previously are located approximately in this region.

Two other geologic features are well illustrated on this Rock Springs image. The beds of the uplift are interrupted by numerous east-northeast striking faults. Figure VI-3c shows a number of these faults or lineaments that can be recognized on the ERTS image. Over 50 faults or lineaments can be recognized by a cursory study of the imagery. One apparent lineament, previously unknown, can be traced for more than 60 miles into the Tertiary terrain east-northeast of the eastern edge of the uplift. Many of these lineaments have been mapped previously; more than 25 appear on the geologic map of Wyoming; (Love et al., 1955) and others have been mapped since 1955. We do not yet know how many of these lineaments are faults because they have not been field checked, nor can we be certain how many represent "new information" without an exhaustive check of the recent literature, but known faults clearly extend beyond mapped limits; and some lineaments not shown on the geologic map of Wyoming exhibit bed offset and are, indeed, faults.

Other geologic features apparent on this image are a series of small intrusives and associated lava flows known as the Leucite Hills. It is possible to map every known body in this volcanic field on the ERTS imagery; but some topographic features (small buttes underlain by rocks of Tertiary age) strongly resemble the intrusives on the images. These volcanic rocks and pseudo-volcanic rocks are shown on Figure VI-3c. If the pseudo-volcanic rocks and volcanic rocks are considered as a unit the mapping in this case has been about 50 percent accurate.

WESTERN BIGHORN BASIN – EASTERN ABSAROKA MOUNTAIN AREA

Figure VI-4 shows two major contrasting types of terrain. The western half of the area is a highland, the Absaroka Mountains, underlain by a thick succession of volcanic rocks. The volcanic flows, tuffs, and breccias that make up much of the Absaroka volcanic field are generally horizontal in attitude, and as is typical of areas of horizontally dipping geologic units this region is characterized by a dendritic drainage pattern that is shown in great detail on the ERTS image. This highland reaches an elevation of 13,153 feet locally and receives approximately 20 inches in rainfall annually whereas the basin to the east is semi-arid and receives annual rainfall of approximately 8 inches. This difference in elevation and rainfall between mountain and basin results in a layer cake distribution of vegetation. Starting at the crests of divides in the Absaroka Mountains (easily identified by noting the drainage pattern) there is an area of light tonal coloration, that is just below the snow covered peaks, which consists of bare rock and tundra; below this are spruce-pine-fir forests that show as a distinct dark layer on the image, and finally at the base of the mountains lighter tones depicting sage-grasslands that show a tonal brightening away from the foot of the mountains toward the lower rainfall parts of the basin.

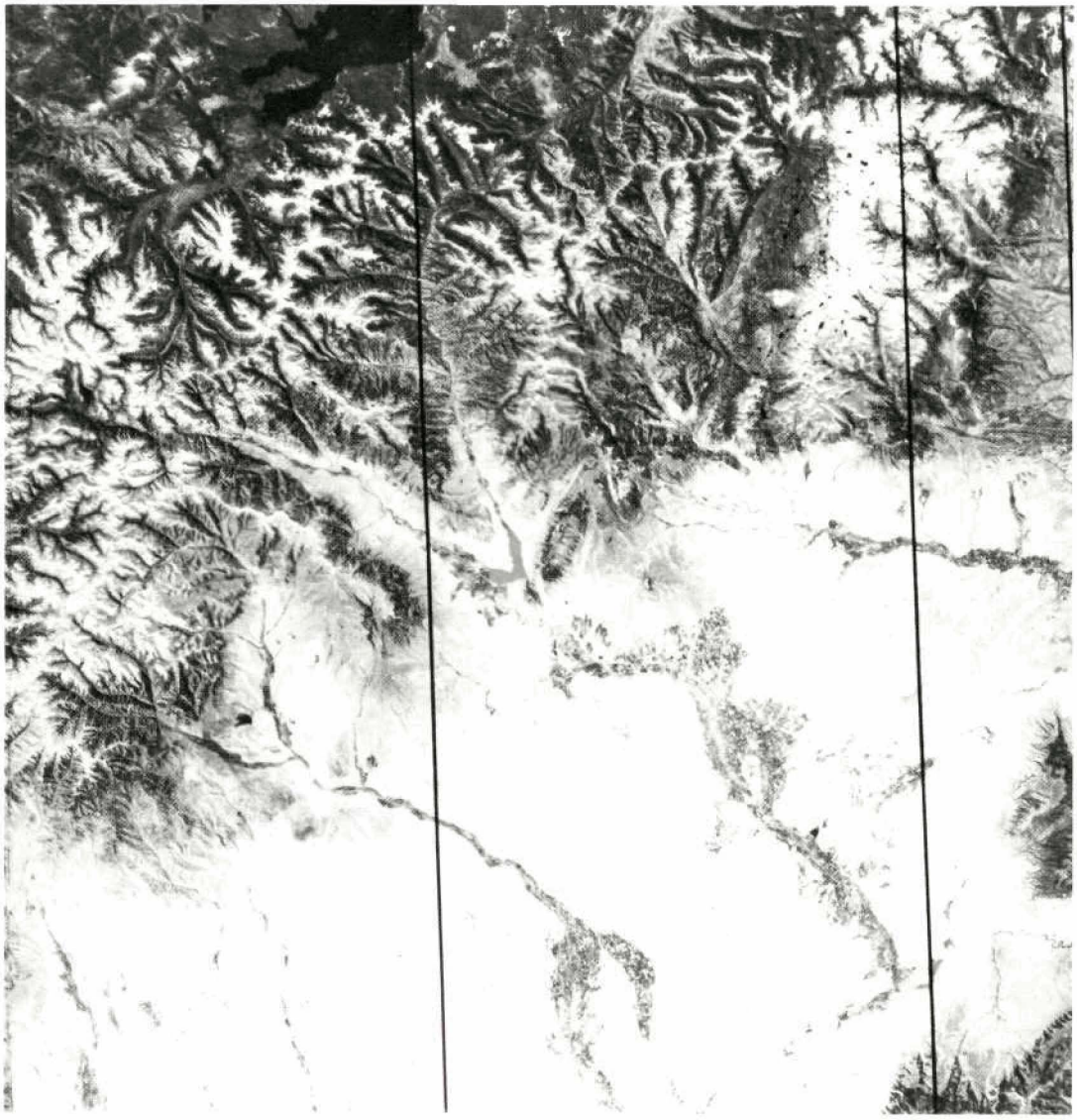

Figure VI-4. ERTS (MSS-5) image of the western Bighorn basin - eastern Absaroka Mountain area of northwestern Wyoming.

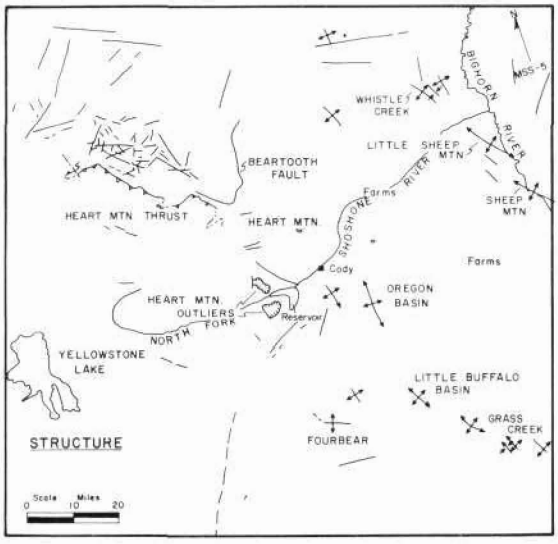

A.

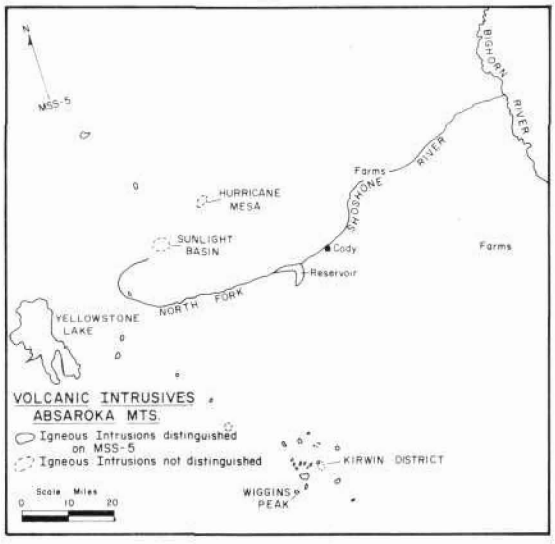

B.

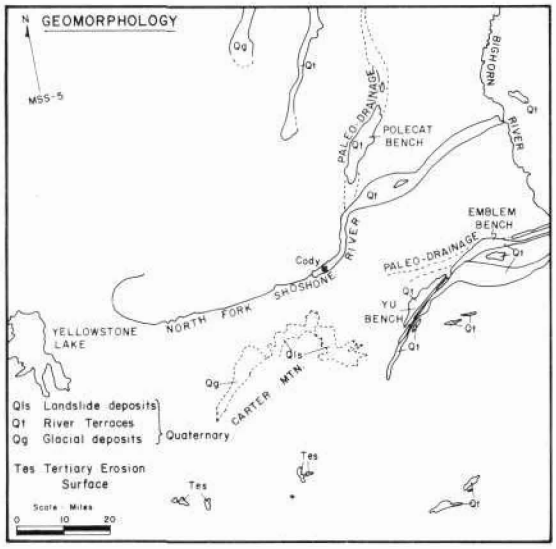

C.

D.

Figure VI-5. Geologic interpretation of western Bighorn Basin - eastern Absaroka Mountain MSS-5 image. A. Tectonic map. B. Intrusive igneous rocks. C. Major geomorphic features. D. Photograph of the Absaroka Mountains near Pickett Creek. Volcanic succession shows in foreground and background. (Photo by W. H. Wilson).

The most prominent physiographic feature of the Absaroka Mountain area is Yellowstone Lake, seen in the southwest margin of the image. The area in the vicinity of Yellowstone Lake shows a different drainage pattern and tonal contrast from much of the surrounding terrain. This plateau is lower topographically and is composed of rhyolite flows and welded tuffs that erupted from the Yellowstone caldera (Boyd, 1961, Keefer, 1971). The northeast rim of the caldera shows on the image in the area north of Yellowstone Lake as a C-shaped line facing west.

The northwest corner of this image is dominated by the Beartooth Mountains of Wyoming and Montana, which appear as a large parallelogram. The Beartooth block is an uplifted mass of Precambrian rock and is much lighter in tone than the Absaroka volcanics. The highest part is covered with snow and pitted with a myriad of glacial lakes. Again, the vertical zonation of vegetation is prominent.

The second major type of terrain shown on this image is the Bighorn Basin which is a broad syncline both structurally and topographically. The image shows roughly the western half of the basin. The basin is largely sage-grasslands that appear in shades of light gray on MSS-5. The river valleys are irrigated and three major irrigated areas can be identified in the northeast one-quarter of the image. Major cultural features in addition to the irrigated valleys are Buffalo Bill Reservoir, a butterfly-shaped body of water, in the center of the image and the Bighorn River located in the northeast corner of the image.

This image has been studied by Roy M. Breckenridge, who has been able to identify most of the major structural and geomorphic features and many but not all of the igneous intrusive bodies that cut the volcanic sequence of the Absaroka Mountains. Figure VI-5a is a tectonic map of this area. In the northwest numerous lineaments can be distinguished in the center of the Beartooth Mountains that are probably faults of Precambrian age. In addition major faults can be recognized in the sedimentary rocks north of the Precambrian-cored uplift.

The Beartooth uplift is bounded by great thrust faults and may be visualized as a wedge-shaped block of basement (Precambrian gneiss, schist, and igneous rocks) pushed up and out over the bounding sedimentary layers. In addition to the major faults at the margin of the uplift, great masses of sedimentary rock are detached from the uplifted area and have simply slid away from the mountain under the influence of gravity (Pierce, 1957). One of the major bounding faults (the Beartooth fault) is readily seen on the ERTS image and perhaps more remarkable a major part of the Heart Mountain thrust, which is a large mass of sedimentary rock detached from the uplift, can be mapped. Large blocks of sedimentary rocks (Heart Mountain and Heart Mountain outlier) that have moved in advance of the main slide block can also be distinguished. The geologist would have to be thoroughly familiar with this area or the literature of the area in order to interpret these structural features accurately, but a first order tectonic map showing major faults could certainly be made by most photogeologists from the imagery.

The Bighorn Basin, like most Wyoming structural basins, is bounded by uplifted blocks. Deformation is more intense at the margin of the basin or at the border of the uplifted

blocks where faulted anticlines and synclines are common. Virtually all of these anticlines can be mapped using the MSS-5 image, and one may note that the structures are indeed concentrated at the margin of the basin. The majority of these anticlines produce petroleum and/or natural gas.

As an example of new structural information from this image a west-northwest striking lineament north of Whistle Creek anticline (northern border of Figure VI-5a) shows apparent offset of sedimentary units and must be a fault. To our knowledge this fault has not been previously mapped.

The volcanic flows, tuffs, and breccias of the Absaroka Mountains are cut by numerous igneous intrusions, shown in Figure VI-5b. Some of these intrusive bodies are mineralized (Wilson, 1964) and are in many respects like the porphyry copper deposits of the southwestern United States. Within the area of the image there are at least forty-four of these intrusive bodies. Breckenridge was able to map twenty-four of the intrusives, shown in solid line on the figure, but none of the mineralized intrusions, shown in dashed line, could be recognized.

Perhaps the most interesting geologic features noted on this image are geomorphic. It is possible to recognize pediment surfaces, terrace deposits, high level erosion surfaces, landslide deposits, and, of course, alluvium. These are shown on Figure VI-5c, and the most striking are the pediment surfaces and their general relationship to terrace deposits of modern rivers. This part of the Bighorn Basin was studied in the 1940's by J. Hoover Mackin (1947), who made a classic interpretation of the origin of the pediment surfaces of the area. Two prominent pediment surfaces are in the northern Bighorn Basin; these are gravel and boulder covered surfaces of low relief referred to as Polecat Bench, Yu Bench, and Emblem Bench. On the ERTS image these show as dark elongate areas. The dark color may be a feature of the vegetation, in part, but is certainly geologic in part, because the gravel and boulders are dark colored mafic volcanic rocks from the Absaroka Mountains. Mackin interpreted these surfaces as old river terraces that were captured by the modern tributaries of the Bighorn River. The capture of the old drainage by the new is clearly shown on the ERTS image and is depicted on Figure VI-5c.

WESTERN WIND RIVER BASIN

The final ERTS image (Figure VI-6) that we will discuss is one that covers most of the Wind River Basin of central Wyoming. The Wind River Basin is like the Bighorn Basin in that it is both a structural downwarp and a topographically low area. This basin has major uplifted areas along its margin.

The uplifted areas are, as follows:

1. The Wind River Range shows as the dark shaded partly forested mass in the southwest corner of the image. The Wind River Range is elliptical in form and has a great series of northeast-dipping hogbacks on the northeast flank that show clearly on the image. The figure also shows the central and southeastern part of the Wind River Range.

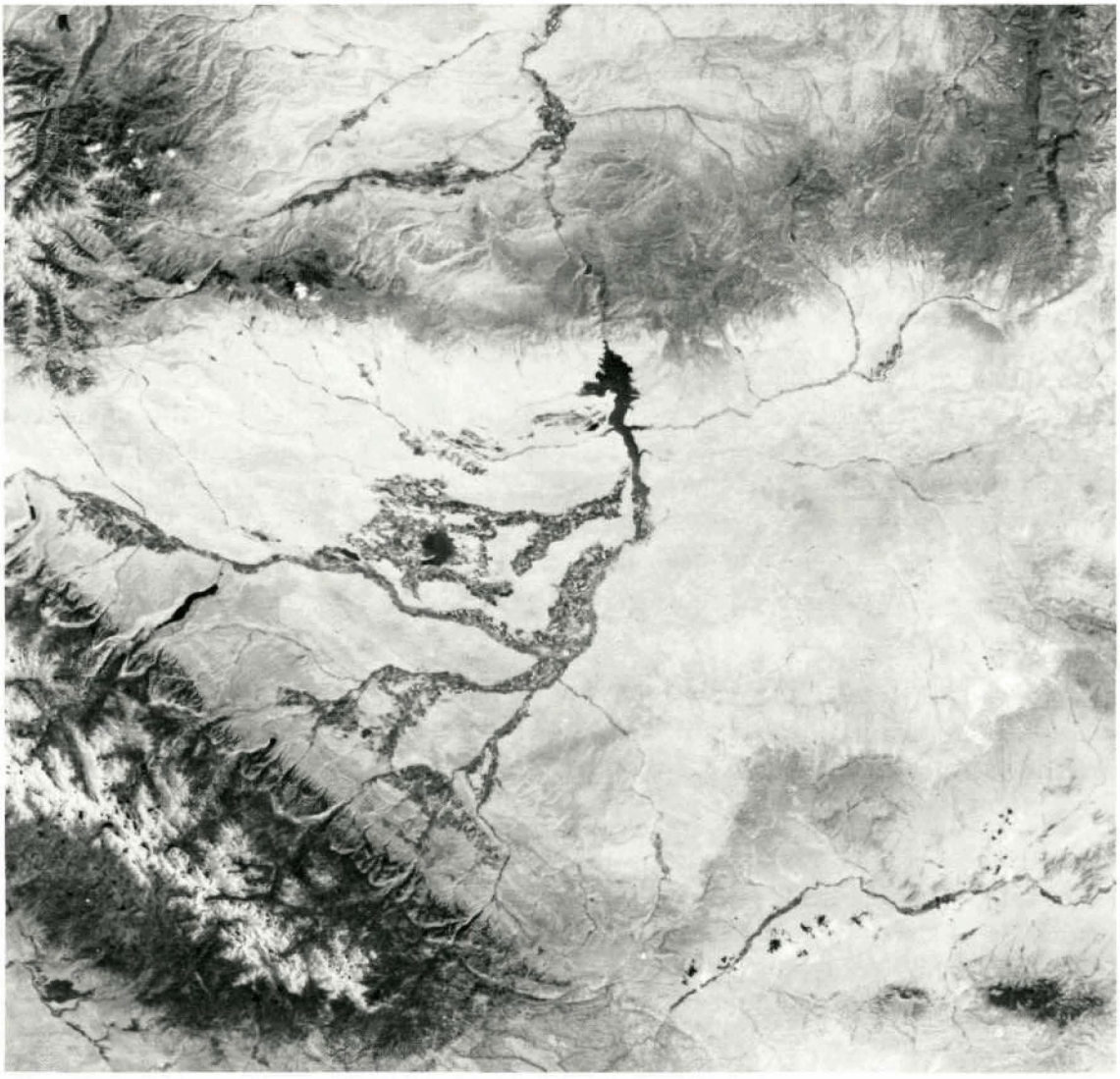

Figure VI-6. ERTS (MSS-5) image of the western Wind River Basin of central Wyoming.

2. The Granite Mountains that show in the southeastern portion of the image north of the Sweetwater River (note a few cumuliform clouds along the river). The Granite Mountains are part of a once great range, like the Wind River Range, that collapsed and was then covered with sedimentary rocks of Tertiary age. The Granite Mountains are irregular isolated highlands of Precambrian rocks that protrude through the dark toned rocks of Tertiary age.
3. The southern Bighorn Mountains that show in the northeast corner of the image as an area of dark tone.
4. The Owl Creek Mountains that are a dark toned area in the north-central part of the image.
5. The southeastern extension of the Absaroka Mountains that show in the northwest part of the image and appear much as they did on the image (Figure VI-4) discussed above.

Major cultural features of this image are two large reservoirs: Boysen Reservoir in the center of the image and Ocean Lake in the west center of the image. Irrigated farmland along the Wind River and its tributaries shows in the center of the image and in the north center of the image. The Wind River cuts a deep canyon north of Boysen Reservoir through the uplifted core of Precambrian rocks of the Owl Creek Mountains. The irrigated valley on the north side of the canyon is actually along the Bighorn River because the name of the river changes from Wind to Bighorn when it enters the Bighorn Basin shown at the north border of this image.

Perhaps the most striking cultural features of this image are the open pit uranium mines and adjacent tailing piles that show as irregular white areas in the east center of the image. These mines are in the Gas Hills Uranium District of Wyoming.

Major vegetation patterns of this basin and adjacent uplifted areas are like those of the Bighorn Basin-Absaroka Mountain area with a dark mantle of spruce-fir-pine forest in the Wind River and Absaroka Mountains separating the sage-grasslands of the basin from the tundra-bare rock areas above timberline. An interesting feature of the vegetation pattern shown by this image is the absence of extensive forests in the Owl Creek, southern Bighorn and Granite Mountains. This is an elevation-rainfall effect in that these uplifts are at lower elevations and thus have less rainfall than the Wind River Mountains, for example, but are higher and receive more rainfall than the Wind River Basin proper. They therefore support a denser vegetative cover and are darker in tone than the Wind River Basin, but do not have adequate rainfall to support the relatively dense forests typical of the Wind River and Absaroka Mountains. This climatic control of vegetation masks to some degree the bedrock geology and clearly more accurate mapping of rock types is possible in the Wind River Basin where rainfall is 8-9 inches annually.

We will report briefly on three geologic studies made of the area covered in this image. Rocks of Precambrian age make up about ten percent of the total exposed rocks in Wyoming. In

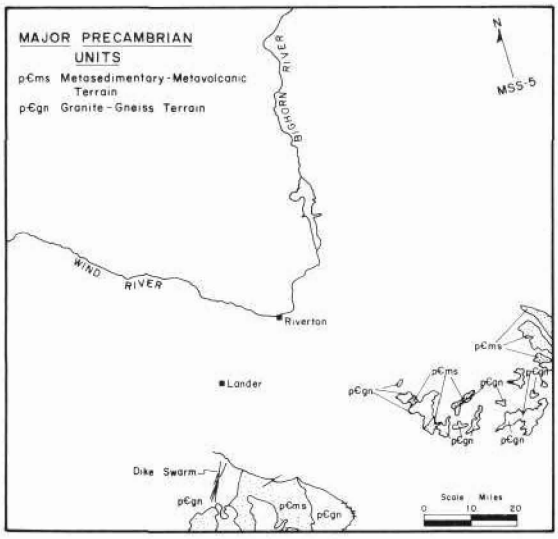

A.

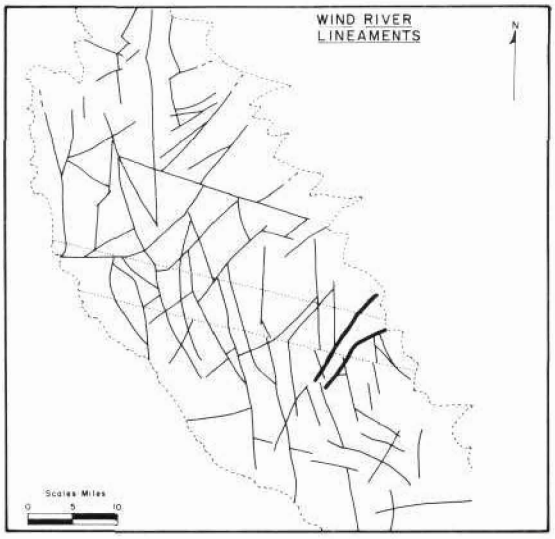

B.

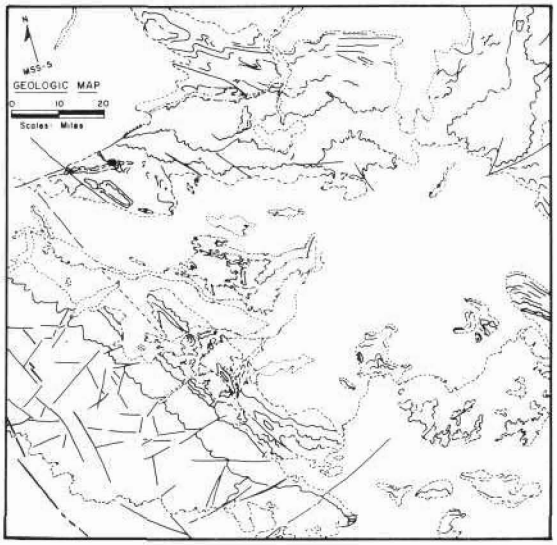

C.

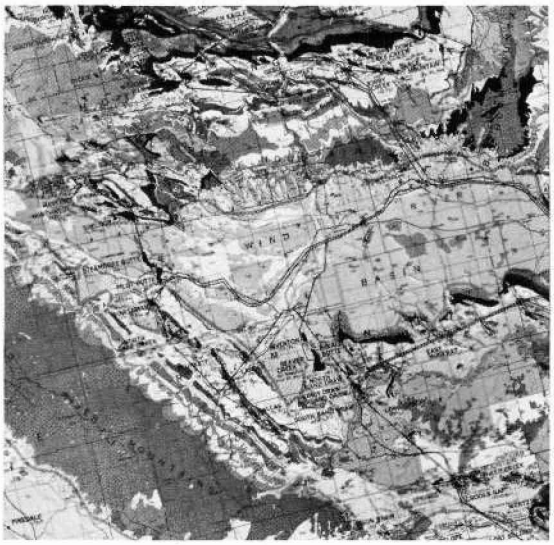

D.

Figure VI-7. Geologic interpretation of Wind River Basin MSS-5 image. A. Map showing distinction made between Precambrian granite-gneiss and metasedimentary-metavolcanic rock terrains. B. Major fractures of the Wind River Mountains as recognized by aircraft-field studies (within dotted line) and from ERTS. C. Geologic map showing contacts, faults, and unconformities recognized on MSS-5 image. D. Geologic map of same area as in C (Geologic map of Wyoming, Love and others, 1955).

much of this area the rocks of Precambrian age have not been mapped. In general, the Precambrian rocks of Wyoming may be subdivided into two major terrains, granite-gneiss terrain and metasedimentary-metavolcanic terrain. Most of the mineral deposits in the Precambrian rocks are in the metasedimentary-metavolcanic terrain so it is economically desirable to distinguish these terrains.

Precambrian rocks are exposed in the Owl Creek, southern Bighorn, Wind River, and Granite Mountains of this image. Vegetative cover in the Owl Creek and southern Bighorn Mountains along with an apparent lack of tonal contrast between Precambrian and Lower Cambrian rocks makes distinctions in Precambrian terrain difficult. Most of the northern and western Wind River Mountains are heavily timbered or snow covered, but the southeastern part of the Wind River Mountains and much of the Granite Mountains show tonal contrasts that are probably a reflection of bedrock. Figure VI-7a is a map prepared of this area that shows the major terrain-subdivisions. Adequate ground truth (Bayley, 1965a-1965d; Bell, 1955) is available for the southeastern Wind River Mountains to verify that this is a good regional distinction in Precambrian terrains. In the Granite Mountains there is inadequate ground truth to check the interpretation, but the three-prong body shown as metasedimentary-metavolcanic terrain in the northeastern part of the Granite Mountains is known to contain some granite gneiss terrain and several igneous intrusives of Tertiary age so the distinction is obviously not fully satisfactory in this area.

A second geologic study is that of fracture systems in the rocks of Precambrian age. A number of studies of fractures in rocks of Precambrian age (Hoppin, 1961; Prucha and others, 1965; Houston and others, 1968) have been made in recent years in Wyoming to try to solve, for example, such geologically significant problems as the relationship between fractures in the Precambrian basement and fractures and other structures in the younger rocks of the basins. Most of this work has been done in small areas along the flanks of the mountains and it has not been generally possible to look at the fractures on a regional basis.

R. B. Parker has begun a study of the fracture system of the entire Wind River Mountains using aircraft images, field checks, and ERTS MSS-5. This study will be reported in some detail in a paper in preparation by Parker, but Figure VI-7b compares a series of major fractures mapped by use of aircraft images and checked in August and September, 1972 in the field. All major fractures recognized by aircraft and ground studies can be mapped using the ERTS image and it is clear that these images will be of great value in mapping regional fractures in terrain of this sort.

The final geologic study is an attempt to see what portion of the regional geology of an area such as the Wind River Basin can be mapped in a short time using ERTS imagery alone. This map (Figure VI-7c) was made by simply mapping major contacts, faults, and unconformities and was made without reference to the geologic literature by a geologist with a good knowledge of the regional geology of the area. If the geologic form map (Figure VI-7c) is compared with the same area on the geologic map of Wyoming (Figure VI-7d), the reader may note that the ERTS interpretation is a reasonably accurate representation of the geology

of the area. The most serious errors are in the Granite, Owl Creek and southern Bighorn areas where vegetation masks geologic contacts.

COMPARISON OF ERTS AND U-2 IMAGERY

The ERTS image (Figure VI-6) showing most of the western Wind River Basin also covers much of the same region overflown on October 21, 1971. Some 50 individual photo frames from this flight have been combined in the photomosaic reproduced as Figure VI-8. Although the resolution in this U-2 mosaic is superior by at least a factor of three, the variations in surface lighting imposed by the one hour needed to obtain the photos and by vignetting within the photos themselves lead to a product which does not give as "clean" a synoptic view as the single ERTS image.

It is instructive to compare individual U-2 red band frames from this flight with the equivalent areas (about 16 statute miles on a side or 250 square miles) as imaged in the ERTS MSS-5 band (Figure VI-9). Figures VI-9a and VI-9b show a portion of the southern Wind River Mountains around Atlantic City south of Lander. Almost without exception, all major surface features (see caption) visible in the U-2 frame can be discerned with equal facility in the ERTS view enlarged to approximately the same scale. This holds true also for the two scenes in Figures VI-9c and VI-9d in which the Beaver Divide, the Conant Creek anticline, and drainage and topographic features in the Tertiary surface to the north, some 20 miles southeast of Riverton, are displayed.

The ERTS view (Figure VI-9c) of the Hoback Range west of Big Piney in the westernmost part of the state is actually more informative than that obtained by the U-2 (Figure VI-9f) as it moved into Wyoming prior to making its run over the Wind River Basin. At the time of this flight, snow had blanketed part of these folded sedimentary rocks in the thrust belt. Both the ERTS and U-2 images appear to delineate the major stratigraphic units to a similar extent.

In all three comparison pairings, the principal structural and geomorphic features can be distinguished to about the same extent in either the ERTS or U-2 scenes. Thus it is concluded that the synoptic capability of ERTS images can be favorably compared with the higher resolution U-2 photos even when the initial products are at notably different scales.

SUMMARY

This first look at Wyoming ERTS imagery is most encouraging from the viewpoint of its value as a tool in photogeologic interpretations. The resolution is adequate for regional geologic mapping, and the images are therefore useful for a variety of scientific and economic studies. In the short time devoted to this study we have new information on the geology of all areas studied, and it is clear that the use of this type of image will save time and thus money in any regional study using photogeologic techniques.

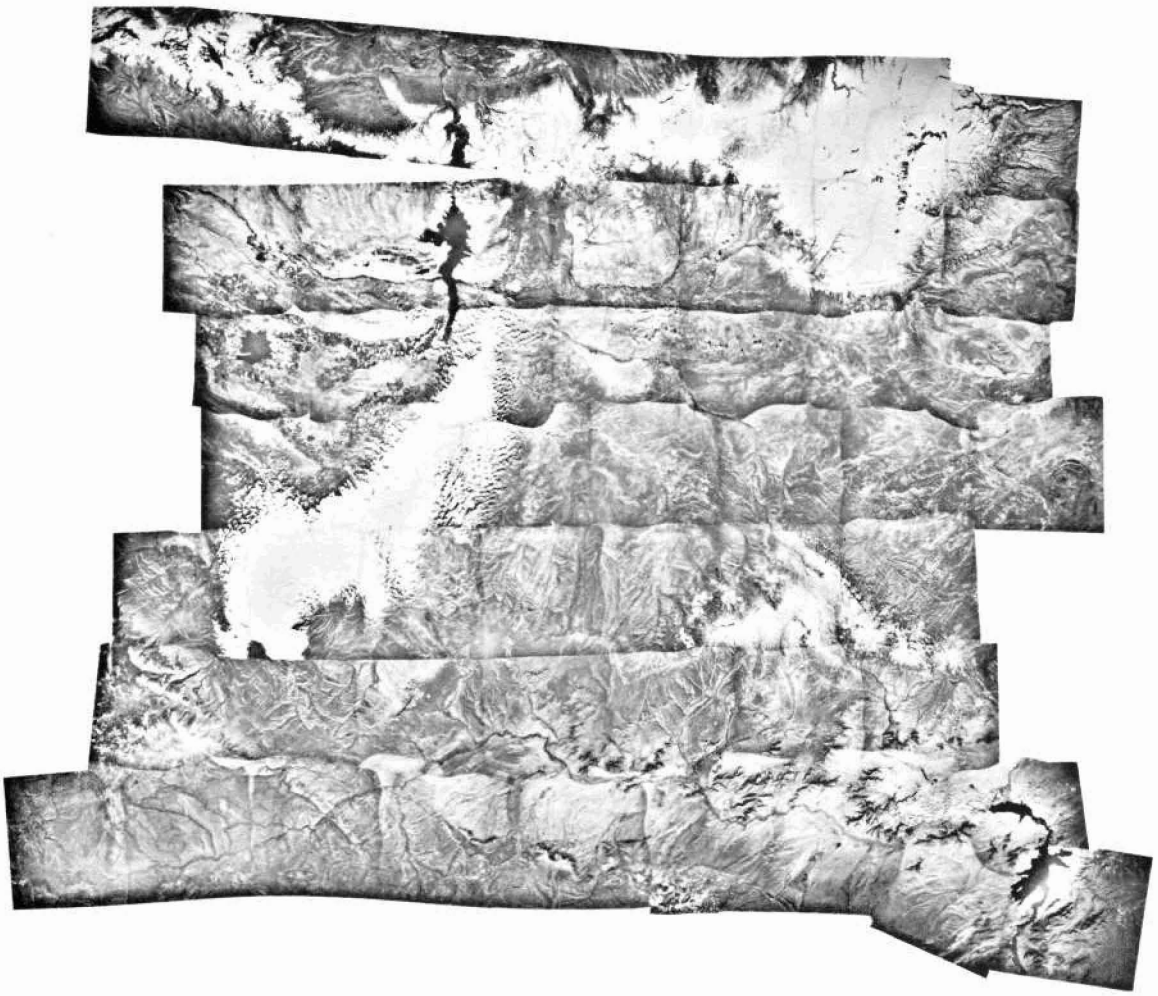

Figure VI-8. Composite mosaic of part of the Wind River Basin (see Figure VI-7d for geological map which includes this scene: Use Ocean Lake as a reference) made from 54 individual photo frames obtained by the red band Vinten camera on the NASA U-2 flight of October 21, 1971. Compare with Figure VI-6.

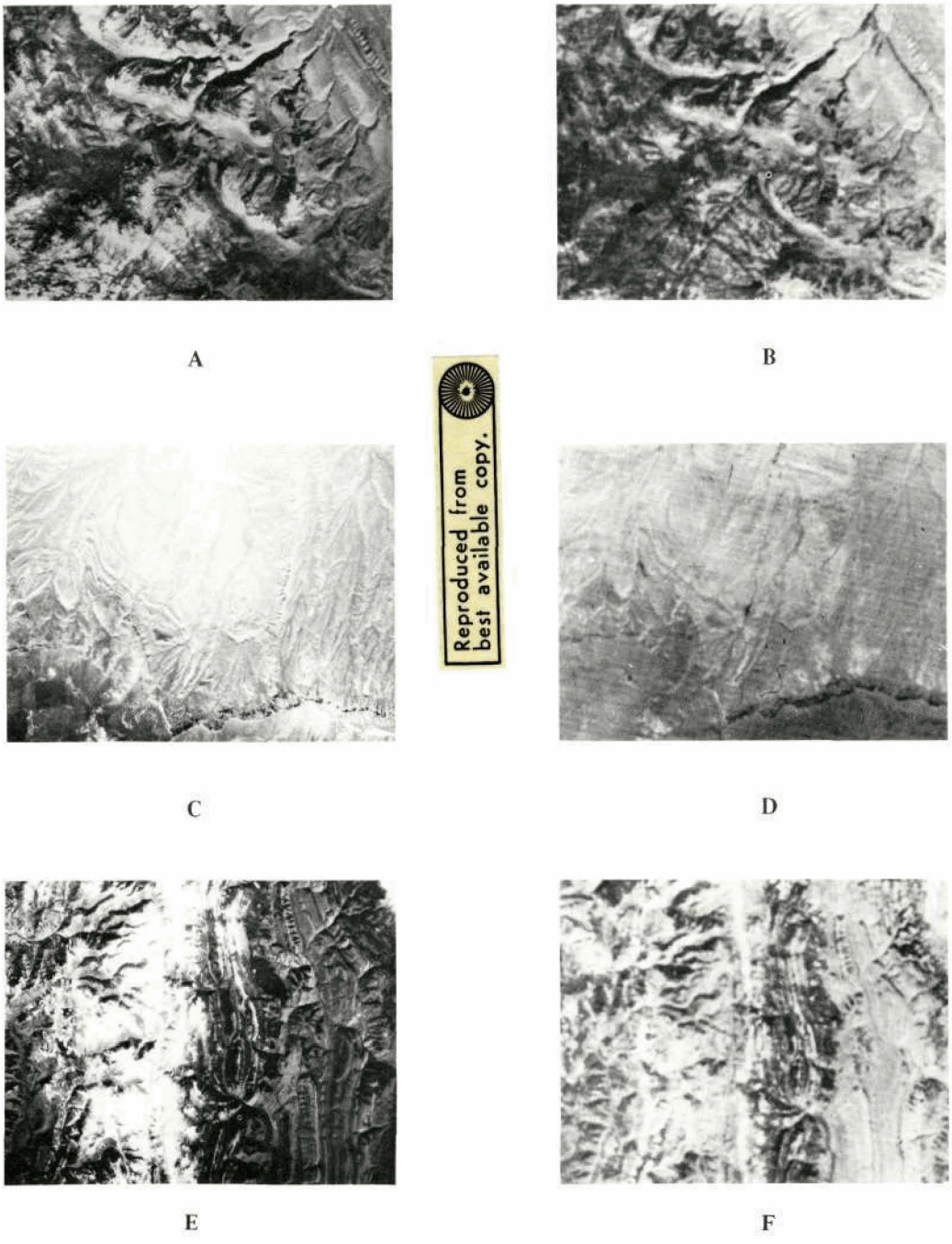

Figure VI-9. Portion of ERTS red band frame (see Figure VI-6) showing area equivalent to that in (a) and (c). U-2 frame (red band) imaging (a) the Beaver Divide (near and subparallel to bottom of photo), (b) the Conant Creek anticlinal structure (near center left), and (c) the dissected Tertiary sedimentary units (upper half of photo) in the Wind River Basin south of Riverton, Wyoming, (d) Area of (c) as seen in ERTS red band frame (see Figure VI-6). (e) U-2 frame (red band) showing part of the folded Paleozoic-Messozoic sequence in the Hoback Range of western Wyoming, west of Big Piney and east of the Idaho border. (f) Equivalent view of area appearing in (e) as extracted from an ERTS red band frame (see Figure VI-1b)

REFERENCES

Bayley, R. W., 1965a, Geologic map of the South Pass City quadrangle, Fremont County, Wyoming: U.S. Geol. Survey Map GQ-458.

Bayley, R. W., 1965b, Geologic map of the Atlantic City Quadrangle, Fremont County, Wyoming: U.S. Geol. Survey Map GQ-459.

Bayley, R. W., 1965c, Geologic map of the Miners Delight Quadrangle, Fremont County, Wyoming: U.S. Geol. Survey Map GQ-460.

Bayley, R. W., 1965d, Geologic map of the Louis Lake Quadrangle, Fremont County, Wyoming: U.S. Geol. Survey Map GQ-461.

Bell, Wallace, 1955, Geology of the southeastern flank of the Wind River Mountains, Fremont County, Wyoming: unpublished Ph.D. thesis, University of Wyoming, Laramie, 204 p.

Boyd, F. R., 1961, Welded tuffs and flows in the rhyolite plateau of Yellowstone Park, Wyoming: Geol. Soc. Am. Bull., vol. 72, no. 3, p. 387-426.

Eugster, H. P., and Surdam, R. C., 1972, Depositional environment of the Green River Formation, Wyoming: Field trip guidebook, Rocky Mtn. Sec. Geol. Soc. America, Laramie, Wyoming, 11 p.

Hoppin, R. A., 1961, Precambrian rocks and their relationship to Laramide structure along the east flank of the Bighorn Mountains near Buffalo, Wyoming: Geol. Soc. America Bull., vol. 74, p. 197-202.

Houston, Robert S., and others, 1968, A regional study of rocks of Precambrian age in that part of the Medicine Bow Mountains lying in southeastern Wyoming -- with a chapter on the relationship between Precambrian and Laramide structure: Wyoming Geological Survey Memoir 1, p. 147-161.

Keefer, W. R., 1971, The geologic story of Yellowstone National Park: U.S. Geol. Survey Bull. 1347, p. 34-52.

Love, J. D., Weitz, J. L., and Hose, R. K., 1955, Geologic map of Wyoming: U.S. Geol. Survey.

Mackin, J. H., 1947, Altitude and local relief of the Bighorn area during the Cenozoic: in Wyo. Geological Assoc. Guidebook, 1st Annual Field Trip, p. 103-120.

Pierce, W. G., 1957, Heart Mountain and South Fork detachment thrusts of Wyoming: Am. Assoc. Petrol. Geol. Bull., vol. 41, no. 4, p. 591-626.

Prucha, John J., Graham, John A., and Nickelsen, Richard P., 1965, Basement controlled deformation in Wyoming Province of the Rocky Mountain foreland: Am. Assoc. Petroleum Geologists Bull., vol. 49, p. 966-992.

Wilson, W. H., 1964, The Kirwin mineralized area, Park County, Wyoming: Geol. Survey of Wyoming Prelimin. Rept. No. 2, 12 p.

GEOLOGIC QUESTIONS AND SIGNIFICANT RESULTS PROVIDED BY EARLY ERTS-1 DATA

W. D. Carter
EROS Program
U. S. Geological Survey

INTRODUCTION

The U.S. Department of the Interior presently has 45 experiments involving over 150 people underway and jointly supported by NASA and the EROS Program to evaluate the uses of Earth Resources Technology Satellite (ERTS-1) data of the United States and selected foreign areas. These studies are in the fields of cartography, land use and management, geology, hydrology, forestry and range management. Our NASA/EROS supported scientists have just begun to receive their satellite data from Goddard Space Flight Center and we are confident that more detailed scientific analyses and results will soon be forthcoming.

We have also established a system to review data as it becomes available and distribute it to regional Department of the Interior experts who are not yet involved in the space program. The purpose is to solicit their assistance and knowledge of local areas in the interpretation of features seen on satellite images but not recorded on available maps. While the system has not yet been perfected, we are beginning to get some return on this effort.

First, we are bringing to the attention of our people the fact that ERTS-1 is in operation and bringing back excellent data. All recipients have been impressed by the synoptic view these data provide, the better-than-anticipated resolution, the spectral response of the individual bands and the overall information content that are contained therein. We have been flooded with requests from within the agency and without as to how people can get more data. In Sioux Falls, S.D., our EROS Data Center is working overtime to supply these requests.

I would like to take this opportunity to briefly describe some highlights of the information we have extracted from data collected during the first two weeks after ERTS-1 was launched on July 23, 1972.

EAST COAST AREA

ERTS-1 images of the Boston-Cape Cod Region have clearly shown the intricate bottom topography of the ocean between Woodshole and Marthas Vineyard in Band 5 (red) where the sea bottom at depths in excess of 70 feet is clearly visible (see E. Yost's paper for New England images). These features, however, are masked out in color composites of the same

area, but the land features are enhanced (see R.B. Simpson's paper for New England color composite).*

Comparisons with aerial photography taken within the last few years show that changes in ocean bottom features have taken place. Some of these changes constitute navigational hazards not shown on existing hydrographic charts. It is believed that ERTS data can provide information useful in updating such charts as well as inventorying near-shore resources, such as sand, gravel and aquatic food sources.

A color composite of the Gainesville, Florida area shows the verdant vegetation of river valleys and swamps as pink (not shown). The drier areas, where water table is low, are shown as yellow to orange in color, perhaps indicating that vegetation is dry or burned out by the late summer sun. This interpretation has not yet been verified in the field. These observations indicate that ERTS-1 data, recording the distribution of verdant vegetation throughout the seasons of the year, can be used as a guide for ground water exploration. Our local Water Resources Division geologists state that the two bright or highly reflective areas in the northeast quadrant of the scene are strip mining operations where titanium ores are being mined. ERTS-1 data can, therefore, assist in locating and monitoring the extent of mine operations and, possibly, provide information on the effects of strip mining activities.

CENTRAL U.S. AREAS

This scene of the Texas/Oklahoma area of the Ouachita Mountains is significant in that it contains two test sites that have been worked on for several years by USDI scientists (Figure VII-1/VII-2). One is a geological test site at Mill Creek, Oklahoma, in the Arbuckle Mountains in the northwest quadrant. The other is Lake Texoma, a large reservoir in the southern half that is of interest to the Bureaus of Reclamation and Outdoor Recreation.

The most striking feature in the scene are the folded sedimentary rocks of Paleozoic age that crop out in the Ouachita Mountains. The ERTS-1 infrared bands (5 and 6) mark the contact between the Cretaceous and younger sedimentary rocks of the coastal plain on the south and their contact with the older rocks to the north. In addition, these bands indicate the distribution of the younger sedimentary rock of the Mississippi Embayment to the south.

WESTERN MOUNTAIN AREAS

The Pyramid Lake and Reno, Nevada area on early ERTS-1 imagery shows a circular feature that is 25 miles in diameter (Figure VII-3). Although it needs to be studied in greater detail, our scientists in the area suggest that it is a resurgent caldera; that is, an old volcanic extrusive center that has uplifted and/or collapsed, or an eroded dome. Tertiary igneous rocks within the circle are overlain by younger sedimentary gravels and sandstones that are warped and

* Perhaps some experimentation in color reproduction could be done to ensure that such information is not lost.

Figure VII-1. Lake Texoma-Ouachita Mountains area of Oklahoma and Texas. MSS Band 5.

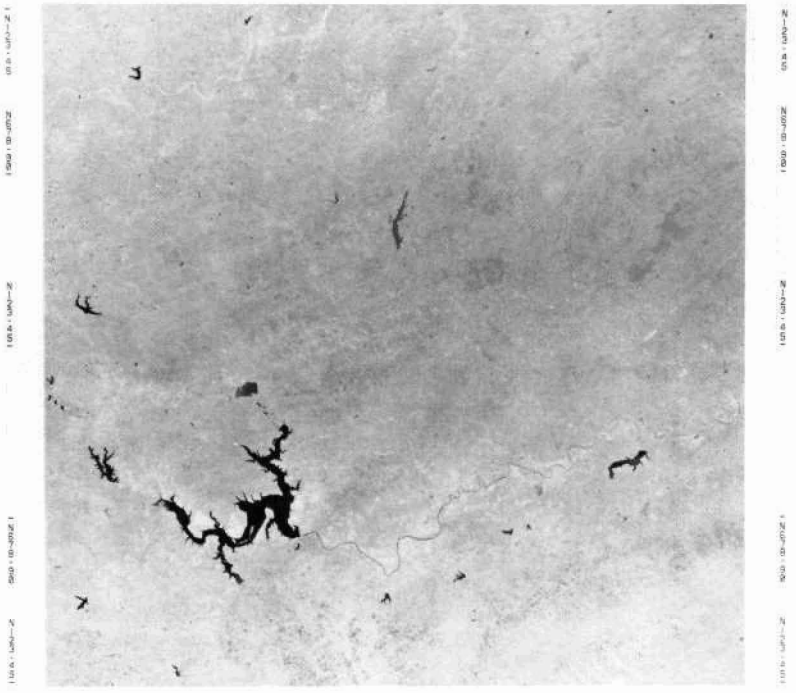

Figure VII-2. Same area as Figure VII-1. MSS Band 6.

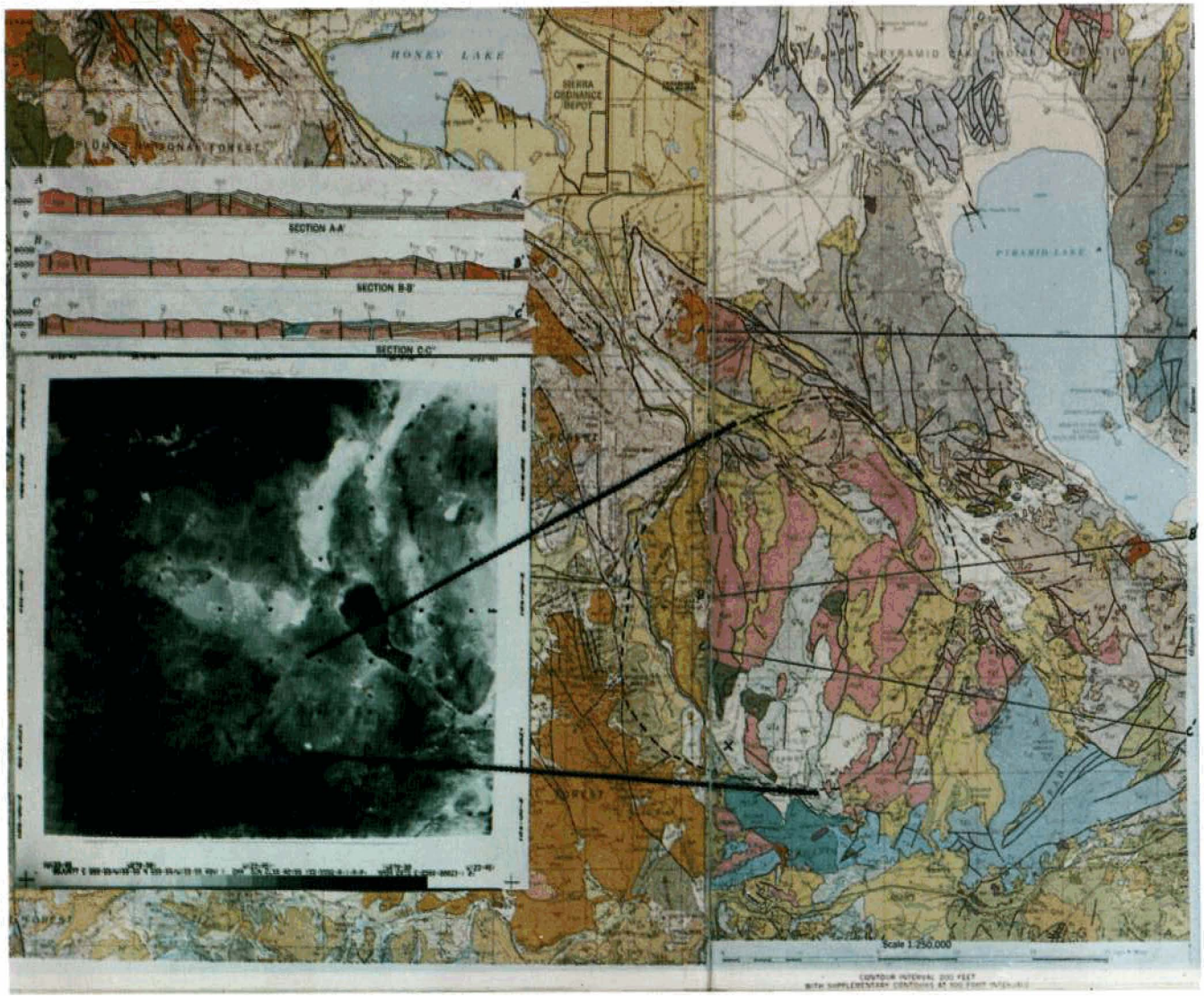

Figure VII-3. ERTS-1 RBV image of the Pyamid Lake area in Nevada, correlated with a geologic map.

titled due to later movement. Hot springs are located in the southeastern part of the circle. Recognition of the feature as a single structural unit is new, for it is not shown on existing maps of the area. It may be important in future studies of the distribution of mineral deposits or geothermal power sources of that region.

It is also interesting to note that in the color composite of this scene at the south end of Pyramid Lake, there is noticeable vegetation or possibly an algae bloom which may be related to pollution coming downstream from the Reno area (Figure VII-4). Comparison with previous maps shows that the lake area has shrunk because of withdrawals from the Truckee River by California and Nevada. The Justice Department filed a suit on September 27, 1972, with the U.S. Supreme Court against California and Nevada on behalf of the Paiute Indians to raise the lake and thereby restore the yield of fish from the Paiute ancestral fishing grounds, their primary livelihood (Treaty 1859).

The scene of Mt. Hood and Portland, Oregon provides a view of the Cascade Range from the Columbia River to the south (Figure VII-5). Several circular and linear features have been identified that are not shown on recent geologic maps of the area. A small circle, about thirty miles due east of the town of Albany, has been identified as Mt. Snow, a relatively recent volcanic cone superimposed on an older volcanic pile. The circle surrounding Detroit Reservoir is related to an intrusive stock which may have uplifted the area into a dome (G. Walker, personal communication). The others, at present, are unexplained but could be domes or calderas somewhat similar to Crater Lake about 100 miles to the southeast. Our preliminary interpretations have been sent to our scientists in Menlo Park, California, and to the Research Center of Volcanology in Eugene, Oregon, for comment. The recognition of such features could be important to our current studies of geothermal resources and in unraveling the geologic history of the Cascade Range.

WEST COAST AREAS

A preliminary analysis of the San Francisco Bay and adjacent central Great Valley area by Ernest Lathram shows three examples of geologic applications in the study of earth resources from space (Figure VII-6). These are:

- Identification of known faults and linears that may be unsuspected faults.
- Recognition of relation of vegetation growth to underlying materials.
- Recognition of ultramafic rock bodies with which minerals of economic value are commonly associated.

Faults

- The trace of the northwest trending active San Andreas, Hayward and Calaveras faults can be clearly seen southeast of the Bay.
- Northwest of the Bay, four nearly north-trending linears, expressed not only in topography but also in abrupt changes in vegetation growth in flatlands adjacent to the

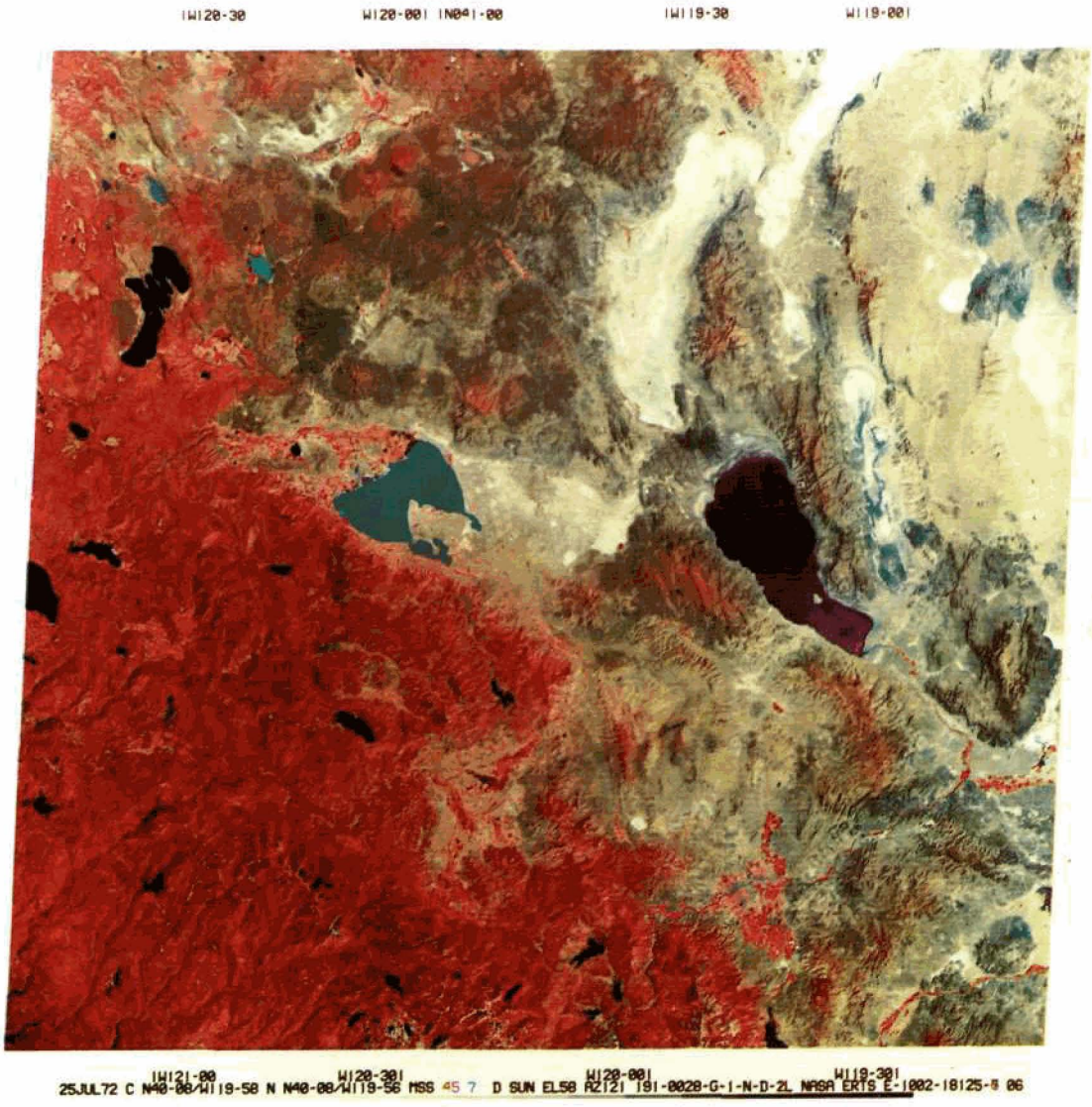

Figure VII-4. ERTS-1 color composite of Pyramid Lake, Nevada.

ERTS-1 IMAGE OF THE
PORTLAND, OREGON AREA
MSS-6 28 JULY 1972

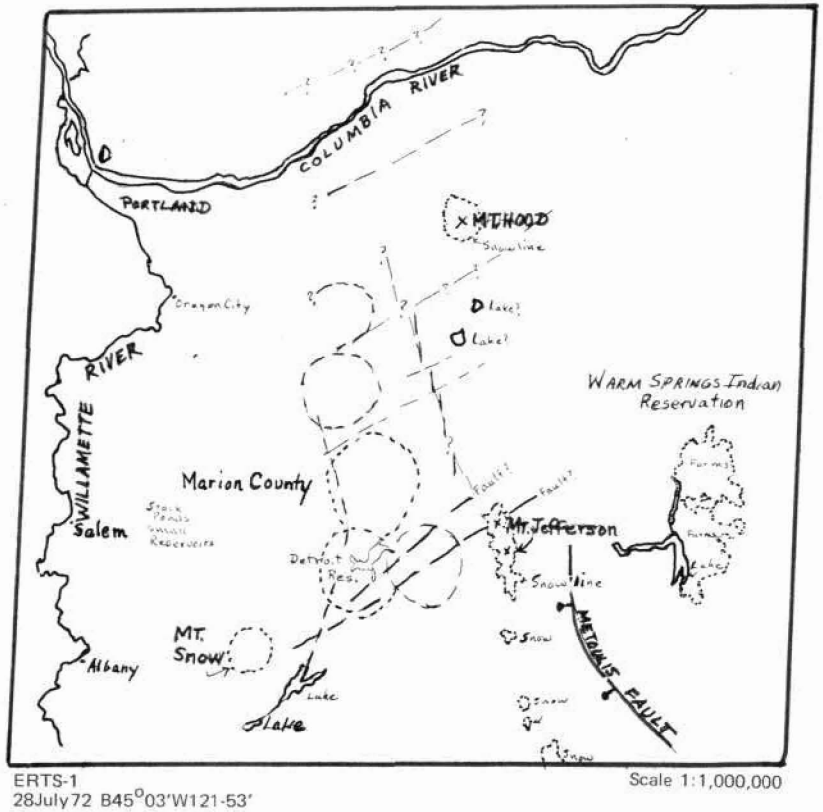

INTERPRETIVE OVERLAY OF PORTLAND
MT. HOOD SCENE SHOWING SUSPECTED
CALDERAS AND FRACTURE SYSTEMS

Figure VII-5. ERTS-1 image of the Cascade Mountains in Oregon with a geologic annotation.

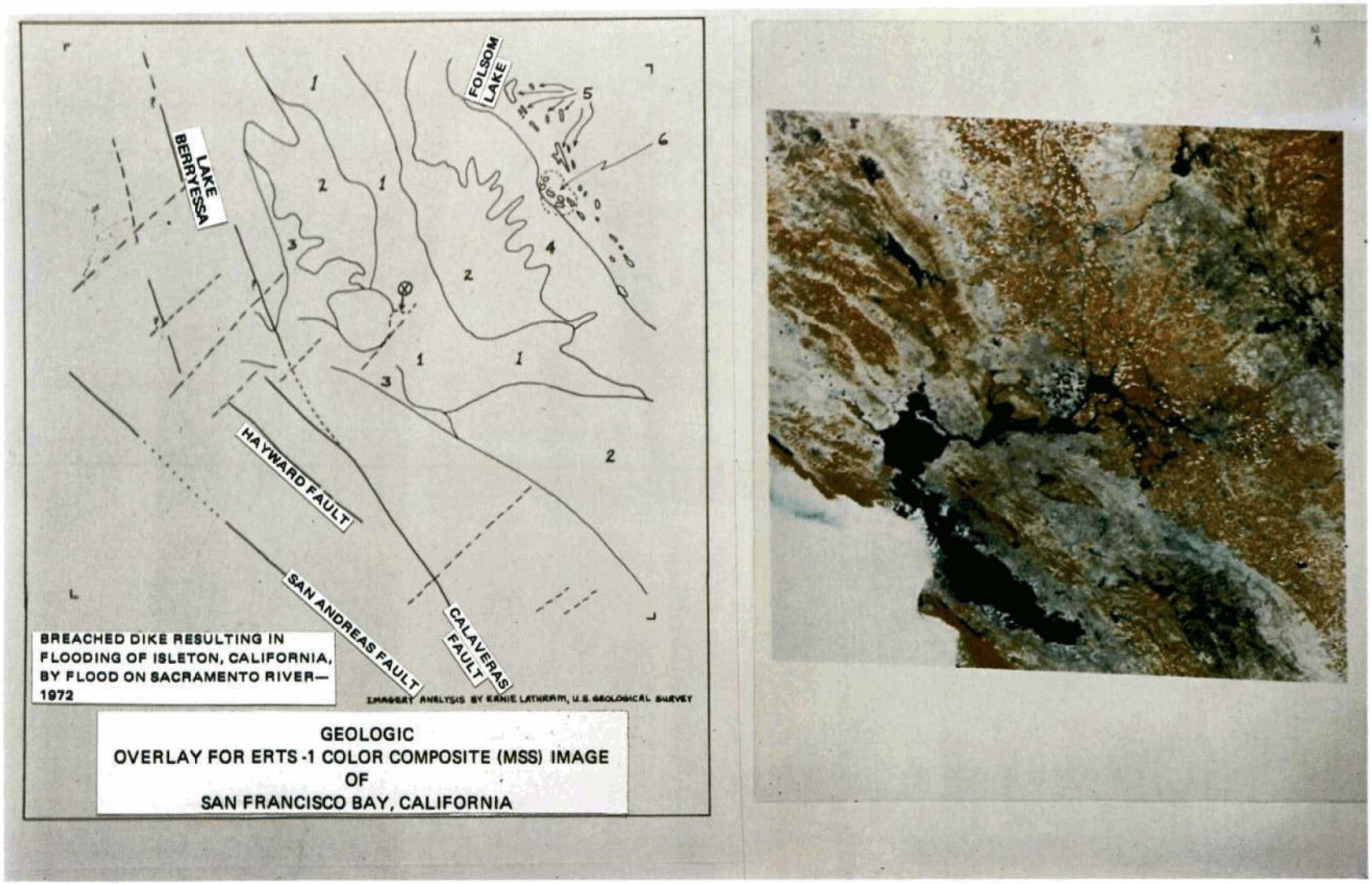

Figure VII-6. ERTS-1 color composite of the San Francisco, California area with geologic interpretation.

Bay, may be unsuspected faults as they are not shown on geologic maps of the area. The easterly linear, whose nothern end, at Lake Berryessa, coincides with the mapped Wragg Canyon fault, extends southerly to Carquinas Straits, and may extend across the Straits beneath the Port Chicago lowland area to the Calaveras Fault. If true, the Calaveras Faults may really extend from Hollister on the southeast to Lake Berryessa on the northwest, rather than terminating at Carquinas Strait as presently shown on geologic maps.

- Both northwest and southeast of San Francisco Bay, between the Great Valley and and Pacific Ocean, a series of northeast-trending linear features transect the dominant northwest-trending geologic structures. These may reflect crustal structures which, coupled with the known northwest-trending faults, may have controlled the location of uplifted blocks (i.e., Jura-Cretaceous strata of the Diablo Mountains) and down-thrown blocks adjacent (i.e., Tertiary basin under San Francisco Bay).

Vegetal growth, reflected by the intensity of reds on the photograph, exhibits distinct areal patterns which are related to the underlying materials. Areas of most intense red (1) and most vigorous growth, are underlain by silts and clays containing a high percentage of organic materials, deposited in basinal areas.

Areas of less intense reds (2) and less vigorous growth, overlie more coarse grained sands and silts, which have less organic content and are better drained, and reflect alluvial deposits from erosion of the Coast Range Mountains and Sierra Nevada in Pleistocene time. Smaller areas of less vigorous growth (3) are underlain by similar materials which may be even better drained, or are the sites of military reservations, ranch lands or in some cases, (Port Chicago) urban development. A distinctive area adjacent to the Sierras which shows poor vegetal growth (4) is underlain by the coarse sands and gravels (poor sub-soil) eroded from the Sierras in Late Tertiary and early Pleistocene time. These are the deposits in which rich placers of gold were found in the Sierra Foothills. One distinctive area (5) shows by a rectangular pattern the evidence of development, but poor vegetal growth. This area, the Mustang Hills, is dominantly ranchland, and is underlain by coarse stream deposits probably eroded from the highlands to the northwest.

Ultramafic Rock Bodies

Ultramafic rock bodies, some with associated mineral deposits rich enough to have been mined, are known in the areas of both the Coast Range and Sierra Foothills shown on the image. These bodies are difficult to identify in the Coast Range, but in the Sierra Foothills area, they have a distinctive purplish brown aspect. Known bodies of ultramafic rock can be readily identified (5). Similar areas (6) may also be ultramafic rocks but are not shown on the 1:250,000 scale geologic map of the area.

At point "X" on the photograph portions of the dike breached by the Sacramento River flood of 1972 can be seen; the dark water area here covers the still-inundated city of Isleton, California, and surrounding farmlands.

ALASKA

Excellent data has been collected over parts of Alaska, generally from the Colville River area and to the south. This color composite is of the area near Kobuk, east of Kotzebue Sound and south of the Brooks Range (for Alaska color composite see paper by D. Anderson). It is of great interest to our Bureau of Land Management because it shows a 50,000 acre forest fire in progress and they are responsible for this area of public land. It also shows the scars of an earlier burn. This data has permitted them to measure and assess, in preliminary fashion, the acreage damaged by such fires and estimate the value of the timber lost.

CONCLUSIONS

The multiband approach is extremely useful with each of the bands providing unique and useful information. There are difficulties, however, in handling the data if all 7 bands are considered. For most current applications, a two-band system (red and infrared) may be sufficient if this would reduce the cost of the satellite and the data reproduction problem. A thermal band, providing coverage on nighttime passes over tropical, volcanic, geothermal and high latitude areas would be extremely helpful and should be considered for future systems.

The mid-morning ERTS-1 orbit has provided sufficient shadowing to enhance landforms for monoscopic viewing. Stereo viewing can be done in high relief areas of overlap and may be very useful as repetitive data is acquired.

The resolution of the images exceeds that which we anticipated and is satisfactory for a large range of applications. Of the multi-spectral bands, the red band (RBV 2 or MSS 5) is important for mapping cultural features, submarine features, and vegetation distribution. The nearest infrared band (RBV 3, MSS 6) is good in mapping water body shorelines but can be fooled by shallow areas or heavy sediment loads in streams or lakes. The farther infrared band (MSS 7) is excellent for vegetation discrimination and infallible for mapping shorelines of oceans, lakes, wetlands, etc. Of the green band (RBV 1, and MSS 4) I have said very little. It is most affected by atmospheric conditions and best serves as an index of such conditions. Its water penetration capability for which it was designed appears hampered by the overwhelming effects of the atmosphere. It should be further tested, however, and studied critically before an attempt to discard it is made.

We are still relatively low on the learning curve with regard to the interpretation of ERTS-1 data. It is clear that in order to keep up with data production, to detect changes in repetitive coverage and to update maps, we must adopt automatic methods as soon as possible. In spite of initial difficulties we think that ERTS-1 is an unqualified success.

CARTOGRAPHIC APPLICATIONS OF ERTS IMAGERY

Alden P. Colvocoresses

U.S. Geological Survey

The Department of the Interior, through the EROS Program, has developed a number of ERTS cartographic experiments. These experiments, which have been accepted by NASA, are summarized as follows:

Experiment	NASA No.	Status
Photomapping of the U.S.	211	Funded
Map Revision	237	Funded
Basic Thematic Mapping	116	Funded
Polar Regions Mapping	149	Funded
Mapping from Orbital Data	150	Funded
Overall Cartographic Application	233	Funded
Cartographic Application of MSS Imagery		Negotiations
Photomapping of Foreign Areas	146	Negotiations

The principal investigators of these experiments have not, as yet, received sufficient data on which to report. However, NASA has asked Interior to take a quick look at selected ERTS-1 imagery and report thereon. The following indicates the results of this quick-look examination with respect to cartographic applications and cartographic products. The term cartographic, as used herein, applies to graphics that have been related to an accepted reference figure of the earth within a prescribed degree of accuracy.

Note that in Table VIII-1 the term resolution is *not* used. With respect to photography, we believe we know how to relate image resolution to a final product. With respect to RBV's and scanners, however, we are not prepared to do this nor are we prepared to discuss the resolution of ERTS. However ERTS image quality in many respects is better than anticipated from preflight experiments. We have asked NASA to install sizeable bar targets for definitive resolution analysis. In the meantime, we are having edge analyses made but do not feel they can at this time be reliably related to resolution as conventionally recorded in terms of bar-target response. As the table shows, we believe that such criteria as spectral consistency and detectability are meaningful indicators of image quality of cartographic products.

Table VIII-1
Nongeometric Relative Image Quality

Form	Spectral Consistency	Object Detectability	Maximum Printing Scales*
RBV, Bulk	Poor to fair	Good	1:250,000 – 1:500,000
MSS, Bulk	Good	Good	1:250,000
RBV, Precision	Poor to fair	Fair	1:500,000 – 1:1,000,000
MSS, Precision	Fair to good	Fair	1:500,000

*Estimate based on samples evaluated by the unaided human eye.

Note that Table VIII-2 refers only to internal accuracy, but external errors must also be considered. The external errors are well known, and they vary from insignificant amounts to several hundred meters. The mapping scales shown are for optimum conditions of minimal external errors. Note the basic conflict between image quality and geometric properties. Based on image quality alone the MSS bulk (system corrected) is the one form which appears suitable for mapping at 1:250,000 scale. However, it lacks the prerequisite geometric properties which are exhibited by the precision (scene corrected) products and the RBV bulk imagery. Perhaps this means that two products are required, one for spatial accuracy and the other for (nongeometric) image quality.

Table VIII-2
Geometric Properties (Preliminary)

Form	Internal Accuracy, Ground Scale	Maximum Scale for NMAS* Products
RBV, Bulk	≈70 meters, rms	1:250,000
MSS, Bulk	>300 meters, rms	< 1:1,000,000
RBV, Precision**	≈50 meters, rms	1:250,000
MSS, Precision**	>50 meters, rms	1:250,000

* National map accuracy standards.
** Requires ground control to produce.

Tables VIII-3, VIII-4, and VIII-5 indicate the various scales and forms that cartographic products might take. On Table VIII-3, note that precision-processed images, as produced by NASA, are recognized as a form of cartographic product. However, we believe such a product should be lithographed to make it generally available at reasonable cost. Note also

that bulk MSS imagery may become a cartographic product by fitting a reference grid to the image. This results in a somewhat warped grid and scale changes. We recommend this procedure only as a last resort. However we do have computer programs developed to print such grids.

Table VIII-3
ERTS-1 Cartographic Products First Phase, Photoimage

Scale		1:1,000,000
Format		Image (185 by 185 km)
Projection and grid		UTM
Mode		B&W and/or color
Final form		Lithographed
Processes:	• Precision – MSS or RBV (NASA)	
	• Bulk RBV – Scaled and Rectified	
	• Bulk MSS – Grid fitted to Image (Not a defined projection)	

Table VIII-4 indicates that a wide range of cartographic products can be made from ERTS data, whereas Table VIII-5 indicates what appears to be an optimum phase or goal.

Table VIII-4
ERTS-1 Cartographic Products Intermediate Phases, Photoimage

Scales	1:250,000 to 1:1,000,000
Format	Image, state, or quad
Projection and grid	Varied
Mode	B&W, Color, or thematic
Final Form	Lithographed

Table VIII-5 ERTS-1 Cartographic Products Optimum Phase, Orthophotoquad	
Scale	1:250,000
Format	1° x 2° (standard quad)
Projection and grid	UTM
Mode	B&W and/or color
Final Form	Lithographed

Table VIII-6 summarizes Interior's cartographic application efforts from ERTS. For the first time, you see revision of line maps mentioned. This is an obvious application with respect to water features but also shows promise in the portrayal of vegetation and gross cultural features.

Table VIII-6 ERTS-1 Summary of Cartographic Applications	
Application	Scale
Photoimage Products, B&W and/or Color	1:250,000 to 1:1,000,000
Thematic Products, B&W (Binary)(Snow and Ice, Water, IR Reflective Vegetation)	1:250,000 to 1:1,000,000
Revision of Line Maps, Gross Features	1:250,000 and smaller

The following figures illustrate some of the products.

Figure VIII-1 is of a standard NASA product. Even though the UTM zone boundary (120° long.) cuts across the image, UTM coordinates can be determined anywhere on the image with a simple coordinate reader. Geographic coordinates can also be read, but this requires considerable effort because of meridian convergence.

Figure VIII-2 illustrates the same scene as prepared for lithography. A full grid and explanation of the process has been added to the NASA precision-processed product.

Larger scale products are difficult to illustrate, but samples of ERTS images enlarged to 1:500,000 and 1:250,000 scale are available in hard copy form for examination.

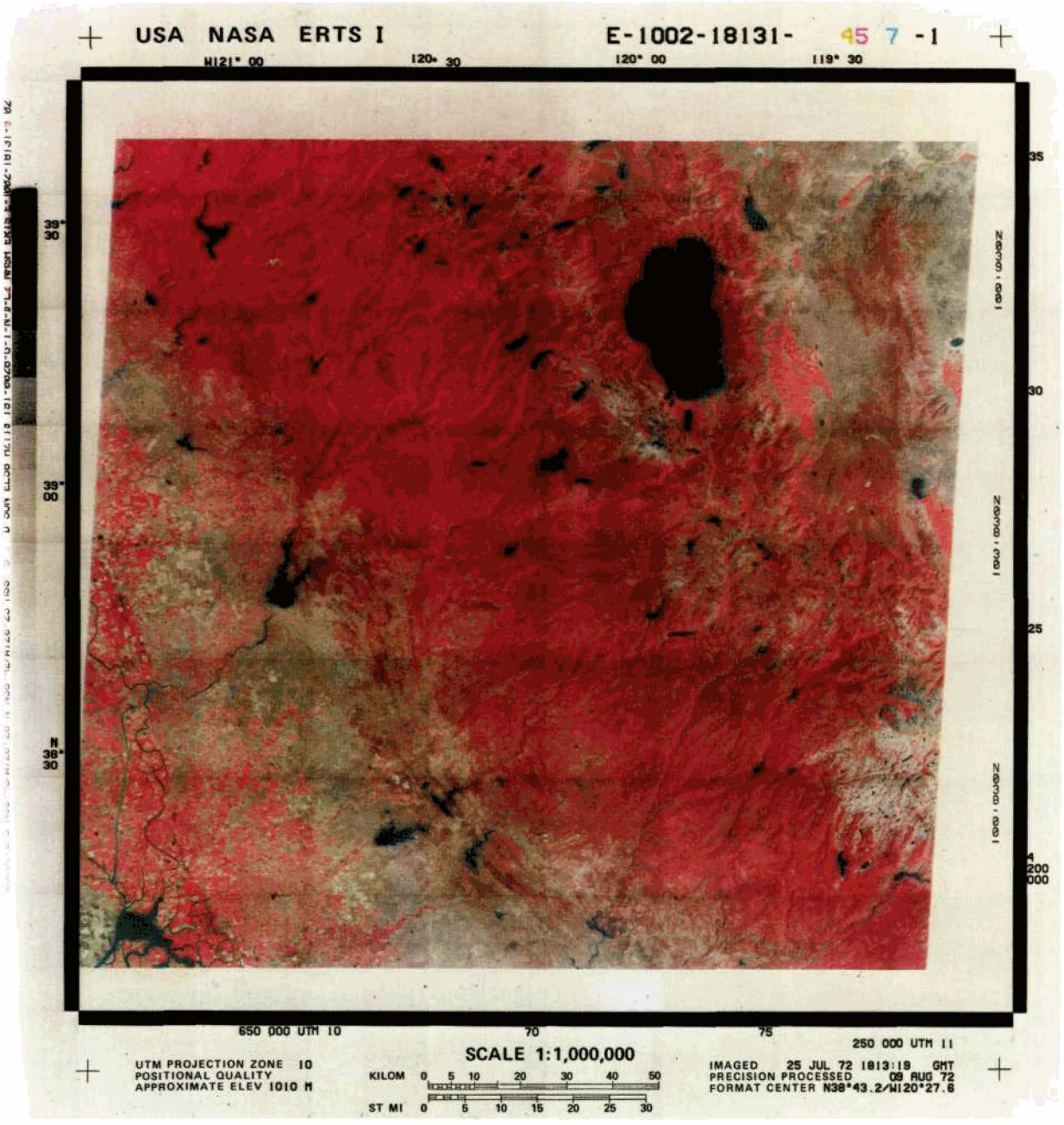

Figure VIII-1. Precision processed color composite of an ERTS-1 image of the Lake Tahoe, California-Nevada, area.

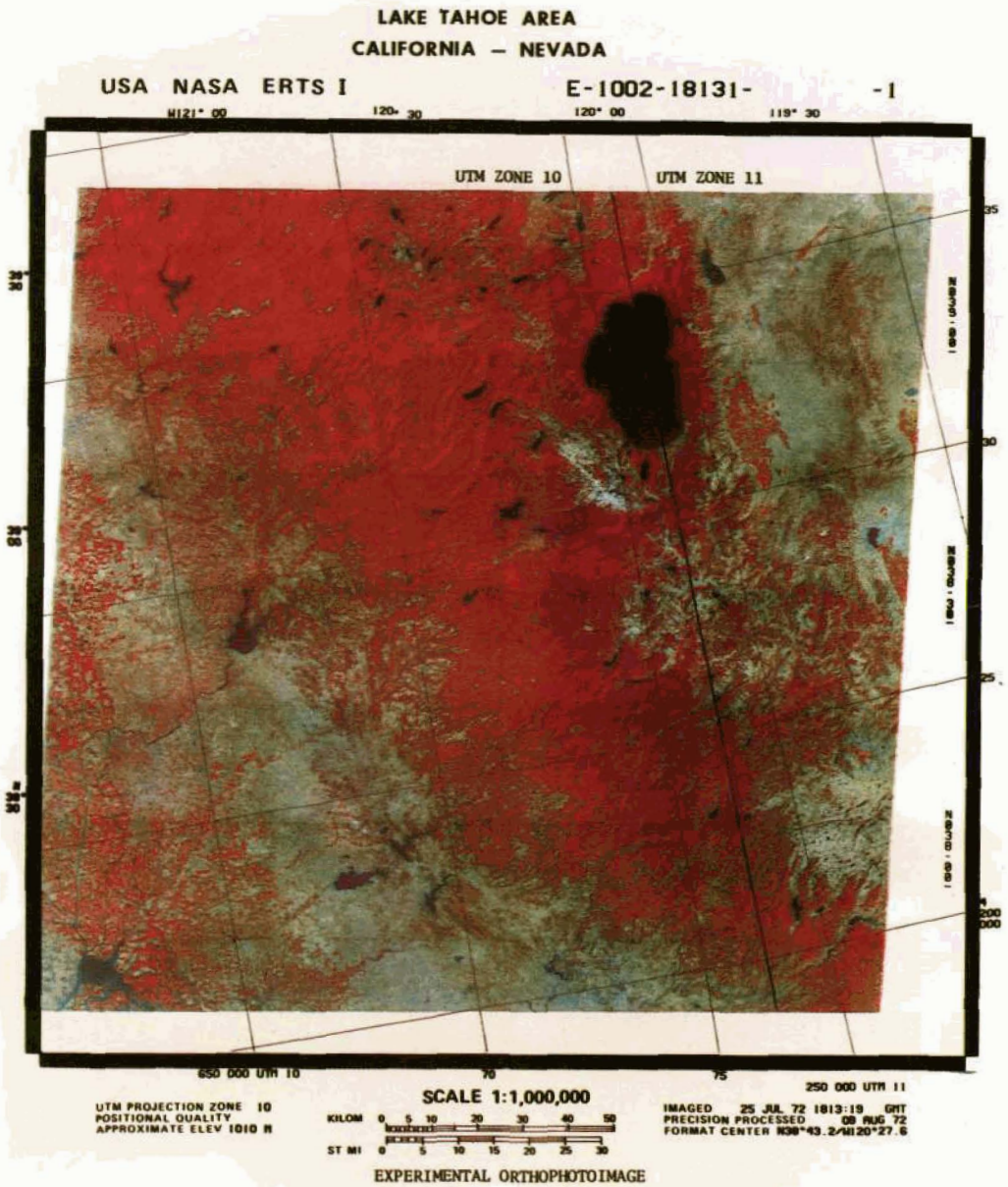

Figure VIII-2. Orthophotoimage produced within 15 days of exposure on semiautomatic equipment at the NASA data processing facility. It is a cartographic product from the Earth Resources Technology Satellite. The satellite is continuously orbiting the earth and recording such scenes at an altitude of 915 km. To provide such images of the earth, sensors of varying wavelengths aboard the satellite provide multiple images of each scene. Three of these initial images at 1:3,360,000 scale have been precisely restituted to ground control points and enlarged to a scale of 1:1,000,000. The three images originally exposed by different spectral bands have been cartographically merged by the USGS and lithographed as a false-color composite. Known geometric and radiometric errors in the initial images were removed and the cartographic quality improved. In the process the ground resolution is reduced. The square shading blocks are a result of the present system of precision processing.

ERTS was never defined as a mapping satellite, and its ability to portray the earth in three dimensions is certainly limited. However, when one treats the Earth's surface as a series of 2-dimensional planes or maps, then ERTS – because of its unique vantage point of 920 km altitude – becomes a powerful mapping tool. It offers the mapmakers something they have never had – an extensive and continuous source of up-to-date data in a form suitable for cartographic expression.

A PRELIMINARY APPRAISAL OF ERTS-1 IMAGERY FOR THE COMPARATIVE STUDY OF METROPOLITAN REGIONS*

James R. Wray
Geographic Applications Program
U.S. Geological Survey

INTRODUCTION

In the office of the Chief Geographer at the U.S. Geological Survey the Geographic Applications Program has been responsible for assessing the role of geographical applications of the remote sensing of environment, especially as they relate to the concerns of the USGS and the U.S. Department of the Interior. This work has been part of the NASA Earth Observations Program and of Interior's Earth Resources Observations Systems (EROS) Program. Underway prior to the ERTS experiment itself, it nevertheless anticipated a demonstration of the role of sensors aboard earth-orbiting satellite as well as aircraft.

The Geographic Applications Program now has three ERTS-related experiments underway. One, under Robert Alexander and William Mitchell, is concerned with multidiscipline research and user applications in the Central Atlantic Regional Ecological Test Site (CARETS). John Place is developing a prototype regional computer land use map model. He updates it from aircraft and satellite imagery, manipulating the inventory and change data in a system of computer mapping. George Loelkes is pioneering an operational user-application of this capability in cooperation with the Ozarks Regional Commission. My task is to concentrate on urban change detection in what has been called the "Census Cities Experiment". All of these tasks anticipate development of a common geographic information system and applications within the USGS and USDI Resource Appraisal and Land Information (RALI) Program. This program is a departmental focus for integrated, multi-discipline resource study and management operations and is now well into its formative stage.

The Census Cities Experiment in Urban Change Detection demonstrates many of the characteristics of the foreseeable operational geographic applications of remote sensing. It also provides a framework for this "Preliminary Appraisal of ERTS-1 Imagery for the Comparative Study of Metropolitan Regions."

At the time of the 1970 Census, we selected a ten-percent rank-size sample of U.S. Urbanized Areas. The Air Force and NASA acquired census-contemporaneous, multispectral, high altitude aircraft photography. Similar photography is being acquired again in 1972, both to provide a basis for comparative analysis of change from 1970 to 1972, and as an underflight for ERTS-1. The census returns represent one kind of ground truth for the 1970

*Publication authorized by the Director, U.S. Geological Survey

high altitude photography, while the interpretation of the 1972 photography represents one basis for evaluating the ERTS imagery. The experiment is viable based on the aircraft imagery alone. Its use as a test of ERTS imagery was never expected to be the likeliest application of the prototype low resolution imagery from the satellite. However, I am greatly encouraged by the imagery I have seen. It clearly portends beneficial geographic applications for and beyond the study of urban change. I welcome this opportunity to share with you some of the preliminary evidence.

In the course of these comments examples are discussed from urban test sites at Dallas, Boston, Seattle, and San Francisco; sample RBV and MSS imagery (both color composites and separate black-and-white multispectral views); sample reproductions provided by both the Goddard and the Sioux Falls data centers; and comparisons of ERTS imagery with that from high altitude aircraft. Sample interpretations and ground truth from the San Francisco test site, offer a preliminary appraisal of the ERTS sensors.

Some of the approaches to ERTS image interpretation implied in these examples may have transfer value in other discipline investigations. Finally, I mention some applications of the role of comparative area analysis by remote sensing which are already being user-tested. These imply a unique role for satellite imagery, despite a parallel need for greater image detail for corresponding *intra*-urban analysis.

The ERTS imagery shows great promise for the inventory of gross land use, and the monitoring of changes in land use. Our understanding of metropolitan regions—in which three-fourths of our population lives—can only be helped by the synoptic overviews which this space imagery provides. This is best done in concert, however, with a back up capability and flexibility such as that represented by a sensing system using high altitude aircraft. More specific comments are offered under subject groupings listed below.

Getting Started

An ERTS image may be acquired by different routes. Once in hand, it is essential for the user to know more specifically where the area depicted is located, what area it covers, and the identification of landmark features. The use of aeronautical charts is recommended for this purpose. These are available at scales of approximately 8, 16, 32, 48, and 80 statute miles per inch (1:500,000, 1:1,000,000, etc. to 1:5,000,000, respectively). The Operational Navigational Chart (ONC) at 1:1,000,000, produced by the Aeronautical Chart and Information Center, is especially useful because it is at the same nominal scale as an ERTS image produced as 9 x 9-inch print or film transparency.

The RBV image frame plots as a square on this chart; the MSS image frame is diamond-shaped because of the scan geometry and because of initial processing provisions.

Direction of the orbit track southward across the U.S. varies from about 15° West of South at the Canadian border to about 11° at the Mexican border. An ERTS-Image Chart Framing Template prepared by the USGS Geographic Applications Program facilitates the task of plotting an image frame at scales of useful reference maps.

An additional aid to image interpretation is the National Atlas of the United States recently published by the U.S. Geological Survey. Especially useful are the double-page thematic maps of the country at 120 statute miles per inch (1:7,500,000) and the place reference maps at 32 miles per inch (1:2,000,000). A prototype ERTS Image Chart-Framing Template for the National Atlas thematic maps has also been prepared. We firmly believe that our geographers will find ways that the ERTS imagery can be used to improve and to up-date thematic maps.

Use of a free-floating classroom globe in a hemispheric cradle is the best way to learn how the satellite's cameras "paint" the earth.

Multispectral Interpretation

(a) The wide range in format of ERTS image products and digital tapes includes provision for compositing separate black-and-white spectral views, once the image sets are brought into proper register. Besides the use of multispectral 70 mm film positives in color additive viewers, we have also found it profitable to cut 70 mm frames from multispectral 9 x 9-inch black-and-white film positives, and then to use these for color-additive viewing. The chief advantage, of course, is the enlargement of the image. Circular sugar beet fields watered by pump irrigation, for example, can clearly be seen in ERTS images of northeastern Colorado. (b) Black-and-white positive prints of any 70 mm multispectral image pair can be viewed as a "stereo pair." This practice is well known to photo interpreters for study of one stereoscopic three-dimensional image from two overlapping air photos. I suggest that editors and authors of articles describing ERTS to the general public will want to experiment with this simple device, too. A reader who can look "cross-eyed" at two different images of the same object, and mentally focus upon the one composite image in his mind's eye, has his own built-in, bi-spectral, additive viewer! (c) Infrared imagery from the multispectral scanner (MSS) shows intra-urban land use details not found in the other sensors. Arteries lined with commercial land use, and large shopping centers, appear as black lines and nodes on black-and-white positive prints, or as dark blue lines and nodes on positive color transparencies. Some vegetation patterns are also prominently shown. In the San Jose area these patterns are highly correlated with detailed land use ground truth maps prepared as part of the USGS Census Cities Experiment. (d) The delimitation of urban areas from ERTS imagery will obviously be more difficult in the more humid areas of eastern United States than in the midwest and southwest. The Boston limits, for example, are less clear than those of Dallas, even if we allow for the scattered clouds over an early New England ERTS scene. (e) For change detection, and for recording boundaries interpreted on the imagery by plotting them on a map base, there is need for an optical transfer aid that can also fit the geometry of the MSS image to the projection of the map base.

Use With Aircraft Underflight Photography

Among the preparations for the ERTS experiments has been the acquisition of multispectral high altitude aircraft "underflight" photography. The 1972 aircraft imagery

seen to date is from two different systems. The results are usable, but differ more or less from imagery acquired in 1970 and 1971 for various change detection experiments. These differences add an extra variable to the task of change detection, but they will also provide insight as to recommended aircraft sensor systems for future work of this nature.

Application of Urban Study by Remote Sensing

During one-and-a-half years of preparatory studies under the Census Cities Experiment we have identified a growing sample of potential applications and the user agencies concerned with them. Some of these applications are: a) Calibrate a traffic flow model and estimate daytime distribution of population; b) estimate water use requirements; c) define "Open Space" land and assess environmental hazards (such as earthquakes and landslides) affecting areas of possible urban expansion; assess environmental hazards on land already urbanized; d) identify prime land which ought to be preserved for agriculture; e) identify open space land to be saved for recreation and "green" space; f) calibrate a waste management model for San Francisco Bay, and monitor possible changes in water quality; g) map susceptibility to land and air pollution; h) assess quality of residential environment; i) project future population densities, and estimate changes in population distribution between censuses; j) prepare for large scale emergencies resulting from foreseeable hazards and for the assessment of environmental impact resulting from gradual as well as catastrophic changes. Many of these applications can be subdivided. For most, there are commercial or military counterparts. This list is a teaser, and a challenge to document specific applications at an early date. (Wray, "The Census Cities Project. A Status Report for 1971," *Fourth Annual Earth Resources Program Review,* Vol. III, Section 73, NASA Manned Spacecraft Center, Houston, Texas, January, 1972.)

These applications are made more feasible because of the nature of remote sensing. However, they are not all dependent on use of a satellite sensor platform. Remote sensing, whether from satellite or not, is especially appropriate for monitoring land use. While mapping of land use is not really our ultimate goal, land use is the visible and measurable evidence of the spatial aspects of Man and Environment relationships at a given time and place. We study land use, therefore, to improve understanding of the less visible processes of resource use, the making of a livelihood, and the quality of life. We make laws about land use to protect quality of life, or to bring about desirable change, hopefully in balance with necessary uses having some undesirable environmental effects.

Unique Role of ERTS

(a) Multistage, multidate, and multispectral remotely sensed data–as Professor Colwell is using these terms–provide more nearly real-time insight as to what the environment is and how it is changing. The satellite platform is one of the stages in an over all, operational, environmental monitoring system. In such a system, the synoptic view from an ERTS, for example, helps to eliminate areas *not* requiring further study while identifying those which do. This knowledge will help planners to establish priorities based upon comparable,

concurrent data. (b) One really unique use of ERTS imagery will be to learn and to teach a really relevant geography of our country, and for us to be prepared better as citizens to participate in decisions affecting our resources and quality of life. The image over San Francisco and central California, for example, dramatizes the breadbasket role of the Central Valley. It provides a meaningful setting for the pros and cons of transporting water from the North four hundred miles across mountains and desert to populous Southern California. It provides a basis for understanding environmental hazards from earthquake and flood, and for preserving accessible open space for two percent of our nation's population, while also identifying risks to urban expansion in areas otherwise easy to convert by bulldozer. The learning and teaching task, to be sure, begins with the work of the scientists and resource managers, but it cannot function at all without responsible participation by the news media and an informed citizenry.

URBAN–FIELD LAND USE OF SOUTHERN NEW ENGLAND: A FIRST LOOK

Robert B. Simpson
Dartmouth College

My colleague David Lindgren and I have revised our expectations upward and downward for a couple of years as NASA added blue chips to the ERTS pile or took them away. But today we are gratified at the amount of information potentially available for urban analysis in the first imagery. Our main question already has shifted from "will we be able to see enough" to "will ERTS continue to get returns long enough, to fill in those cloud gaps?"

The project I am basing my remarks on is relatively small. But of course, if only big projects produce good results none of us would be here today, for ERTS never would have gotten started.

The Dartmouth contribution to the ERTS program deals with that critical social and economic problem, urban sprawl, and conversely, with that disappearing resource: open space. Our ERTS objectives are:

- Map and digitize land use of northern megalopolis
- Identify urban–rural interface
- Identify special–interest areas
- Attempt limited prediction of future trends
- Evaluate ERTS as planning tool

The area within which our study is taking place is *large,* because ERTS is a large-area tool. Many specialists study cities, but until recently their studies have been at the local, small-area level; or at a *slightly* higher level, that of the metropolitan area. This is changing. Let me illustrate. Nothing less than three-state coverage will embrace metropolitan – or megalopolitan -- New England as seen by the Bureau of the Census. The New England Regional Commission, an innovative, large-area group, began examining in 1969 an even more extensive area as a possible palliative for the problems of megalopolitan New England. Two-and-a half additional states must be added to the original three to encompass the New England Regional Commission study area.

So, large-area regional planning already is under way. It needs a large-area data base. We have hoped that ERTS could help.

ERTS PRODUCTS AVAILABLE TO DATE

Eighty-five percent of our first-look work has been focused on a single color additive transparency. This is the rather widely distributed MSS image taken on 28 July over southeastern New England (Figure X-1). The photo center is near Providence, Rhode Island. The picture shows most of Boston under clouds, but the Naragansett Bay area fared somewhat better, and the completely non-urban eastern half of Connecticut is clear as a bell.

Two other color composites, also from July, have been useful for comparative purposes. Our first BW multiband images now have been received, but too late for posting on this graphic.

FIRST–LOOK FINDINGS

Product Utility

Suspension of the RBV pictures was for us small loss, but we do regret the absence of scene-corrected imagery. Our systems-corrected color composites appear to average a scalar distortion of about 5 percent, which is more than a quarter of an inch discrepancy across a 9 x 9 print. Much adjustment will be required when we transfer land use maps drafted as overlays to these photos, onto base maps which meet (or nearly meet) national map standards of accuracy.

In addition to our main reliance on color composites, we expect to make frequent use of BW transparencies in Band 5. From them we will get additional cultural detail, and more edge-acuity. For us Band 7 promises little, in spite of its ability to shrink clouds. We are investigating false color, density slicing, and edge enhancement, but in general favor a more simplistic approach.

What the ERTS Reveals

Figure X-1 is the image on which we have focused our preliminary investigation. Since Boston is largely cloud covered, and New Haven, which we have also studied intensively, was off the photo, we have zoomed in on an area that is less familiar to us, around Narragansett Bay. It includes such agglomerations as Providence-Pawtucket, Woonsocket, Fall River and Westerly. It also affords a spectrum of settlement patterns down to almost unpopulated woodland.

At 9 o'clock last Saturday (23 September) morning Professor Lindgren and Research Assistant David Ruml started to map land use of the state of Rhode Island. They mapped at a scale of 1:250,000, using as a base a four-times magnification of the Rhode Island portion of the ERTS photograph. At 7 PM Sunday the map was completed. Time invested was a little less than 40 man-hours. Since Rhode Island embraces 1200 square miles, they mapped an average of 30 square miles per man-hour. We believe the product warrants optimism regarding mapping land use of the United States at this scale perhaps as a supplement to the present USGS 1:250,000 map series. Figure X-2 shows an enlarged portion of the ERTS color composite and Figure X-3 shows the land use patterns for the state of Rhode Island.

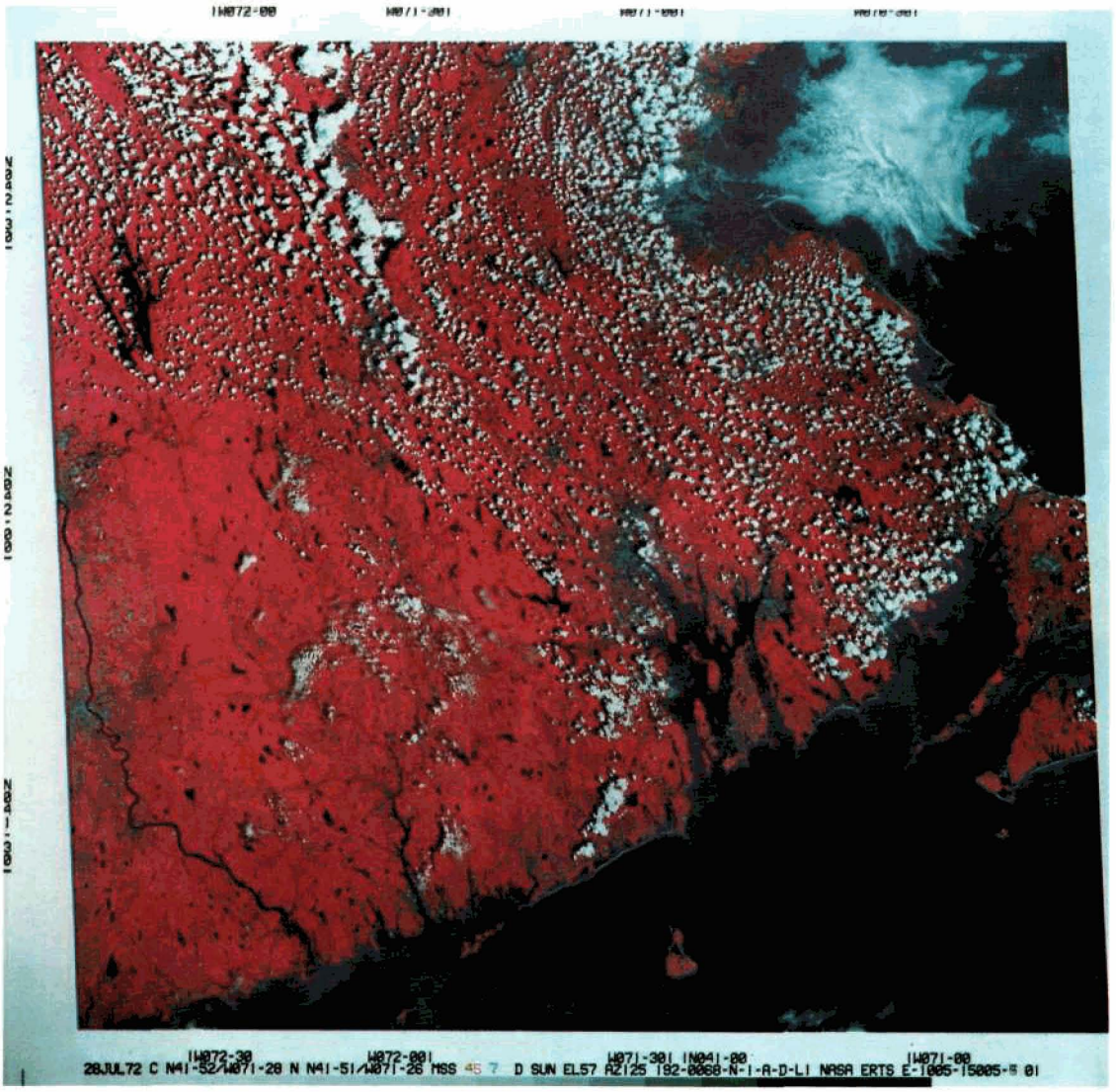

Figure X-1. July 28, 1972 color composite image from ERTS-1, showing a portion of New England.

Figure X-2. An enlarged portion of the New England ERTS-1 color composite showing essentially the state of Rhode Island.

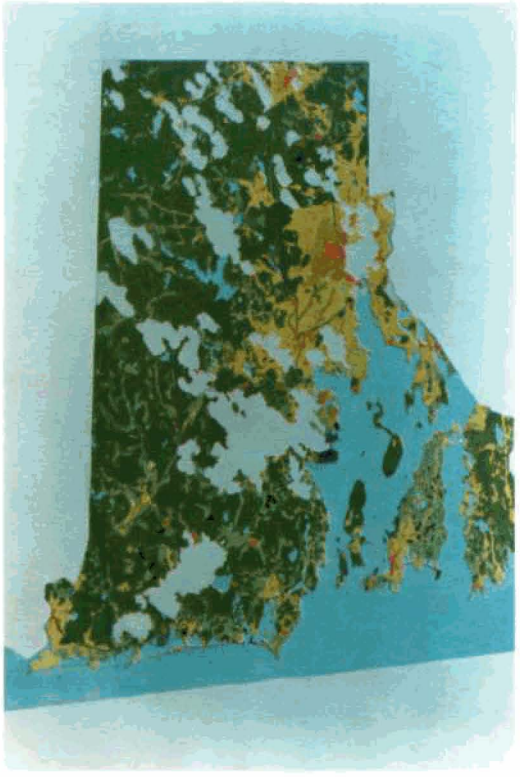

Figure X-3. Preliminary Land Use Map of the State of Rhode Island compiled from the color composite shown in Figure X-2. See text for explanation.

The amount of land use detail which can be extracted confidently from the ERTS images is encouraging. In addition to the white areas, which denote clouds or their shadows, this map has eight land use categories (Table X-1).

Table X-1
Land-Use Categories

Yellow	Single family residential (dense)
Orange	Mixed single-multiple family residential
Red	Commercial and manufacturing
Black	Transportation and utilities
Lt. Green	Rural residential and open space
Dk. Green	Woodland
Brown	Agricultural (row crops)
Blue	Water
Blank	Obscured by clouds

Commercial and industrial uses have been combined in a single category. There was no great difficulty in separating areas of high density, mixed multi- and single-family housing from areas of purely single-family dwellings; nor of separating the cleared areas which flank most rural roads, from the accompanying woodland. Significant areas of cultivated crops largely are limited to the island on which Newport is located, where they can be recognized clearly. However only one bridge, one sector of power line, and no railroads are shown. In part this may be a function of the limited time available for close examination.

As shown in Table X-2, eight categories of land use were delineated, using ERTS imagery, compared to 11 for RB-57 legends.

The fact we did not attempt an Institutional category does not mean that no institutions were recognized. The University of Rhode Island campus, for example, was quite apparent, and included indicators which helped discriminate it from other phenomena in the commercial-industrial category, to which it was assigned. Many golf courses were recognized, but we decided against attempting to aggregate them into a recreational category, and assigned them to open space.

Finally, a look at some thresholds of detection. In Figure X-2 it is possible to see the urban-rural interface on the north edge of North Providence, a golf course, and two groups of oil tanks.

Figure X-4 shows the interface of North Providence in more detail, on RB-57 imagery; a fully urban population density of 1800 people per square mile on the south side of the interface, a rural population density of 800-900 on the north side of it.

Table X-2 Land-Use Categories	
RB-57	ERTS
Residential, Single-family	X
Residential, Multi-family	X
Commercial	X
Industrial	X
Cultivated Agricultural	X
Transportational	X
Woodland	X
Water	X
Institutional	NO
Recreational	NO
Non-cultivated, open, or vacant	Rural residential and open space
Total	
11 Categories (Plus 6 special-use categories)	8 Categories (No special-use categories)

Figure X-5 shows the island on which Newport, Rhode Island, is located. Its "moth-eaten velvet" pattern stands for well-developed but small-field agriculture patterns, plus sprawl with urban population density: over 1,000 people per square mile. The rather thready pattern is common in New England rural wooded areas. Here it accompanies a population density of only 60 people per square mile. Cleared fields in a linear pattern along the rural roads are the cause of the threads. Curiously, comparable population densities are often attained without the threads.

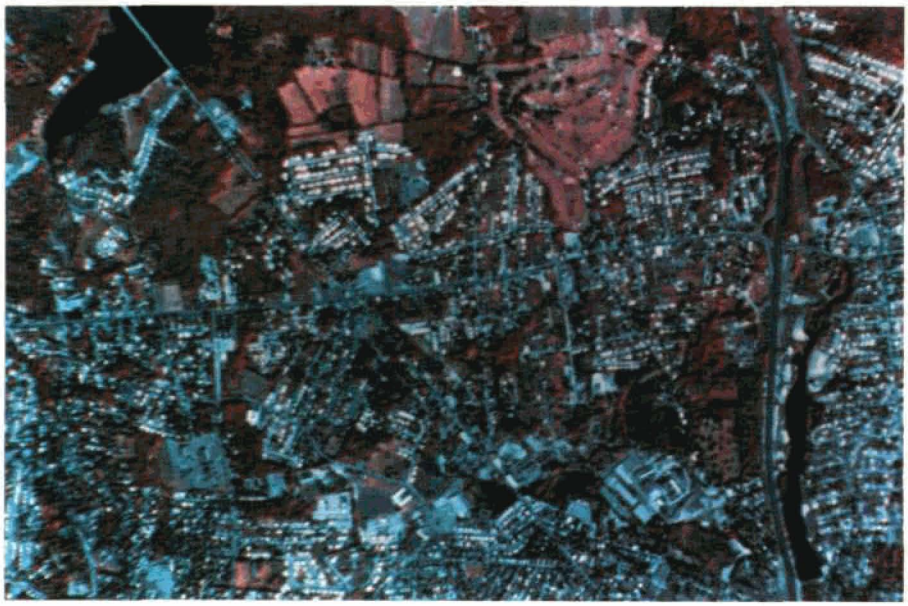

Figure X-4. RB-57 underflight imagery depicting the urban-rural interface in North Providence in the upper portion of the scene.

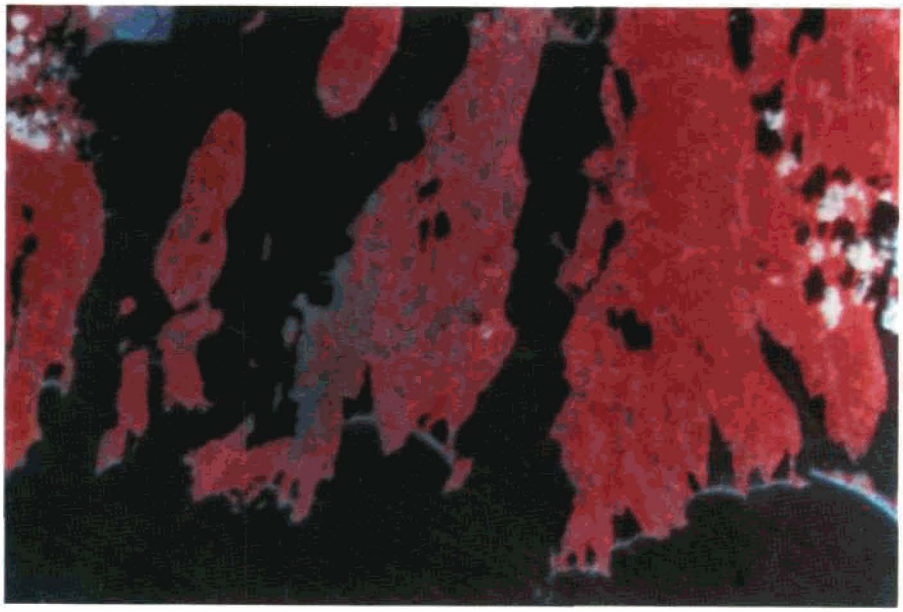

Figure X-5. Enlargement of the New England ERTS-1 color composite showing land use patterns. Newport, Rhode Island, urban complex is visible in the southwestern portion of the larger center island.

To summarize some of the informational thresholds we have encountered:

Some Informational Thresholds

Consistently recognize

- Ponds down to 300 feet diameter
- Urban cores of 7,000 population cities

Normally recognize

- Commercial and industrial sites down to 800 feet square
- Major highways
- Rural roads, if flanked by clearings

Occasionally recognize

- Railway lines, power lines, golf courses, cemeteries, bridges, tank farms, small intra-city canals

In conclusion I would like to summarize all I have said in a single sentence: The stated objectives are feasible, providing timely cloud-free coverage is available from ERTS-1.

USE OF ERTS-1 IN COASTAL STUDIES

Orville T. Magoon
Coastal Engineering Research Center
U.S. Army, Corps of Engineers

The strong private, public and federal interest in our nation's shorelines is readily apparent from material in the published press and in past and pending legislation. This presentation reflects the federal involvement in shore protection and planning and also reflects congressional and public recognition of beach and shore erosion as a local as well as a regional problem.

The physical processes which shape our shorelines are extremely complex and diverse. Both natural forces and man-induced changes affect the movement of and supply of sediments along a shoreline. The shores of the United States include practically all known land forms consisting of many materials and at various stages of geologic evolution. These land forms and materials have different vulnerabilities to wave action and their responses to the powerful forces which they oppose form a very broad spectrum. In order to effect realistic coastal planning and sound coastal engineering, it is necessary to quantifiably determine the movement of sedimentary material along the coastline under consideration. Although littoral processes are conceptually understood, it is not yet possible to adequately describe or quantify long or short term forecasts of the effects of improvements or modifications to the shoreline. In some instances, past shoreline changes have resulted in costly damage worth millions of dollars. Research in coastal processes at the Coastal Engineering Research Center is currently directed toward efforts to improve the state-of-the-art on qualitative and quantitative approaches to this problem. These efforts are based in part on tedious, extremely complex and short-lived in situ sediment transport measurements and experiments.

In addition to the examination of in situ sediment movement at specific locations, it is also necessary to describe and quantify the major coastal processes which occur over large physiographic reaches of our nation's shores. Of the 84,000 miles of the United States' ocean and Great Lakes shorelines, about 25% is undergoing significant erosion. Almost 3,000 miles of the nation's shoreline are undergoing critical erosion. The cost of remedial measures to halt such erosion, if desired, would be about two billion dollars plus major annual costs. From a practical standpoint, it is impossible to make detailed in situ measurements to describe and quantify the coastal phenomena in all these areas sufficiently to enable the planner and engineer to provide economically and environmentally viable solutions of these problems.

One thus looks for new tools that advance our capabilities in coastal studies. This material will summarize a few of the exciting possibilities of the use of ERTS-1 imagery in coastal studies. The material presented here is very preliminary and is a result of the synergistic

contributions of personnel of the NASA-Goddard Space Flight Center and the Coastal Engineering Research Center.

ERTS-1 SATELLITE

The ERTS-1 satellite and its user oriented applications are described in NASA-Goddard Space Flight Center Data Users Handbook, Earth Resources Technology Satellite, Document 71SE4249 with appropriate revisions (1). Analysis of multispectral images is given in reference (2). The nation's shorelines are discussed by Sheppard and Wanless in reference (3) and in the Report on the National Shoreline Study (4). Coastal applications of the ERTS-1 satellite are given in (5), (6) and (7). General coastal processes are contained in the Shore Protection Manual (9).

REGIONAL VIEWS

An obvious application of the ERTS-1 imagery is in obtaining regional views of extended coastal areas. An example of this is shown in Figures XI-1 and XI-2 which show multispectral scanner (MSS) bands 4,5,6 and 7 and a color composite from Orbit 0333, NASA E-1024-15073 and NASA E-1024-15071 and NASA E-1024-15080. Note that a clear line of demarcation along the New Jersey coastal areas is seen on the color composite view. Black and white views show a similar effect. Although readily compiled from ERTS imagery; mosaics made from aerial photography are often extremely difficult to match due to problems inherent with variation of sun angle and camera geometry. This is especially true when comparing the large, well-defined sediment plumes seen in ERTS with attempts to prepare mosaics of areas over water. We thus see in ERTS for the first time the structure of the large coastal and lacustrine plumes associated with sediment producing areas in many parts of the world. The four channels of the multispectral scanner show increasing sediment with decreasing MSS channel number. As shown on Figure XI-3 taken near Admiralty Island, Alaska (Orbit 0266 NASA E-1019-19430) and consistently shown in other coastal locations, minimum sediment is shown on MSS-7 gradually increasing to maximum sediment on MSS-4. In ERTS imagery where atmospheric haze is a problem on MSS-4, good sediment patterns are shown on MSS-5. Well-defined sediment sources indicate the direction of coastal currents away from the source. A large number of types of sediment plumes have been discussed in the literature. Considerable work on this subject has been supported by the Office of Naval Research and in particular, the Geography Branch. Material in this regard is available from Evelyn Pruitt, Chief of the ONR Geography Branch. The major sediment sources that have been seen in ERTS imagery appear to be derived from river discharges and to a lesser extent from cliff erosion. Sediment plumes are also seen in the Gulf of California near Mazatlán, Mexico (Orbit 0111, NASA E-1008-17062, not shown).

COASTAL CONFIGURATION

Information on the predominant direction of littoral movement is often derived from a number of specific shoreline configurations or changes. Particular work in this regard has

MSS 4

MSS 5

MSS 6

MSS 7

Figure XI-1. ERTS-1 images of the New York–Long Island area showing all MSS bands.

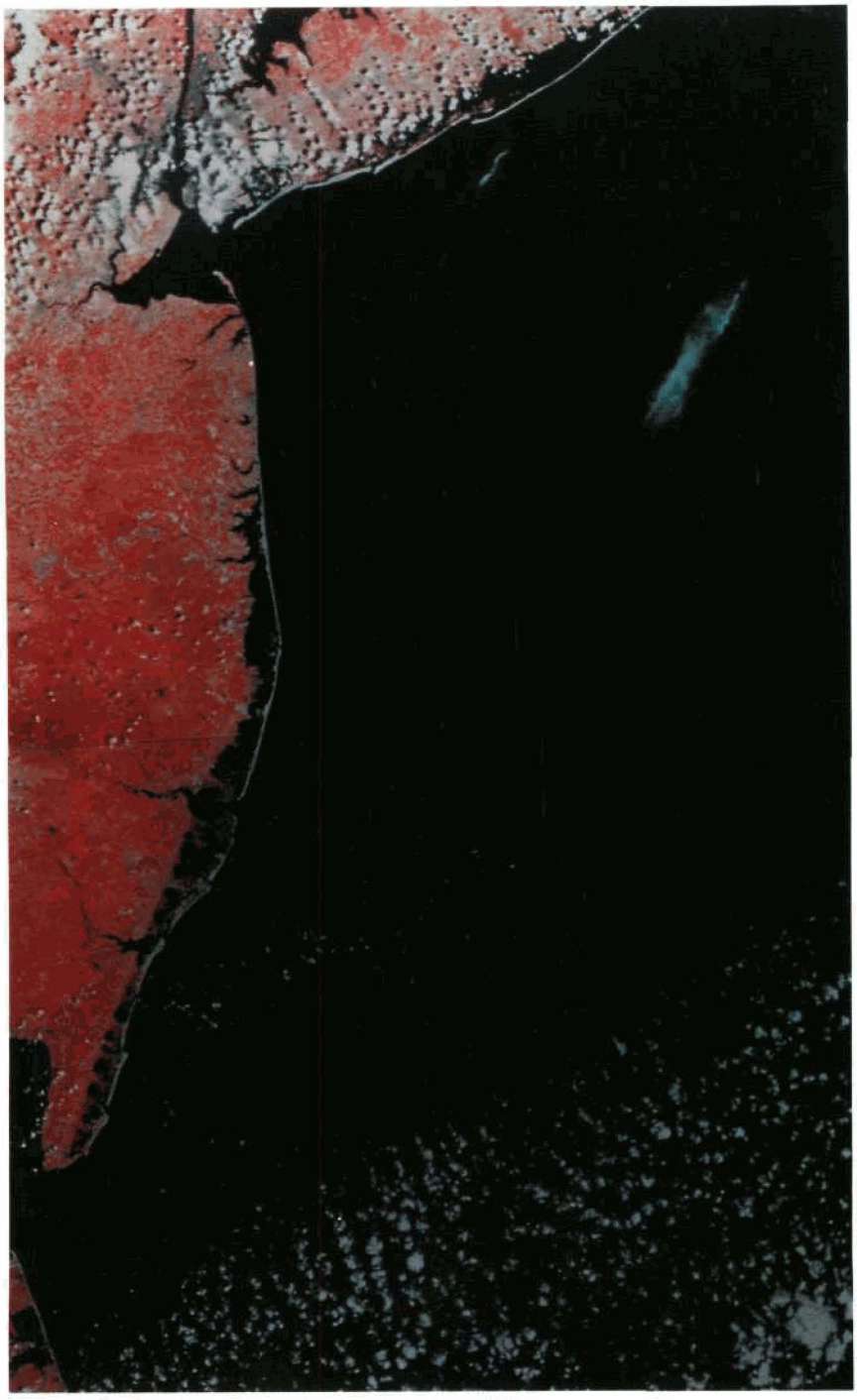

Figure XI-2. Color composite mosaic of the New York–New Jersey coastal zones made by combining consecutive ERTS images.

MSS 4

MSS 5

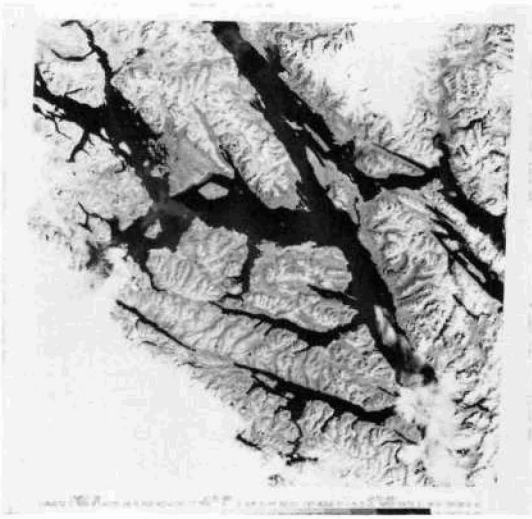

MSS 6

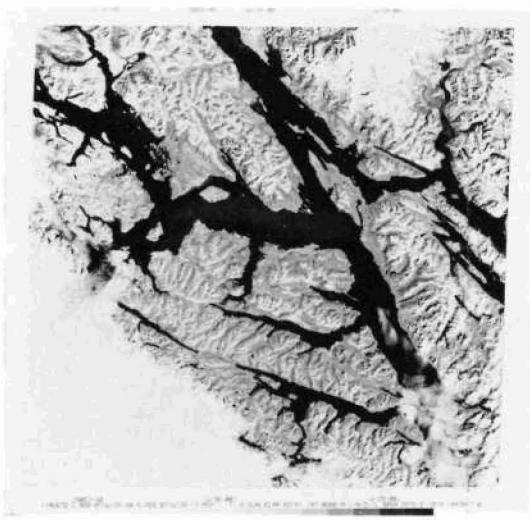

MSS 7

Figure XI-3. ERTS-1 images of the Admiralty Island–Lynn Canal area near Juneau, Alaska showing all MSS bands.

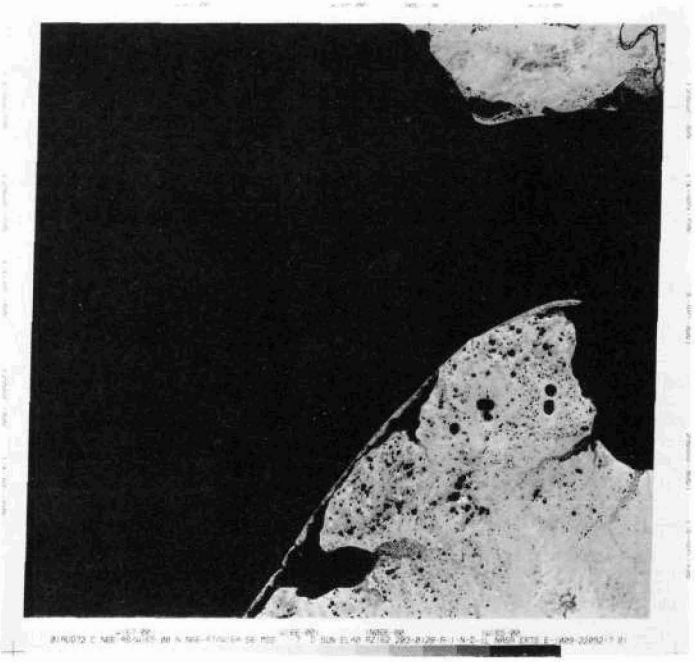

Figure XI-4. ERTS-1 MSS Band 7 showing the coastal zone west of Kotzubue Sound in the Seward Peninsula, Alaska.

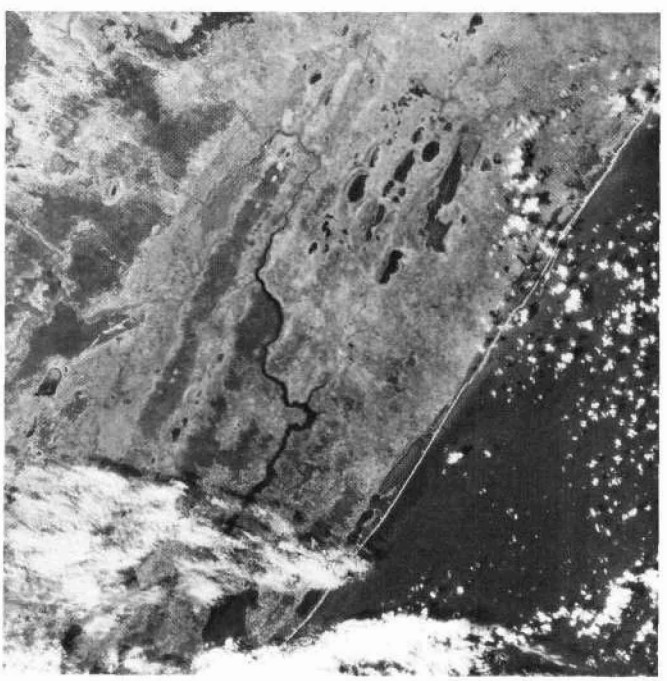

Figure XI-5. ERTS-1 MSS image of Lake Marangua area on the southeastern African coast just south of the Tropic of Capricorn.

been published by Galvin regarding coastal inlets (8), and also in the Shore Protection Manual (9). Note particularly on the barrier beaches seaward of Long Island, the strong overlapping entrances indicating drift towards New York Harbor (Figure XI-1 and Figure XI-2). Note the similarly occurring spit pointing toward the entrance to New York Harbor. Although shown in the figures, and more easily seen on the 70 mm originals, the pronounced offset at some coastal inlets is an example of an indication of the direction of littoral drift.

BARRIER ISLANDS

One of the major types of natural protection to the shore and thus of great interest to the coastal planner and the coastal engineer are the barrier islands. Due to the large extent of these islands, it is relatively difficult to obtain good synoptic coverage of major portions of the islands after severe storms. One important use of ERTS will be in studying the changes in barrier beaches and barrier islands after severe storms or hurricanes. The precise location capabilities of ERTS will be particularly useful in the measurement of the changes in these islands. Some idea of the capability of ERTS to resolve small features in barrier beaches was shown on a random comparison of a section of ERTS imagery with the Army Map Service scale 1:250,000 sheets. An example is Shishmaref and Kotzebue, Alaska (Figure XI-4). The particular area (Orbit 0128) shown is located between Arctic Lagoon and Cape Essenberg, roughly latitude 66°, 30′ north, longitude 165° west. Note that very small features in the smallest channels are clearly seen. A new inlet or closed inlet would be easily detected. I would estimate that the inlet channels are in the range of three to four hundred feet wide. The interface between land and water is, of course, particularly enhanced by the infrared bands.

UNDERWATER PENETRATION

During examination of the ERTS imagery, it is clear that considerable underwater penetration is possible under the appropriate conditions. This will be particularly useful in detecting, for example, changes in underwater sand formations such as those located between Florida and the Bahamas. Considerable penetration was also observed in ERTS imagery of tropic waters where the comparison between various bands of the multispectral scanner gives an indication whether the phenomena being observed is at the surface or under water. Analysis of results from specific test sites will be required before detailed results can be presented. An interesting fringing reef which shows up well on RBV1 around Poeloe Besar, Flores, Indonesia (see HO Chart 3090) (Orbit 46, NASA E-1004-01241, not shown).

COASTAL WAVES

In viewing ERTS imagery of coastal areas, particular attention was paid to areas where coastal waves might be present. Breaking waves were identified on the coast and around a coastal bay mouth bar located along the Spanish-Sahara coast (Orbit 0205, NASA E-1015-01523, not shown). Waves are in the series of small dots along the coast and out over the bay mouth bar. Breaking waves along a bar ten miles in length are seen on the coast of

Mozambique (Orbit 0119, NASA E-1009-07064) (Figure XI-5). Breaking waves also appear on the north side of bars along the New Jersey coast (Orbit 0333, NASA E-1024-15073) (Figure XI-2). Additional analysis will undoubtedly reveal other areas of breaking wave identification. In areas of high waves in deep water with appropriate sun angles, it is expected that long straight deep water waves as seen in the U-2 simulation flights will be observed in ERTS imagery.

CONCLUSIONS

Only a few samples of the ERTS-1 imagery to coastal studies have been presented. Even with the limited inspection possible of available imagery, a number of clearly demonstrated applications of ERTS to coastal studies have been described.

ACKNOWLEDGEMENTS

Acknowledgement is gratefully made to the personnel of NASA/Goddard, particularly Messrs. Bill Nordberg and Tom Ragland for their support. This presentation would not have been possible without the assistance of Dick Holmes, Jack Palgen in Building 23 and Clair Hill and others who kept the ERTS Browse Room open many evenings while I was scanning ERTS imagery. A special thanks is given to the sympathetic understanding of Miss Gail Blackmore in actually obtaining the ERTS imagery shown here. Acknowledgement is also made to the following CERC investigators who viewed the ERTS imagery and commented on its applications: Mr. Jim Balsillie, Mr. Dennis Berg, Mr. Charlie Chesnutt, Dr. Dave Duane, Dr. Craig Everts, Dr. Jerry Galvin, Dr. D. Lee Harris, Mike McClenan and Dr. Don Woodard. Acknowledgement is also made for Herb Bruder for mounting mosaics, Jim Dayton for producing the slides and Barbara Fletcher for typing the manuscript.

Data presented in this presentation, unless otherwise noted, were obtained from research conducted by the United States Army Coastal Engineering Research Center under the Civil Works research and development program of the United States Army Corps of Engineers. Permission of the Chief of Engineers to publish this information is appreciated. The findings of this paper are not to be construed as official Department of the Army position unless so designated by other authorized documents. The review and comments on the manuscript and continued support by LTC Don S. McCoy, Director, CERC are gratefully acknowledged.

REFERENCES

1. NASA/Goddard Space Flight Center Data Users Handbook, Earth Resources Technology Satellite, Document 71SE4249.

2. Short, Nicholas M. and MacLeod, Norman H., "Analysis of Multi-Spectral Images Simulating Earth's Observation", NASA/Goddard Publication X-430-72-118.

3. Sheppard, F.P. and Wanless, H.R., "Our Changing Coastlines", McGraw-Hill, 1971.

4. National Shorelines Study – Summary Report, Dept. of Army, Corps of Engineers, Washington, D.C., August 1971.

a. Shore Management Guidelines, Dept. of Army, Corps of Engineers, Washington, D.C., August 1971.

b. Shore Protection Guidelines, Dept. of Army, Corps of Engineers, Washington, D.C., 1971.

c. Regional Inventory Reports for Entire U.S. Coastline, published by various Corps of Engineers Division Offices.

5. Magoon, O.T., Jarman, J.W., Berg, D.W., "Use of Satellites in Coastal Engineering", Proceedings First International Conference on Port and Ocean Engineering Under Arctic Conditions, The Technical University of Norway, Trondheim, Norway, August 23-30, 1971.

6. Magoon, O.T., Jarman, J.W., Perry, Doug M., "Coastal Engineering Application of the ERTS-A Satellite", Proceedings 13th International Conference on Coastal Engineering, Vancouver, British Columbia, Canada (in press).

7. Magoon, O.T., Perry, Doug M., "Use of Remote Sensing in the Study of Coastal Processes", Proceedings 13th International Conference on Coastal Engineering, Vancouver, British Columbia, Canada, July 1972 (in press).

8. Galvin, Cyril J., Jr., "Wave Climate and Coastal Processes", The Water Environment and Human Needs, Massachusetts Institute of Technology, Symposium, October 1-2, 1970.

9. Shore Protection Manual, Coastal Engineering Research Center, Washington, D.C. (Replacement for Technical Report No. 4, Shore Protection Planning and Design) (in preparation).

10. Schubel, J.R., Carter, H.H., Schiemer, E.W., Whaley, R.C., "A Case Study of Littoral Drift Based on Long-Term Patterns of Erosion and Deposition", Chesapeake Science Vol. 13, No. 2, p. 80-86, June 1972.

11. Szekielda, K.H., Kupferman, S.L., Klemas, V. and Polis, D.F., "Element Enrichment in Organic Films and Foam Associated with Aquatic Frontal Systems", Journal of Geophysical Research, Vol. 77, No. 27, p. 5278, September 20, 1972.

THE ESTUARINE AND COASTAL OCEANOGRAPHY OF BLOCK ISLAND SOUND AND ADJACENT NEW YORK COASTAL WATERS

Edward Yost, Rajender Kalia
Sondra Wenderoth, Robert Anderson*
Rudolph Hollman**

NASA Test Site 151, in particular the Block Island Sound area from the tip of Long Island to Martha's Vineyard, is the subject of this report. These coastal waters contain a mixture of different ocean masses, including the discharge of brackish water from the Connecticut and Thames River estuaries. Complex surface current patterns exist, particularly in the area between Block Island and Montauk Point on Long Island and southeast of Point Judith, Rhode Island, as well as at the interfaces of Narragansett Bay and Buzzards Bay with Rhode Island Sound and in Vineyard Sound, north of Martha's Vineyard. Underflight and ERTS imagery were analyzed in order to determine the hydrologic features of the water mass, including current patterns, particulant in suspension, and the contacts between different water masses.

The ERTS imagery exposed on 28, 29, and 30 July was received from the Goddard Space Flight Center in both positive and negative form. The spectral bands included the 500-600 nm, 600-700 nm, 700-800 nm, and 800-1100 nm regions. Unfortunately, the data for 29 and 30 July was not useful because of the large extent of cloud cover over the New York area. Figure XII-1, on the following page, shows the general region covered by the frame of ERTS data which has been analyzed using additive color techniques.

Quick-look analysis of the NASA second generation negatives indicated that:

- The green spectral band lacked contrast, owing perhaps to the presence of some haze; it was also overexposed.
- Red spectral band was of acceptable contrast, although somewhat overexposed.
- The infrared bands were overexposed for the land areas, but the exposure was good for the water. The land areas fell almost completely on the shoulder of the curve (gray scale number vs. image density), while the water was along the upper toe portion. Almost no areas of interest fell along the straight line region of the curve.

The characteristic curves of the NASA-processed ERTS positive imagery are shown in Figure XII-2. The slopes of the multispectral records are well matched, although the

*C. W. Post Center, Long Island University.

**New York Ocean Science Laboratory.

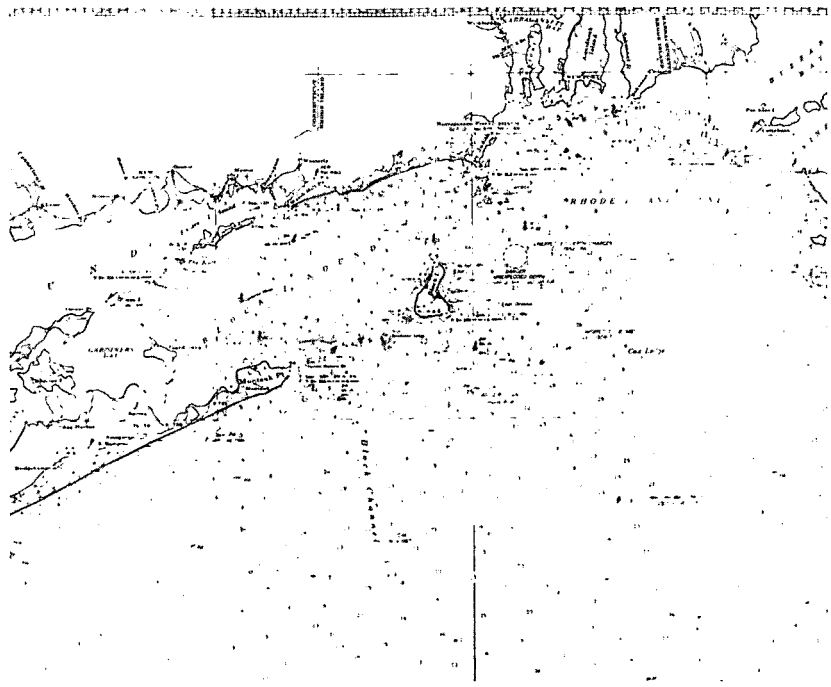

Figure XII-1. Hydrographic chart of the coastal area between Montauk Point and Block Island Sound.

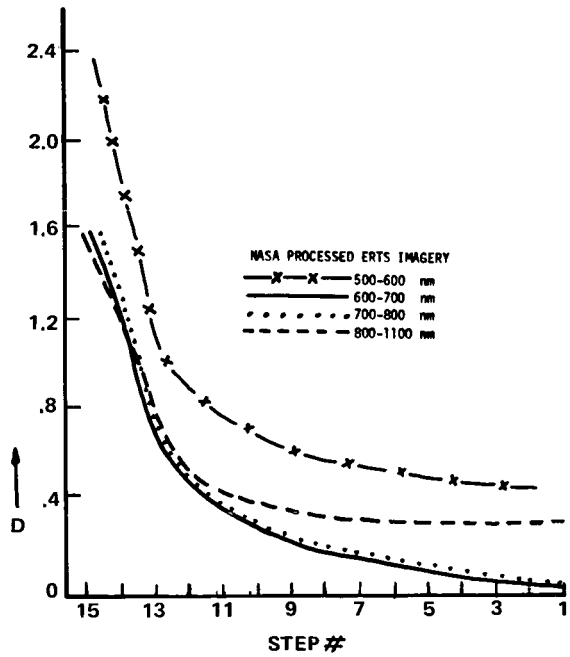

Figure XII-2. Curve of gray scale number vs. density of the positives supplied by NASA.

minimum density of both the green and far-infrared images is excessive. These curves were generated plotting the gray scale step number which appears at the bottom of the ERTS chips on the x axis with its density plotted on the y axis. Unfortunately, all the highlights of the scene fall along the toe portion of the curves where the density differences are relatively small for a large change in gray scale number. The darker regions of the imagery lie between the toe and the straight line portion of the curve where the density-brightness gradient is less than optimal.

A visual analysis of the NASA positives indicated the following:

- The green spectral band was extremely flat with a high D_{min} due to overexposure.
- The red spectral band was of acceptable contrast.
- The infrared bands lacked detail in both the water and land areas.

The NASA supplied positive imagery shown in Figure XII-3 was placed into the Spectral Data Model 64 viewer and the spectral records were projected as follows:

500-600 – Blue	700-800 – Red
600-700 – Green	800-1100 – Red

A photograph of the viewer screen presentation is shown in Figure XII-6. Only one of the infrared records was projected at a time with the two visible bands. The large urban areas are apparent, although most detail in the land is missing because of the heavy infrared exposure. Of all the records, the red has the most detail in both land and water. No obvious differences in water mass are apparent in this color composite image. Because of the non-optimal development of the MSS data for either the highlights (land) or the shadows (water) the NASA imagery was reprocessed at Long Island University.

The negatives supplied by NASA were used to generate a second set of positives which would enhance any small detail in the water mass as shown in Figure XII-4. Both the exposure and processing were altered to place the low brightness regions on the straight line portion of the characteristic curve shown in Figure XII-5 on the following page. Notice that those regions which existed between the toe and straight line of Figure XII-2 are now imaged along the straight line portions of Figure XII-5. The minimum density has also been reduced on the red and near infrared records. Due to the poor exposure of the green band, little could be done to create any significant change in the high minimum density without losing the little detail which the image contained. Contrast increased by using EK 2420 duplicating film and processing in D-19. The scene brightness range for both water and land is small so that a single reproduction of the green record has been used for the enhancement of both water and land areas. A more accurate comparision of the effects of reprocessing can be made by noting the density differences in the water between NASA and Long Island University processing. The water mass is represented by step wedge steps # 14-16. The Δ density between these steps for NASA processed infrared positives is .7, while the Δ density of the water for the reprocessed infrared positives is 1.35. The Δ density in the

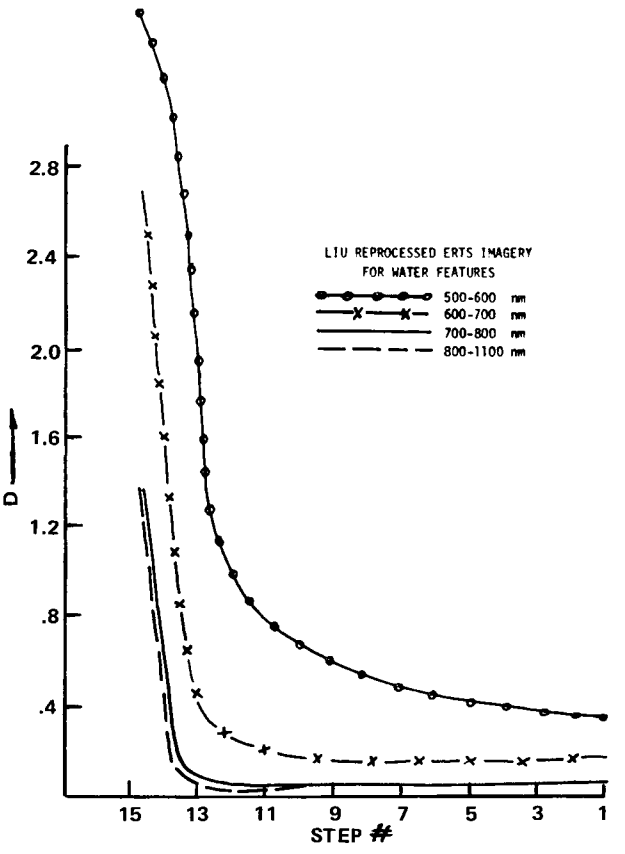

Figure XII-5. Curve of gray scale number vs. density for positives reprocessed to enhance water detail.

red region is .6 for NASA processed film and .8 for Long Island University reprocessed images. It should also be noted that the lower D_{min} makes the water differences more obvious when projected by increasing the brightness level on the viewer screen.

Figure XII-7 is a composite color rendition of the positive imagery reprocessed to enhance water detail. Notice that all detail in the land areas has been lost since highlights have been placed along the toe of the curve of Figure XII-5. Distinct outpourings from the Connecticut and Thames Rivers are apparent as a cyan color. Some turbidity also exists in the vicinity of Newport, as well as between Martha's Vineyard and Cape Cod. Attention is called to the water mass south of Martha's Vineyard. The light grayish-purple hue is indicative of the high reflectance of the water in the red spectral region. We believe that this image could be related to the infestation of poisonous algae that invaded the New England coast from Cape Cod to upper Maine known as the "red tide".

Red tides, composed of many different types of pigmented algae ranging from green to brown, are more often than not harmless, but toxic varieties periodically invade the coastal waters around the world. New England waters, which are cold and have a good tidal flush,

are generally inhospitable to red tides, but a "seed" condition is endemic. It simply awaits the combination of proper conditions to achieve sufficient concentration for a "bloom". The conditions necessary for the reproduction of these organisms are thought to include much sunlight, low salinity, warm water, and a sudden upsurge in nutrients. Distrubances of the ocean floor are known to stir up mineral particles that provide the life-giving nutrients. Data is being analyzed to relate water samples with the multispectral color image shown in Figure XII-7.

This photograph shows bleeding of the infrared record along the shoreline. This is due primarily to the heavy exposure given to the positive in order to place the areas of the water on the straight line of the characteristic curve.

The NASA negatives were also reprocessed in order to enhance the land areas, the results of which are shown in Figure XII-9. The infrared bands required making an interpositive, an internegative, and finally the projection positive. This procedure was done in order to build up the contrast without losing too much land detail. It was not possible to obtain sufficient contrast using a single step. The characteristic curves of the final reprocessed positives are shown in Figure XII-9. Most of the information for the land areas was contained in the infrared records. Notice that the long toe region for the infrared bands shown in Figures XII-2 and XII-5 have been picked up and now exist on the straight line portion of Figure XII-9. Those land regions for which only small density differences existed previously have been greatly enhanced. The Δdensity of the land improved from .1 (NASA processed) to .7 (Long Island University reprocessed) in the infrared regions and the minimum density of all records was decreased considerably for projection.

A color composite of the reprocessed positive imagery for land detail is shown in Figure XII-8. The 700-800 nm near-infrared band has been projected as red, the red band as green, and the green band as blue. No detail in the water region is possible since all low brightness areas fall on the shoulder of the curve of Figure XII-9. The heavily wooded and cultivated lands appear as a bright red, while the urban regions such as New Haven, Boston, Groton, and New London, are a vivid cyan. Less lush agricultural areas are a gray-magenta.

These photographs indicate that it is necessary to expose and process the multispectral imagery for the scene brightness range under consideration. Unfortunately, some of the reprocessed film is grainy, which is a natural consequence of trying to develop the film to a sufficiently high contrast in order to get good projected color.

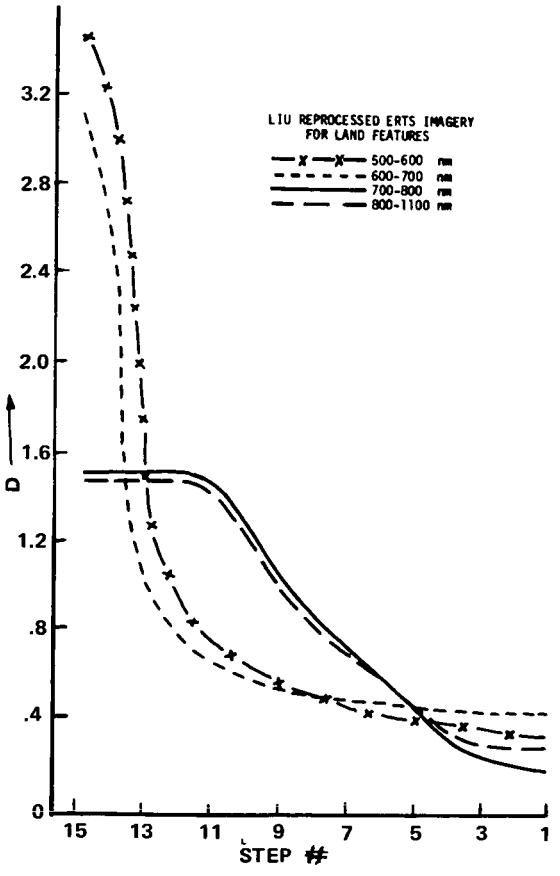

Figure XII-9. Curve of gray scale number vs. density of positives reprocessed to enhance land features.

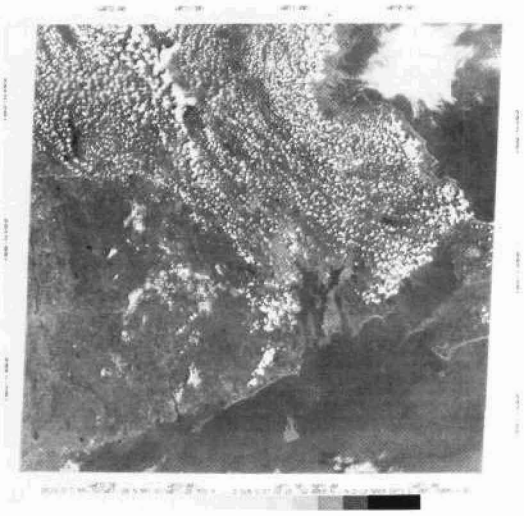

500 – 600 nm Band

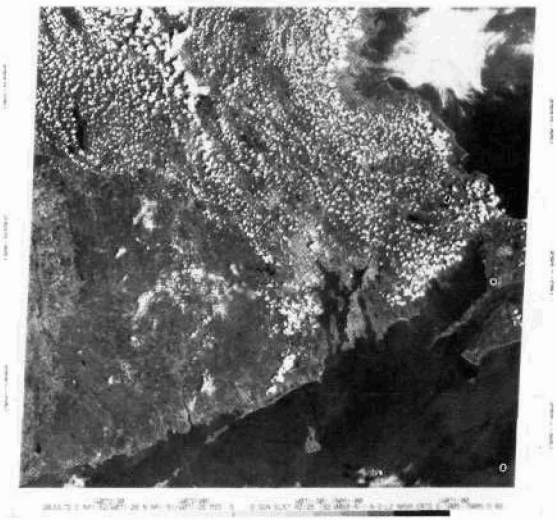

600 – 700 nm Band

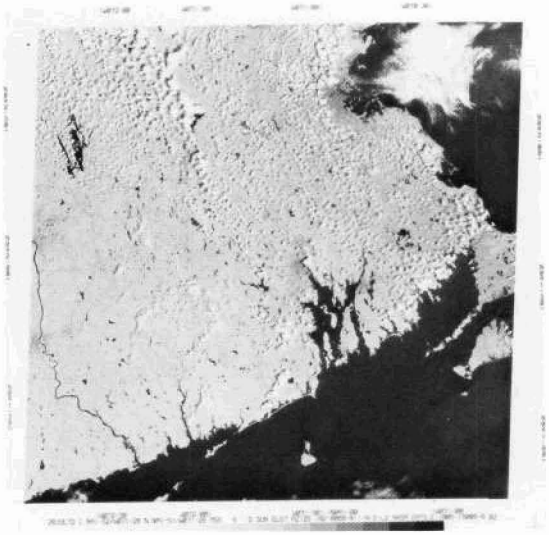

700 – 800 nm Band

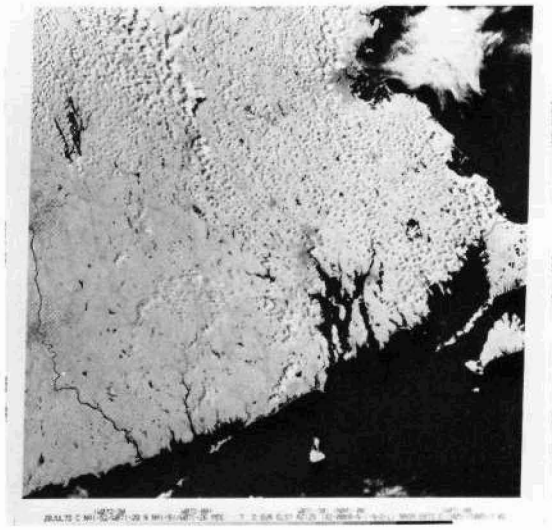

800 – 1100 nm Band

Figure XII-3. Four multispectral scanner film transparencies as received from NASA.

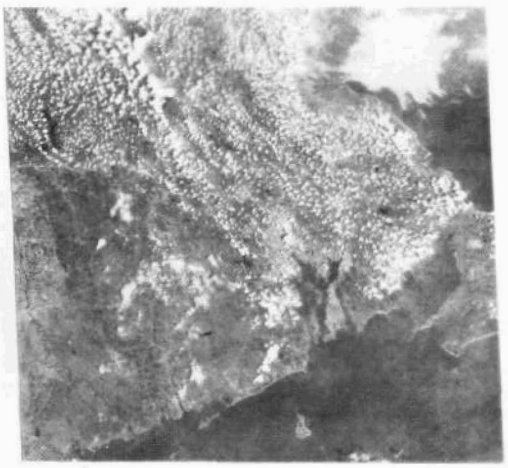

500 – 600 nm Band

600 – 700 nm Band

700 – 800 nm Band

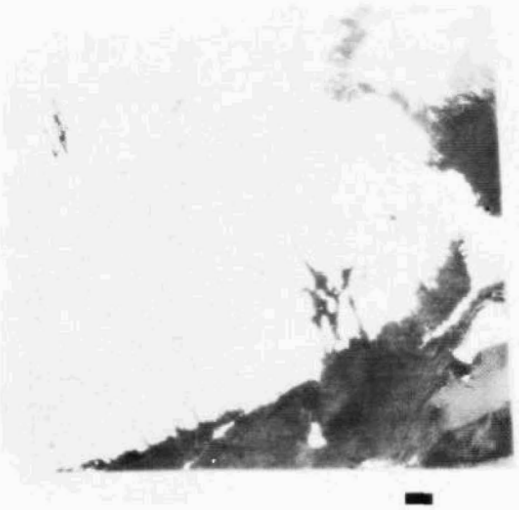

800 – 1100 nm Band

Figure XII-4. Four multispectral scanner positives reprocessed to enhance water detail.

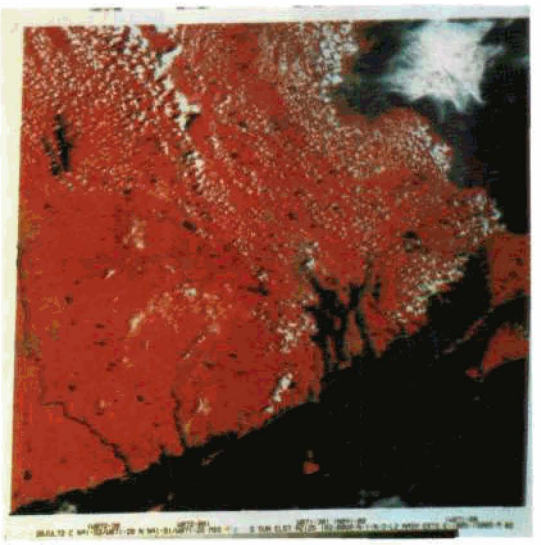

Figure XII-6. Additive color image using NASA supplied MSS bands 4, 5, and 6.

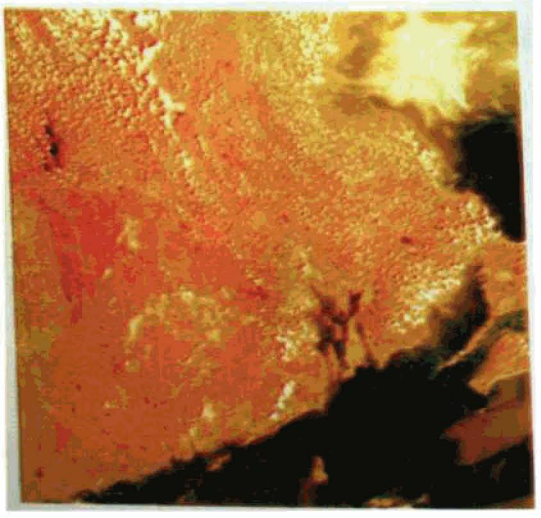

Figure XII-7. Additive color image of MSS bands 4, 5, and 6 reprocessed to enhance water detail.

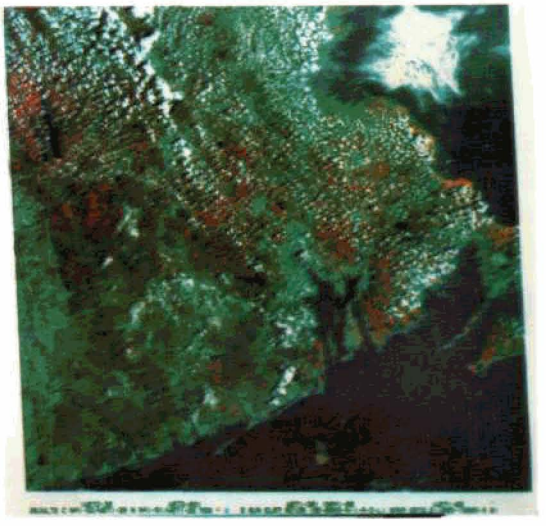

Figure XII-8. Additive color image of MSS bands 4, 5, and 6 reprocessed to enhance land features.

PRELIMINARY ASSESSMENT OF THE ERTS-1 DATA COLLECTION SYSTEM*

James F. Daniel
U.S. Geological Survey

As of September 1, 1972, ten Data Collection Platforms (DCP's) were successfully transmitting messages to ERTS-1. Of these ten, five were known to be transmitting "dummy" data and five were transmitting real data. The lack of other transmitting DCP's was due to an unexpected delay in shipping reliable units from the NASA Contractor, coupled with an expected delay due to a period of familiarization with new equipment by field personnel.

Data from three operating platforms in the Delaware River Basin have been found to be of excellent quality. During one two-week period of operation, only one message was received in garbled condition. Other messages were obtained at the rate of two to three messages per pass, two to three passes per morning and evening periods. As the entire Delaware network is implemented (20 sites) the exceedence of ERTS-1 specifications is anticipated.

These platforms relay water quality data for four parameters: dissolved oxygen, water temperature, pH, and specific conductance. When data are received a screening process takes place in order to assess their validity. A summary report on conditions is then prepared and transmitted from the U.S. Geological Survey's Current Records Center in Philadelphia, Pennsylvania, to the operating agencies in the basin. Such agencies include the Delaware River Basin Commission (DRBC) and the National Weather Service.

Near real-time relay has been promised by NASA Data Processing Facility (NDPF) to commence October 2, 1972. This service will transmit data via hard line from Goddard Space Flight Center to the Current Records Center after each pass. The screening process will be performed and transmission of the summary via teletype is initially anticipated by 1400 hours, Eastern Standard Time, daily. In effect, this is approximately a four-hour delay for quality control and re-formatting of the released data. This is within the present data requirements of the DRBC.

*Publication authorized by the Director, U.S. Geological Survey.

DETECTION OF ICE CONDITIONS IN THE QUEEN ELIZABETH ISLANDS

E. Paul McClain
National Oceanic and Atmospheric Administration

It has been demonstrated with Nimbus 3 data that melt water on ice packs can be detected by the sharp drop in reflectance that occurs in the reflective infrared portion of the spectrum, reflectance in the visible being changed little. This same useful characteristic has been found in the much higher-resolution, multispectral imagery from ERTS.

Figures XIV-1 and XIV-2 can be used to compare a visible band (MSS 4) with the near-IR (MSS 7) in the area just west of Melville Island (near 76N, 115W) on 28 July 1972. Most of the areas that appear distinctly darker in the near-IR than they do in the visible are inferred to be covered with melt water. A few small and very dark areas, mostly near the coast, show up in both bands indicating that these are open water. This is clearly shown in a false-color composite of MSS-4 and MSS-7 where in the melt water areas on the ice show up pink and the open water appears nearly black (not shown).

Canadian Ice Central charts for 24 July 1972 showed consolidated pack (10/10 total concentration) in the Melville Island area. Two to four-tenths of this was multi-year ice, four-tenths was second-year, and two to four-tenths was first-year. Three to four-tenths puddles on the ice were reported. Mould Bay (77 N, 120 W), the nearest meteorological station, reported surface air temperatures from 37-43°F. near noon during this period.

In conclusion, we think that using the visible bands (Bands 4 and 5) in conjunction with the near infrared band (Band 7) is a very useful means of monitoring not only the ice itself but some important characteristics of the condition of the ice; namely when there are pronounced meltwater areas present on the ice and also the open areas such as the leads and polynyas.

(See page 128 for figures XIV-1 and XIV-2.)

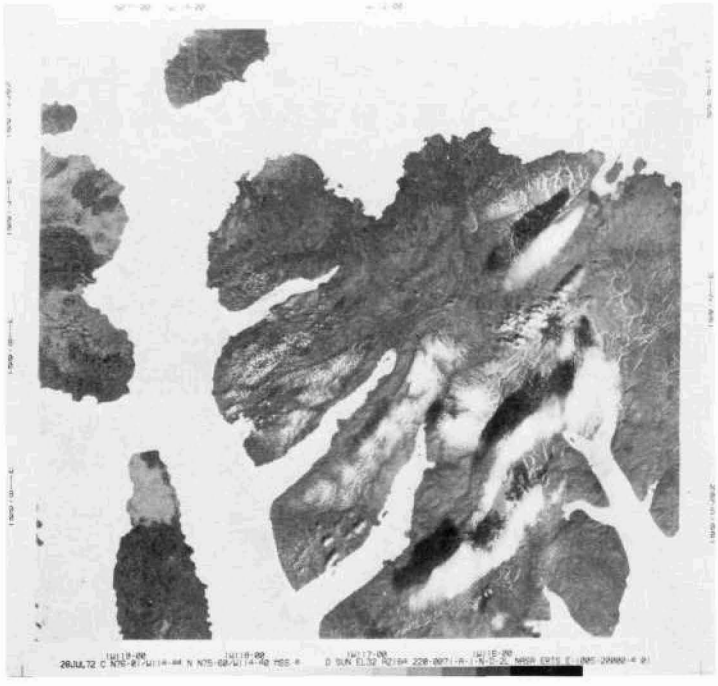

Figure XIV-1. MSS Band 4 image of area immediately west of Melville Island.

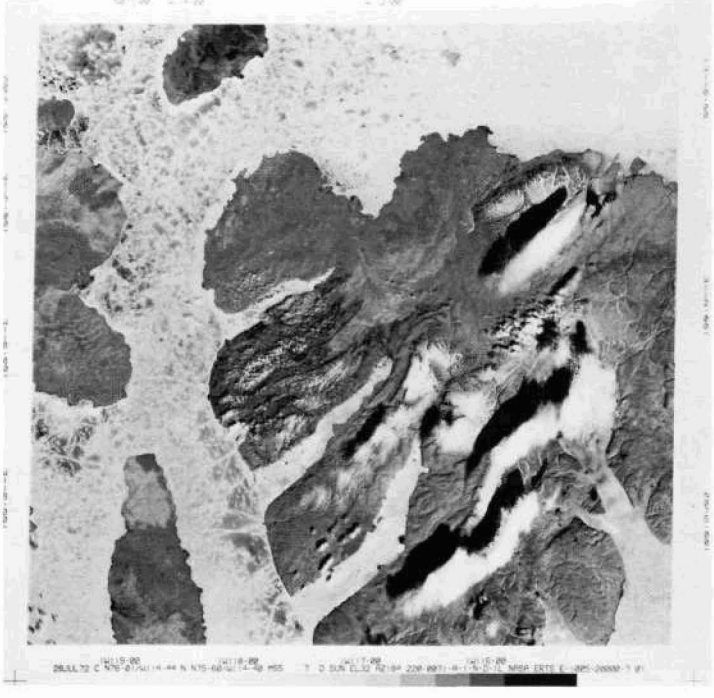

XIV-2. MSS Band 7 of the same image. Note dark areas, especially near the coast in the northwestern portion of the image.

ANALYSIS OF ARCTIC ICE FEATURES

William I. Campbell
U.S. Geological Survey

Previously available satellite pictures from ITOS and Nimbus have been useful for ice surveillance, but their relatively coarse ground resolution limited their detection capabilities to only the major ice boundaries and the largest ice features. The ERTS imagery is clearly the best sequential, synoptic data on ice ever taken by means of remote sensing for purposes of ice dynamics studies such as those being conducted as part of the AIDJEX project. It is of the highest importance for these investigations that ERTS coverage of the western Beaufort Sea area be maintained as long as illumination conditions are adequate. Four of six IRLS transmitters emplaced in the ice are still functioning.

Figure XV-1 (MSS 7) illustrates a variety of ice conditions in the vicinity of Cornwall Island (approximately 78N, 95W) on 27 August 1972. Figure XV-2 (MSS-7) shows the same area a few days earlier (23 August), and the significant ice movements in some areas are readily apparent. Surface air temperatures at Resolute (approximately 75N, 95W) were near or slightly below freezing at local noon during this period. The Canadian Ice Central reported total ice concentrations varying from open pack (6/10) to consolidated pack (10/10). Multi-year and second-year ice each ranged from 1/10 to 4/10, with first-year ice varying from 2/10-4/10. Some puddles, 6/10 frozen, were reported.

Rather different ice conditions than in the earlier figures were observed in the 27 July 1972 image for the Cape Bathurst area (near 70N, 127W, Figure XV-3). The Canadian Ice Central reports open (4/10) to very open (2/10) pack with many open water areas in this region for that period. Only multi-year ice is present, and surface air temperatures at Sacha Harbor (72N, 125W) were in the range 37-57°F during this time.

(See page 130 for figures XV-1, XV-2 and XV-3.)

Figure XV-1. Vicinity of Cornwall Island, Canada. Note the pack ice and the more open ice condition between the two islands in the lower right portion of the image. MSS Band 7 image.

Figure XV-2. Same general location as Figure XV-1. Note the presence of a considerable quantity of loose pack ice in the passageway itself. MSS Band 7 image.

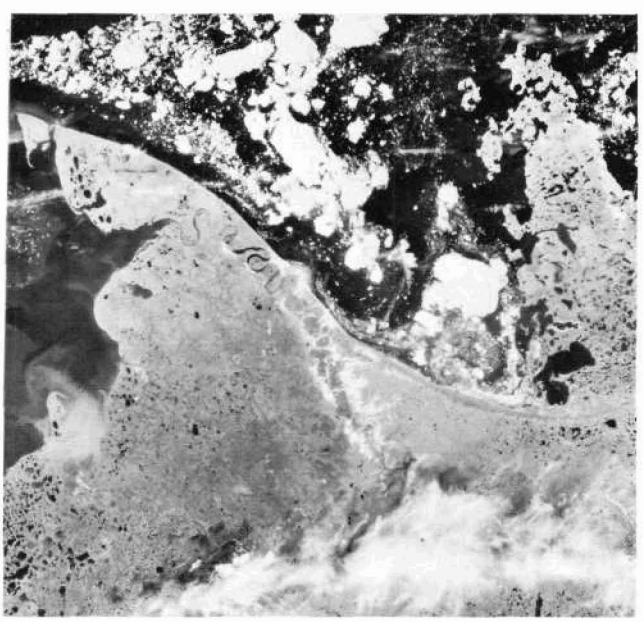

Figure XV-3. Cape Bathurst in the Franklin Bay area of northern Canada. MSS Band 5 image.

DETECTION OF SNOW CONDITIONS IN MOUNTAINOUS TERRAIN

Donald R. Wiesnet
National Oceanic and Atmospheric Administration

SNOWLINE DETERMINATION

ERTS-1 imagery of Washington taken during Orbit 70, July 28, 1972, clearly shows the snowline in the Cascade Mountains. Using this imagery, the snowline elevation on Mt. Rainier was found to range from 5100′ to 5800′ above msl in four different sectors with an overall average of 5500′ msl. The U.S. Geological Survey's glaciologists in Tacoma, Wash., give a mean firn line on Mt. Rainier at 6000′ msl. The snowline in July ranges from 5,000′ to 10,000′. This year's record snowpack would make 5500′ a very reasonable figure.

MELTING SNOW DETECTION

Previous studies of the differential spectral reflectance of melting snow and ice using Nimbus III HRIR data indicate that melting snow reflects less energy in the near-IR range than in the visible range of the spectrum. Preliminary examination of ERTS-1 MSS imagery from the Cascade Mountains of Washington as well as from British Columbia in Canada tentatively confirms this finding.

Enlargements of two frames from the ERTS-1 70 mm imagery from Orbit 70 (July 28, 1972) over the Cascades are shown in Figures XVI-1 and XVI-2. Band 4 (.5-.6 μm) is shown in Figure XVI-1 and Band 7 (.8-1.1 μm) is shown in Figure XVI-2. Snow-capped Mt. Eldorado (8868′) lies in the northeast corner. The snow area south of it includes Snowking Mountain (7438′) and Spirepeak Mountain (8261′).

Comparing the .5-.6μm band with the .8-1.1μm band reveals that snow reflectance is greatly reduced in the near IR (.8-1.1μm) except in the Spirepeak area, indicating that melting snow conditions prevail. The same effect is clearly seen in Orbit 42 (July 27, 1972) imagery of the Revelstone area of British Columbia (not shown). The air temperatures in the Cascade area ranged from 60-85° F (1000 PST.). Rawinsonde 700-millibar charts place the 10,000 foot level temperatures near 11° C in Oregon and -3° C in northern British Columbia.

In conclusion, although the ERTS-1 revisit time is unsatisfactory to some hydrologists, the resolution of the ERTS-1 multispectral scanner is certainly sufficient for determining snow-line elevation in mountainous terrain for all but the most stringent hydrologic requirements.

Figure XVI-1. Enlargement of ERTS-1 imagery of the Cascade Mountains. MSS Band 4.

Figure XVI-2. Enlargement of ERTS-1 imagery of the Cascade Mountains. MSS Band 7.

DETECTION OF CIRCULATION FEATURES IN THE GREAT LAKES

A.E. Strong
National Oceanic and Atmospheric Administration

Nearly two inches of rain flooded the Duluth, Minnesota, area between 5 and 7 August 1972. As this water drained off the land flowing out into Lake Superior it carried a vast load of sediment, mostly clay and silt. On 12 August ERTS-1 viewed the area and witnessed western Lake Superior to be very turbid. The sediments served expeditiously to color the currents thereby revealing circulation patterns over much of the lake west of the Apostle Islands. A cyclonic gyre, approximately 25 miles in diameter was revealed by the turbid waters, immediately off Duluth-Superior (Figure XVII-1). The waters along the entire southern shoreline showed an eastward transport through the Apostle Islands.

The same storm produced suspended sediments along the western Lake Michigan shoreline that ERTS-1 viewed 9 August (Figure XVII-2). Concentrations of turbidity were greatest near Milwaukee and Chicago. Coastal currents were southward.

As expected, the red (0.6-0.7μm) channel is optimum for revealing turbid features. Intensity correlates well with surface turbidity measurements. Not only are currents in these Great Lakes waters easily identified, but diffusion and dilution of these currents can be demonstrated through the use of ERTS-1 imagery.

(See page 134 for figures XVII-1 and XVII-2.)

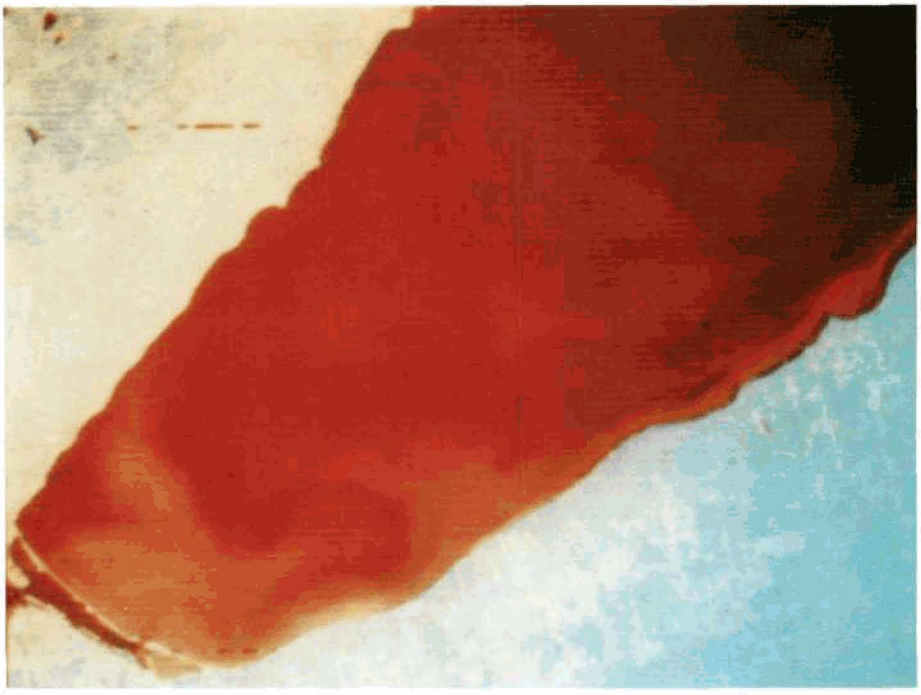

Figure XVII-1. Enlarged portion of ERTS-1 imagery, 12 August 1972, showing circulation patterns in Lake Superior offshore from Duluth, located in the lower left corner.

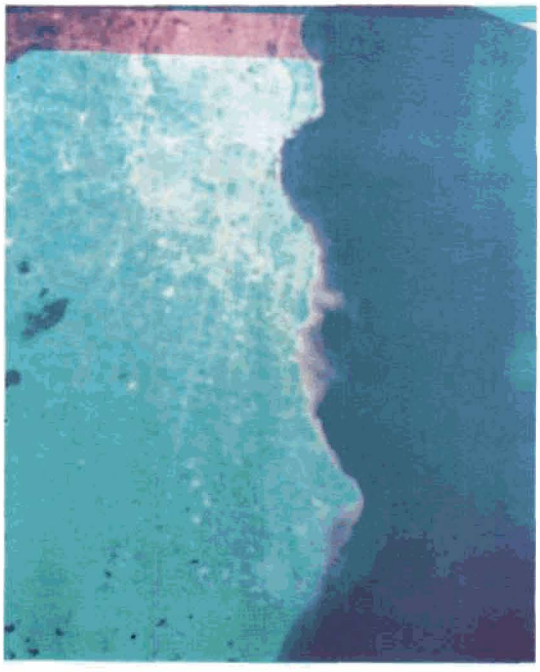

Figure XVII-2. Enlarged portion of ERTS-1 imagery showing areas where sediment is being transported into Lake Michigan in the vicinity of Milwaukee.

DELINEATION OF PERMAFROST BOUNDARIES AND HYDROLOGIC RELATIONSHIPS

Duwayne M. Anderson
U.S. Army Cold Regions Research and Engineering Laboratory

We have analyzed the ERTS-1 MSS color composite of the Koyukuk-Kobuk River area, Alaska and RBV scenes of adjoining regions in the Brooks Range to the north (Figure XVIII-1). An interpretation team consisting of a geographer, a soil scientist, a geologist and a hydrologist studied tones, textures and patterns evident in the imagery. These were subsequently compared with existing maps and other data on surficial geology, vegetation, topography and permafrost. We believe that the tonal differences in the MSS color composite relate to vegetation density as well as species composition. Four density levels have been identified and mapped in this scene. They are:

- High density tones (very dark red) occurring along streams, resulting in a galaria forest type pattern.
- Medium density tones (dark red) on the upland areas are believed to be associated with the well developed white spruce forest. Recently burned areas within this unit appear as very high density black tones.
- Low density tones (reddish gray) occur in the extensive lowland areas. These areas are essentially treeless bogs and are punctuated by many thaw lakes typical of alluvial, poorly drained permafrost areas.
- Very low density tones (gray with very little red) probably indicative of old burn scars. In these areas shrubs are the dominant vegetation.

Eight surficial geology units have been recognized and mapped (Figure XVIII-2). They are:

b	Bedrock and colluvium deposits
Q_o	Outwash deposits
Q_{ag}	Undifferentiated alluvial, glaciofluvial deposits
Q_{fl}	Fluvial and Lacustrine deposits
Q_e	Eolian deposits
Q_u	Undifferentiated deposits
Q_f	Fluvial deposits
Q_{al}	Undifferentiated Alluvium-Lacustrine deposits

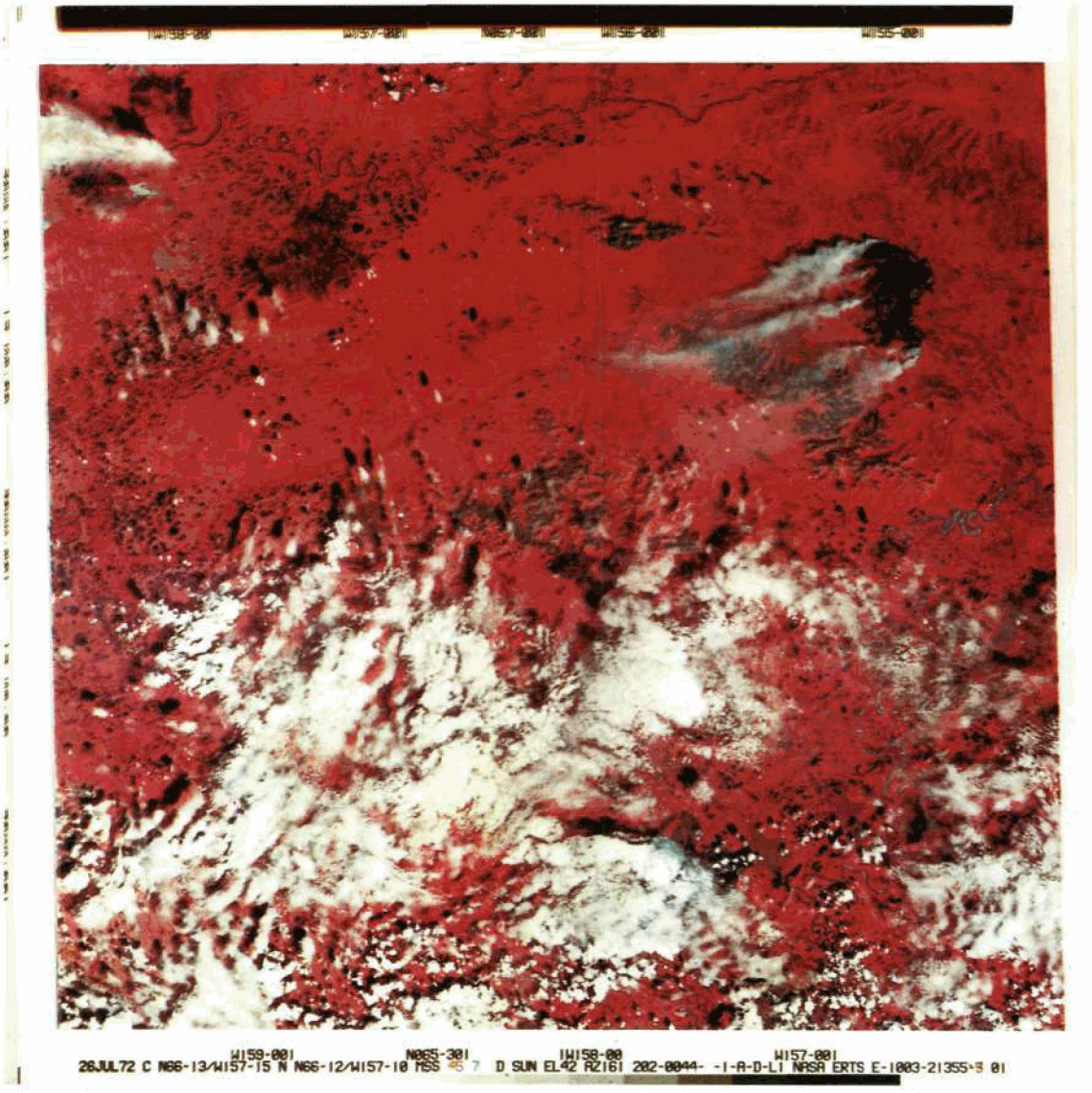

Figure XVIII-1. MSS composite some 200 miles north of Fairbanks, Alaska in the Koyukuk River region. Smoke plumes from a forest fire are seen in the upper right portion of the photograph. The meander pattern of the Koyukuk River is visible in the upper left part of the photograph.

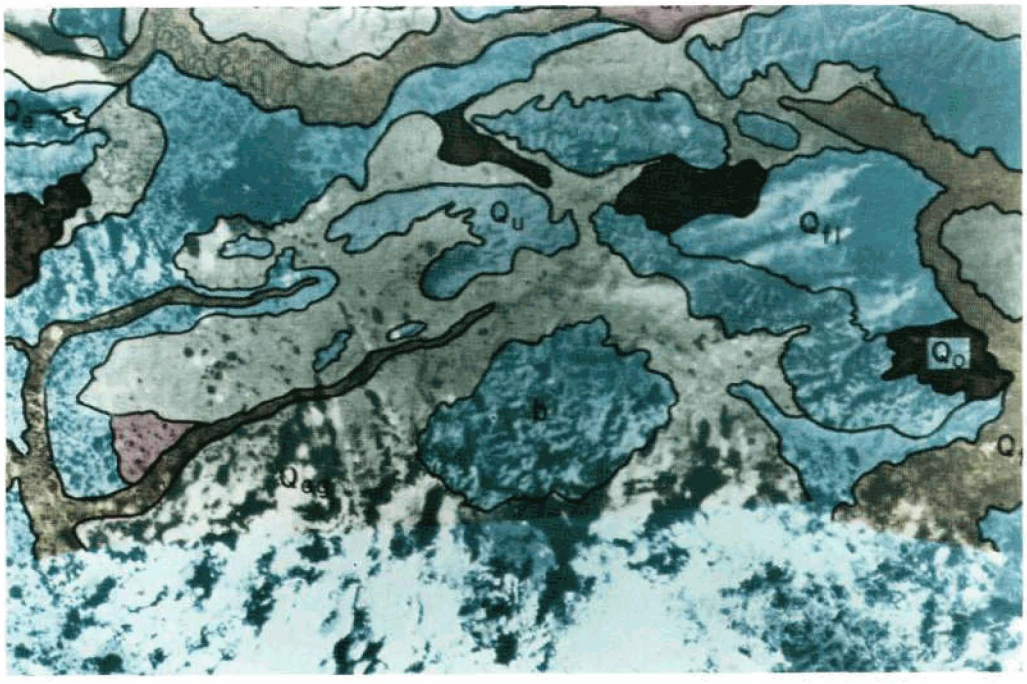

Figure XVIII-2. Enlargement of the upper portion of Figure XVIII-1. Mapped units represent the surficial geology units.

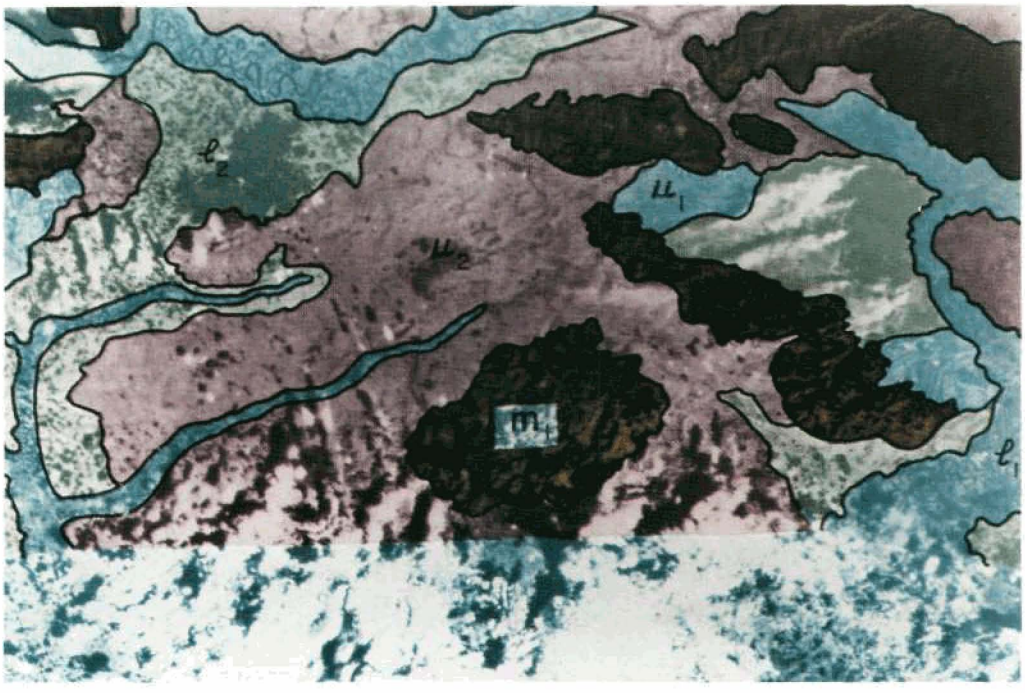

Figure XVIII-3. Enlargement of the upper portion of Figure XVIII-1. Mapped units represent permafrost categories.

Five categories of permafrost have been recognized and mapped. In this preliminary interpretation it was found most convenient to employ geologic terms as category descriptors (Figure XVIII-3). They are:

M_1 Bedrock and colluvium scattered taliks; moderate seasonal thaw. Includes alpine vegetation grading into white spruce forest below timberline.

U_1 Dissected alluvial deposits. Numerous taliks. Solifluction probably active. Alpine vegetation. Thaw depth; moderate.

l_1 Active floodplains. Numerous taliks, vegetation dense shrubs interspersed with black spruce. Deep seasonal thaw.

l_2 Abandoned floodplains. Scattered taliks primarily in close association with large water bodies. Vegetation predominantly grasses, sedges, and small shrubs. Depth of thaw; shallow.

U_2 Alluvial-Colluvial deposits. Continuous permafrost, vegetation white spruce forest on well drained slopes grading to shrubs and grasses in less well drained sites. Thaw depth shallow where drainage is poor to moderate on south facing well drained slopes. Thaw depths: Shallow $<.5$m; Moderate .5-2m; Deep >2m.

The increase in size of an active burn area (Pah River fire) during the period July 8 to July 26 was determined by color densitometer planimetry to be 20,000 acres in 18 days.

CHLOROPHYLL STRUCTURE IN THE OCEAN

Karl-Heinz Szekielda
University of Delaware
Robert J. Curran
Goddard Space Flight Center

Before we started our program we simulated an experiment with the spectral response of the 0.5 to 0.6 μm region of the MSS over oceanic regions with different chlorophyll concentrations. It showed a significant relationship between the obtained signal and the chlorophyll concentration in water. Our studies in upwelling areas with ERTS-1 make it necessary to estimate the chlorophyll concentration. Since sediments in near coastal areas respond in a similar way as chlorophyll within the spectral response of the MSS, it was intended to differentiate in a qualitative study between the effect of sediments suspended in water and chlorophyll on the different channels.

The target for a representative estuary with sediment discharge was the St. John's River in the south of the United States as shown in the color composite from channels 4, 5 and 7 (Figure XIX-1). Over cloud-free areas the river discharge is indicated by a higher reflected energy in the visible compared to the open ocean. Clouds are very easy to distinguish from sediment loaded water masses.

The black and white imagery of the channels 0.5-0.6 μm; 0.6-0.7 μm; 0.7-0.8 μm; and 0.8-1.1 μm was color enhanced to display the reflective properties of chlorophyll concentration (Figure XIX-2). Channel 4 (0.5-0.6 μm) monitored the effect of chlorophyll as well as sediments and exhibits a diffuse structure in the response of the MSS. The next channel, located at 0.6-0.7 μm indicates a very pronounced gradient within the sediment plume. This is caused by the position of the second absorption band of chlorophyll at 0.66 μm and the increased absorption of water which limits the photon penetration depth. The recordings in the near infrared (0.8-1.1 μm) gave a response only in the near coastal areas, thus indicating near surface parameters. The transport of sediments is limited to the coast and is in agreement with the direction of near coastal currents.

Pure phytoplankton populations should cause a response principally in channel 4. This response is the result of increased reflectivity at short wavelengths and the compensation of reflection by absorbtion in channel 5.

Our ground truth measurements indicated chlorophyll concentration up to 20 $\mu g \cdot \ell^{-1}$. The visibility measured with the secchi disc is only several meters, which shows that the topography does not affect the signal obtained with ERTS-1. Since channel 5 showed no

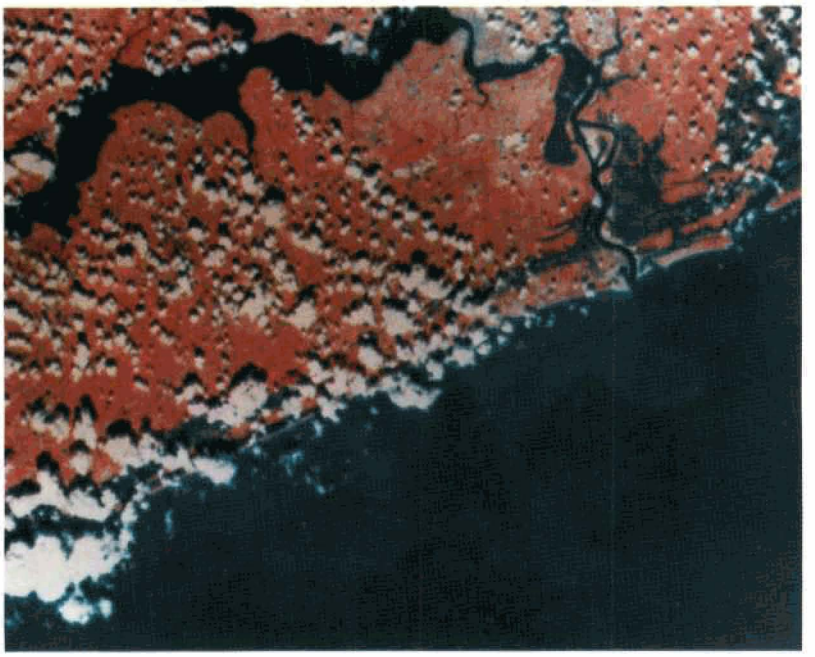

Figure XIX-1. Enlargement of MSS color composite of St. John's River Estuary in Florida.

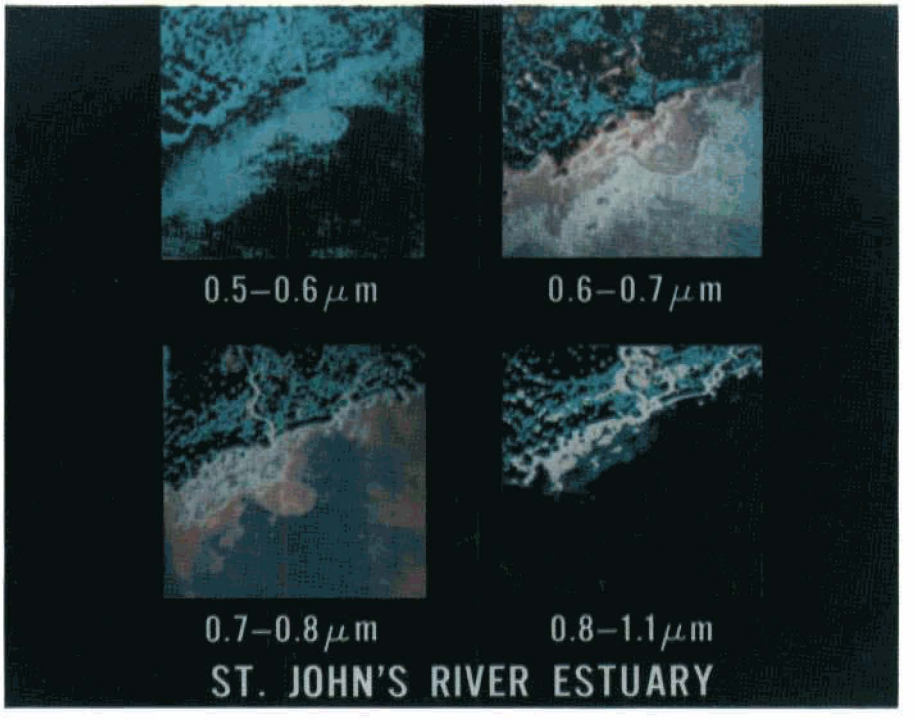

Figure XIX-2. Color enhanced density slices of each of the four MSS bands of the same general area shown in Figure (XIX-1).

visible structure, and also sediment transport by river discharge is absent we can conclude that the structure visible in channel 4 is due to the distribution of chlorophyll.

The oscillation of chlorophyll boundaries as well as the separated zones with high chlorophyll content, as seen with ERTS-1 was also recognized by continuous chlorophyll measurements carried out with a fluorescence technique aboard a research vessel in the same area.

BARGE DUMPING OF WASTES IN THE NEW YORK BIGHT

C.T. Wezernak
F.J. Thomson
Willow Run Laboratories
University of Michigan

A variety of municipal and industrial wastes are disposed of by barge dumping in the waters of the New York Bight, including sewage sludge and acid wastes (Figure XX-1). Disposal of these wastes by barge dumping produces surface films and waste fields whose fate and effects are not completely defined.

An important element in present and future programs for managing ocean disposal of wastes at this and other locations is the requirement for a monitoring system which will (1) document authorized discharges to verify compliance in terms of discharge location, (2) detect unauthorized dumps or accidental discharges, and (3) provide data regarding the movement of wastes. Monitoring systems are required not only for the detection of small spills and discharges but also for monitoring large scale processes and phenomena. The present investigation is an example of the latter.

The specific objectives of this investigation are as follows:

1. Provide data regarding the surface spread and movement of wastes discharged by barge dumping
2. Delineate major spectral anomalies and relate to existing waste disposal practices
3. Provide data regarding surface circulation in the New York Bight

A preliminary analysis of aircraft and spacecraft data collected on 16 August 1972 (ERTS Image ID E-1024-15071-4, E-1024-15071-5, E-1024-15071-6) clearly shows the distribution of an acid-waste discharge, sewage sludge dump and major suspended sediment inputs into the study area (Figures XX-2, XX-3 and XX-4). Additionally the data analysis shows the surface drift patterns of the waste inputs and major waste masses at the time of observation. The data also indicate that under the sea-state conditions existing at the time of observation, the disposal of acid waste produces a suspension which tends to remain in a distinct pattern for extended periods of time.

Earlier studies of surface circulation (using drift bottles) indicate a complex circulation pattern. Adequate definition of these patterns will require synoptic coverage over a large area of the type available from satellite altitudes.

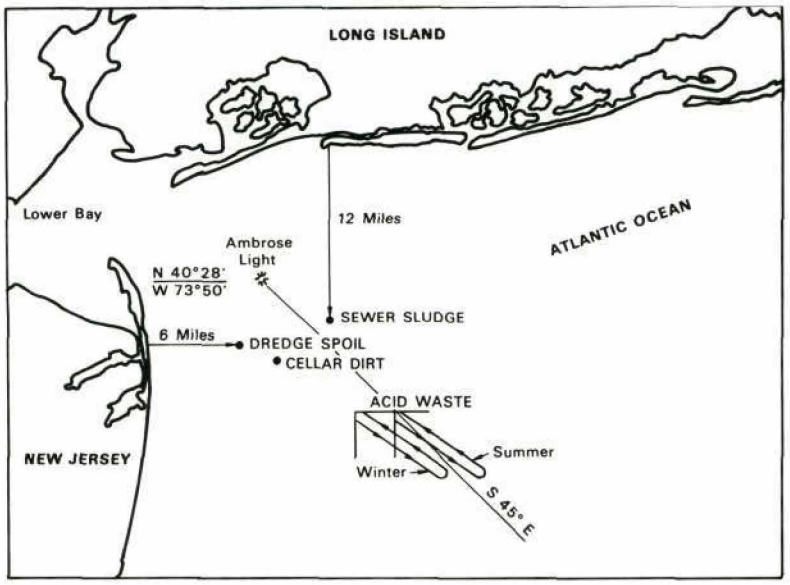

Figure XX-1. Map showing waste disposal sites in the New York Bight.

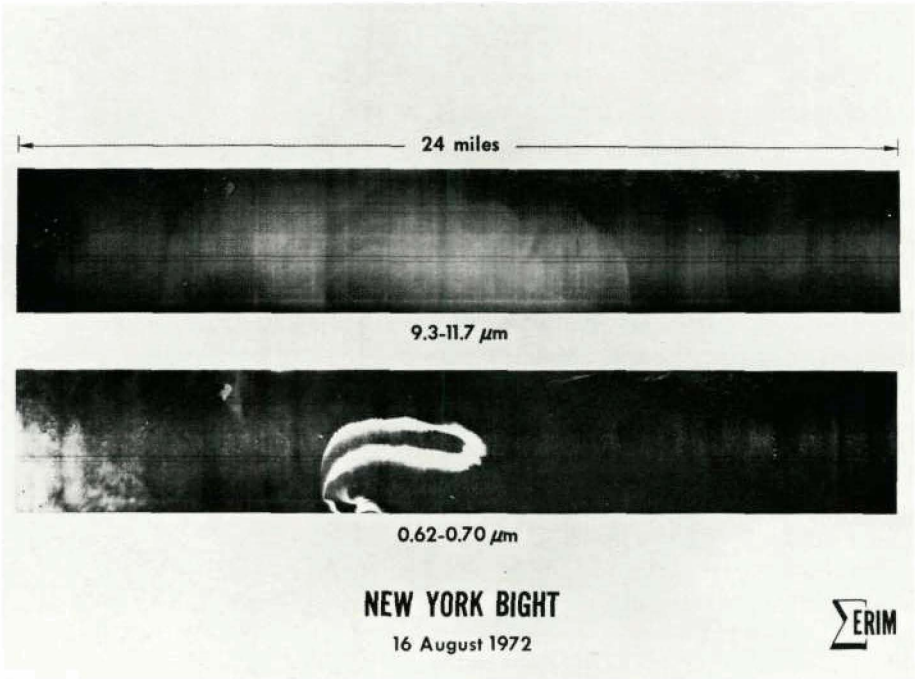

Figure XX-2. Aircraft data obtained with the University of Michigan C-47 aircraft and 12-channel multispectal scanner. The aircraft underflight was nearly simultaneous with the ERTS transit.

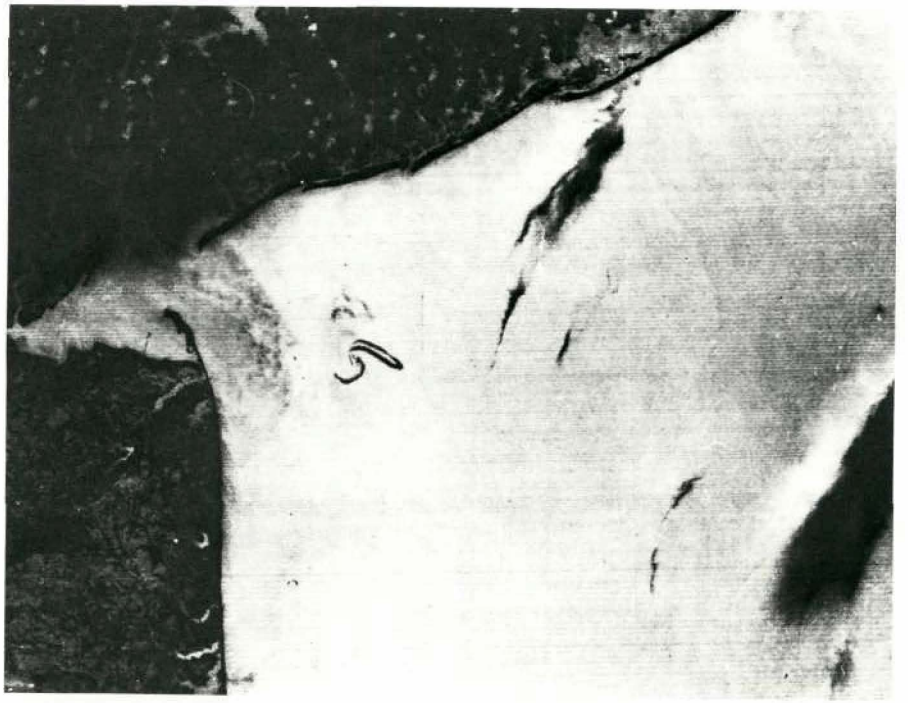

Figure XX-3. Enlargement of an ERTS-1 image 16 August 1972, MSS Band 5, 0.6 to 0.7 μm. Note the clearly defined acid waste area. Full-frame ERTS image is reproduced in Figure XI-1.

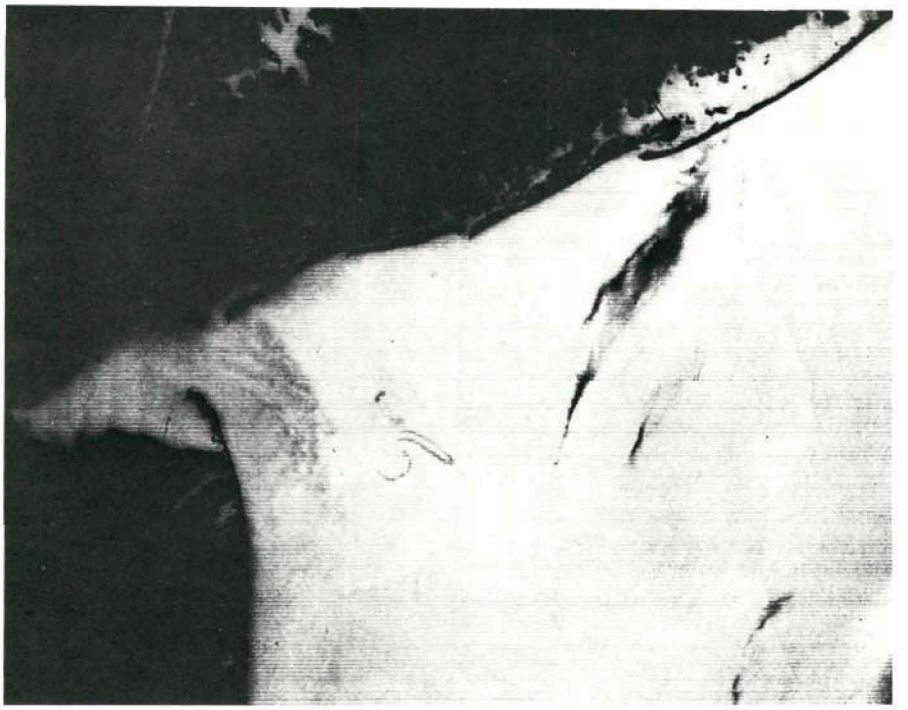

Figure XX-4. Enlargement of an ERTS-1 image 16 August 1972, MSS Band 6, 0.7 to 0.8 μm. Note less detail of sea surface features. Full-frame ERTS image is reproduced in Figure XI-1.

Preliminary analysis of ERTS data indicates that the remote sensing program is providing information which will contribute towards an understanding of the environmental effects of marine dumping.

COASTAL OCEAN OBSERVATIONS FROM ERTS

R. Charnell and G. Maul
National Oceanic and Atmospheric Administration
Miami, Florida

The Earth Resources Technology Satellite (ERTS-1), made a transit over New York Bight on 16 August, 1972. This image supplies valuable information on the utility of using a satellite for large area synoptic oceanic observations (see Figure XX-3 in Wezernak and Thomson's article). The Hudson River plume is easily distinguished and appears to be 18 miles long and 2 miles wide. Two transects across the plume on August 10 and August 22 show a drop in surface salinity in the plume of about 2%. Evidence of waste disposal is also seen in the frame. The lineal feature 15 miles east of Sandy Hook is probably the waste acid dump while the diffuse patch just to its north is residence from sewer sludge dumping.

This single image, taken in an area of complex oceanography and high population density, demonstrates the utility of satellites such as ERTS, equipped for surveying water quality changes, such as location of river discharge plumes and the effectiveness of waste dumping procedures. It seems likely that satellites with sensors optimized to view the ocean in visible and infrared wavelengths, supplying synoptic wide-area data, will make management of the coastal zone on a broad scale much more realistic.

INTERPRETATION OF WETLANDS ECOLOGY FROM ERTS-1

Richard R. Anderson, Virginia Carter, Bill McGinness
The American University

ERTS-1 images of wetlands along the South Carolina–Georgia coastline and the southern New Jersey coastline have been given preliminary analysis for ecological conditions in wetlands. The objectives of the research are as follows: (1) plant community composition; (2) successional trends; (3) identification of man-made or other causes of reduction in productivity of wetlands; and (4) delineation of shallow, productive waters around the wetlands.

RBV and MSS bands have been analyzed singly and collectively using the Spatial Data Corporation, Datacolor System, the Multispectral Image Analysis System (MIAS) and the I^2S Digicol and Addicol systems. Each system apparently is going to provide certain pieces of information and no one system will provide all necessary data.

The following preliminary results have been obtained:

- The red band on both RBV and MSS appears to be the least useful for density analysis of individual bands.
- MSS bands 6 and 7 are very similar and one or the other may be used for density analysis or additive color enhancement.
- The wetland-dryland interface is clearly defined, particularly on the IR bands and is well delineated using additive color procedures.
- Tonal structure with wetlands is good when color additive viewing is utilized. This tonal structure is interpreted as species differences including *Spartina alterniflora* and *Spartina patens.*
- Transition zones from wetland to dryland are tonally unique and may be used to judge successional trends in wetlands.

MULTISPECTRAL SCANNER IMAGERY OF THE SIERRA NEVADA: GEOLOGIC ANALYSIS

Paul D. Lowman, Jr.
Goddard Space Flight Center

As part of a preliminary geologic evaluation of ERTS-1 imagery, a multispectral scanner color composite (Figure XXIII-1) covering the northern Sierra Nevada, California, has been studied. The objective was to determine the geologic value of MSS images by drawing a structural map from the color composite.

The general approach taken was to compare the MSS picture in 18 X 18 cm-size, with a scale of 1:1,000,000, with the 1:250,000 scale Geologic Map of California (Chico, Sacramento, and Walker Lake Sheets). The section of the picture's area lying in Nevada was not studied. The reasoning behind this approach was that the 1:250,000 maps, all published later than 1958, should in principle show at least four times as much structural detail as the MSS picture, and perhaps more, since the MSS picture used was enlarged from a 70mm original.

The picture was first examined for previously-mapped geologic features, in particular lithologic contacts and faults. Contacts proved to be difficult to find on the MSS picture unless they had strong physiographic expression. The main lithologic contacts that could have been drawn with any confidence were those between bedrock and Quaternary alluvium; in addition, the Pliocene volcanics around Relief Peak could also be delineated. This problem was due not only to general lack of physiographic and tonal/color expression, but also to the heavy forest cover in the Sierra Nevada and the extensive cultivation in the Great Valley. Experience with previous orbital photography (Lowman and Tiedemann, 1971) had indicated this to be a probable difficulty, and stress was therefore placed on structural features.

This analysis was essentially conventional, consisting of construction on a light table of a drainage overlay (Figure XXIII-2). The principle behind such analysis is that any departure from dendritic drainage (i.e., a random pattern) probably reflects bedrock control, at least in areas of moderate slope. As applied to the MSS picture, unusually straight valleys or aligned segments of valleys, if not corresponding to mapped lithologic contacts or dipping strata, were interpreted as fracture-controlled. These fractures were plotted as dashed lines to distinguish them from mapped faults. In addition to those plotted, a fracture or fault zone probably controls the course of the Stanislaus River (lower right).

The nature of these fractures is difficult to determine without field-checking or study of air photos; specifically, it is not possible to distinguish faults from joints. Parallelism between fractures plotted from the MSS picture and mapped faults strongly suggests that at least some of the former are faults. However, the description of regional joints of the

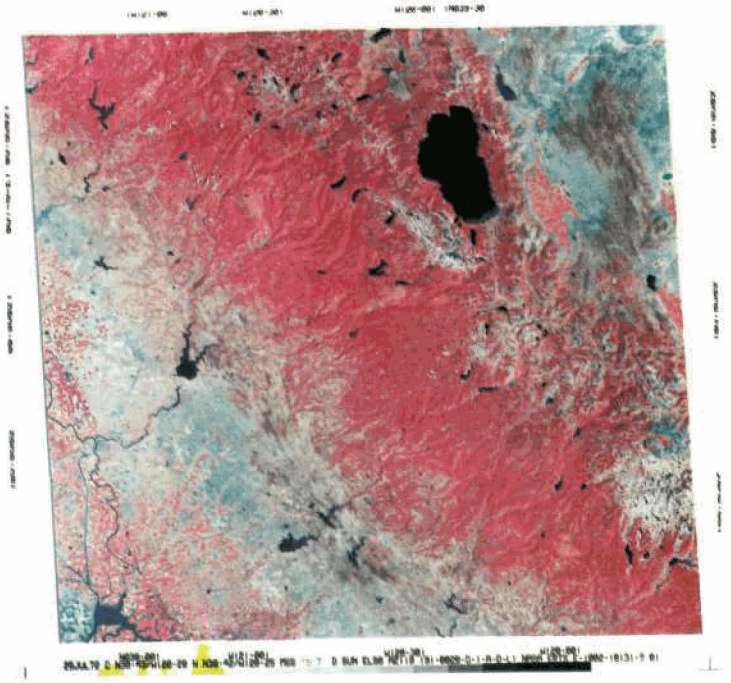

Figure XXIII-1. ERTS-1 multispectral scanner color composite, bands 4, 5 and 7, taken July 25, 1972, showing the northern Sierra Nevada, California. Center of photograph N 38 ° 43′, W 20° 28′; sun elevation 58 °, azimuth 119°.

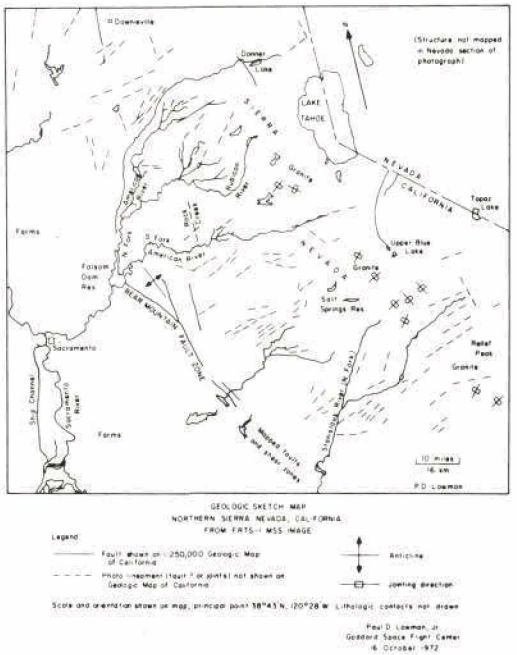

Figure XXIII-2. Geologic sketch map drawn from ERTS-1 color composite (Figure XXIII-1). Stanislaus River (lower right) is probably fracture-controlled, although not shown as such. Crest of Sierra Nevada lies just west of Lake Tahoe and trends northwest.

Sierra Nevada by Bateman and Wahrhaftig (1966) indicates that joints are also prominent. The closely-spaced lineaments in areas of exposed granite have accordingly been mapped as joints. A third type of structure (not plotted), found east of Salt Springs Reservoir, consists of closely-spaced curved lineaments. Similar features in the southern California batholith seen on Apollo 9 photography (Lowman, 1972) have proved to be the topographic expression of flow structure and xenoliths in the intrusions making up the batholith. Further geologic interpretation would be beyond the scope of this report, which is intended primarily as an evaluation of the MSS imagery rather than as a geologic investigation.

In summary, the MSS color composite of the northern Sierra Nevada has provided a convincing demonstration of the geologic value of this imagery. Many geologic structures, many of which may be faults, not shown on recent 1:250,000 scale maps are visible on the ERTS picture. A possible explanation for this is that the California geologic maps used are actually compilations of previously published larger scale maps. Several of those covering the northern Sierra were published in the 1890's, before the availability of aerial photography. It is therefore clear, as Jennings (1966) points out, that much remains to be done in the geologic mapping of California. The ERTS-1 data should be extremely useful in this work.

REFERENCES

Bateman, P.C. and C. Wahrhaftig, 1966, Geology of the Sierra Nevada, in *Geology of Northern California* (ed. E.H. Bailey), California Division of Mines and Geology, Bulletin 190, San Francisco, pp. 107-172.

Jennings, Charles W., Introduction: State Geologic Maps of California – a Brief History, in *Geology of Northern California* (ed. E.H. Bailey), California Division of Mines and Geology, Bulletin 190, San Francisco, pp. 3-16.

Lowman, P.D., Jr., 1972, *The Third Planet: Terrestrial Geology in Orbital Photographs,* Weltflugbild Rinhold A. Muller, Feldmeilen, Zurich, Switzerland, 170 p.

Lowman, P.D., Jr., and H.A. Tiedemann, 1971, *Terrain Photography from Gemini Spacecraft: Final Geologic Report,* X-644-71-15, Goddard Space Flight Center, Greenbelt, Maryland, 75 p.

QUICK LOOK ANALYSIS OF LOS ANGELES TEST SITE SCENE WITH GENERAL ELECTRIC MULTISPECTRAL INFORMATION EXTRACTOR SYSTEM (GEMS)

Richard Economy
General Electric Co.

The analysis reported here is from the ERTS E1018-18010 scene, a 9.5 inch color transparency with MSS bands 4, 5, and 7 received a few days ago. The analysis on the GEMS was done during half-a-day on the system with some real-time communication with the Test Site Coordinator, Mr. Jene McKnight, of the county of Los Angeles Regional Planning Commission over long distance phone. A color print of the scene was made available to Mr. McKnight whose visual observations and comments helped in selecting and analyzing the topics and areas selected to report here. He was very impressed with the imagery even though it is not as sharp as the Monterey scene print he had seen earlier.

The two topics for quantitative analysis were:

- Agricultural Inventory in a portion of the Antelope Valley (Figures XXIV-1, XXIV-2 and XXIV-3).
- Surface water bodies in the western county (Figure XXIV-4).

The ground truth data for the field crops for 1972, is being obtained by Mr. McKnight from the County Agricultural Field Representative in Lancaster, California to verify the GEMS-analyzed acreages. The RPC supplied the 1971 crop data for the Alpine Butte quadrangle as well as the average data over a few years gathered for their Environmental Design Guide program.

The water body surface areas as analyzed from the ERTS imagers by GEMS, both in the CRT display form as well as the digital printouts are being obtained by Mr. McKnight from the two major agencies under whose jurisdiction the public water management falls:

- The State Water Resources Board
- The Los Angeles City Water and Power Department

In summary, it can be said that the purpose of this experiment, which is to derive planning information from ERTS-1 images to be used by the Los Angeles Regional Planning Commission, is an achievable goal.

Figure XXIV-1. Display of 9x9 mile area in eastern Antelope Valley, obtained by GEMS analysis of an ERTS-1 image of Los Angeles. The grid is a superimposed map of the major section line roads in this area. The road intersection near the letter "D" is East Ave. and North 100th street. Based on preliminary ground truth data the superimposed pink area represents alfalfa fields under irrigation; the pink area represents 3.6% of the scene, or 1870 acres.

Figure XXIV-2. A GEMS normalized display of the same area shown in Figure XXIV-1. This enhancement aids the GEMS operator in identifying and interpreting various objects in the scene, for example the field structure and the difference between crops are more apparent after normalization. The dark blue fields are wheat and the reddish brown areas are alfalfa.

Figure XXIV-3. GEMS display of the same area shown in Figure XXIV-1. In this scene the irrigated alfalfa is superimposed in white and the total cultivated area is shown in white and purple. The total cultivated area is 12.3% of the scene, or 6400 acres.

Figure XXIV-4. GEMS processed area from the Los Angeles ERTS-1 image for a region north of Newhall, California. The water reservoirs have been identified and their areas totalized and superimposed on the enlarged section of the ERTS-1 image. The water areas in percent of scene, or acres, are available for readout and are stored in the computer for further analysis. In all, 24 water bodies in the ERTS image were identified and measured.

CROP CLASSIFICATION USING ERTS-1 DIGITAL TAPE DATA

Charles Sheffield
Earth Satellite Corporation
Ralph Bernstein
IBM Corporation

Earth Satellite Corporation, in conjunction with the IBM Corporation, has performed experimental crop classification in the San Joaquin Valley of California. The analysis has been restricted to images obtained by ERTS-1 on July 25, 1972, and uses wholly digital processing of multispectral scanner data obtained directly from the bulk MSS digital tapes.

The objectives of this work were twofold:

(1) To determine the general quality and utility of the information contained on the digital tapes provided by NASA, and to explore the feasibility of all-digital processing.

(2) To provide quantitative information about a conjecture that had often been made prior to the launch of ERTS-1. This conjecture can be summarized briefly as follows: The ERTS-1 spacecraft and orbit were designed to diminish the effects of certain variable factors that complicate crop classification by multispectral analysis from aircraft images. These uncontrolled (or unmodeled) degrees of freedom include the variation in sun angle, the variation in look angle, and variations in altitude and weather. In some sense, therefore, classification from the ERTS-1 spacecraft data should be "easier" or "better" than classification from aircraft.

We have given this proposition a somewhat different emphasis, and addressed the question: What quality of classification results can be achieved using ERTS-1 data with a minimum of prior aircraft and ground truth information? An answer to this question is important for several reasons. First, ERTS-1 is imaging many parts of the world in which aircraft and ground truth information are very hard to come by – this is particularly true in foreign investigations. In addition, however, the value of ERTS data will be considerably diminished in the United States if every ERTS overflight must be accompanied by costly aircraft and ground support in order to be used.

The classification procedure adopted was as follows:

- Intensity shade prints were generated directly from the MSS bulk digital tapes for each of the four spectral bands.
- Based on these intensity prints, areas of particular intensity ranges were selected by land use specialists as probably representatives of particular ground cover classes.

- Based on the selected areas as training samples, crop classification was performed on a large portion of the image (about 250 square miles). Two computer programs were used to perform the classification – the LARS program, developed by Purdue University, and a proprietary program, termed Program III, designed by EarthSat and implemented by IBM for use in an interactive environment.

Minor radiometric inconsistencies in the NASA-generated tapes existed for the July 25 data, and apparently have not yet been removed from subsequent tapes. The main effect is a slight intensity error on every sixth line of picture elements. This has the effect of producing occasional crop mis-classification. The effect of such errors on the tapes can be fairly easily removed by a simple image smoothing procedure applied to the digital tape itself, and any users of digital tapes should perform intensity consistency checks to determine whether or not the tapes they receive suffer from inconsistencies in intensity calibration.

The classification results obtained may be summarized as follows:

- Major land use classification can be performed using ERTS-1 data with excellent results. By this we mean that major broad categories of crops and land use can be clearly distinguished.
- Each picture element of the digital tape represents an area of about 5/6ths of an acre (0.4 hectares). Fields as small as 20 acres are successfully classified by the programs.
- More subtle crop classification cannot be performed from a single set of four ERTS-1 images obtained at a single moment of time. Thus, for example, on the frame we analyzed it was not possible to distinguish wheat from barley. Both crops were close to harvest, and human interpreters also proved incapable of distinguishing these crops by analysis of the imagery. The use of data at different times of the year is, therefore, necessary to make distinctions between such crops.
- The classifications obtained proved to be consistent across large regions of the ERTS image, supporting the idea that within a region of homogeneous climate ERTS will permit crop classification to be performed successfully based on a small localized training set.

The results stated above were validated by the use of aircraft photographs and ground truth tests performed shortly after the ERTS-1 image had been obtained. It should be emphasized, however, that the basic major classification was made by EarthSat analysts before any supporting evidence was available, and that the original categories defined from the intensity shade prints of the digital tapes stood up very well in the light of the subsequent ground- and aircraft-derived data.

COMPUTER PROCESSING OF ERTS-1 MSS DATA FROM THE "SAN FRANCISCO" FRAME

F.J. Thomson
M. Gordon
J. Morgenstern
F. Sadowski
Environmental Research Institute of Michigan

IBM 7094 digital computer analysis of ERTS-1 MSS data was initiated to identify important water, soil, and vegetation classes in the Sacramento Valley portion of the "San Francisco" ERTS-1 frame E1003-18175. Figure XXVI-1 shows a color infrared composite of the northwest portion of frame E1003-18175, with Lake Berryessa in the left center and Sacramento just off the photo to the lower right center. The study area of approximately 25 nm east-west and 15 nm north-south is enclosed in black lines.

This area comprises the major portion of two Bureau of Reclamation water irrigation districts near Woodland, California. Important agricultural crops in the area are rice, safflowers, barley, and various truck crops such as tomatoes and melons.

ERTS-1 MSS data was computer processed to recognize the important crops using spectral signature information collected by the MSS scanner. The color coded recognition map is shown in Figure XXVI-2. Computer estimates of acreages for the major crops are also shown. Preliminary analysis and field visits to the site show that rice, safflowers, and barley stubble (most barley had been harvested at the time of the overflight) can be reliably discriminated. Continuing work will focus on attempting to recognize the various truck crops and other green vegetation categories.

(See page 156 for figures XXVI-1 and XXVI-2.)

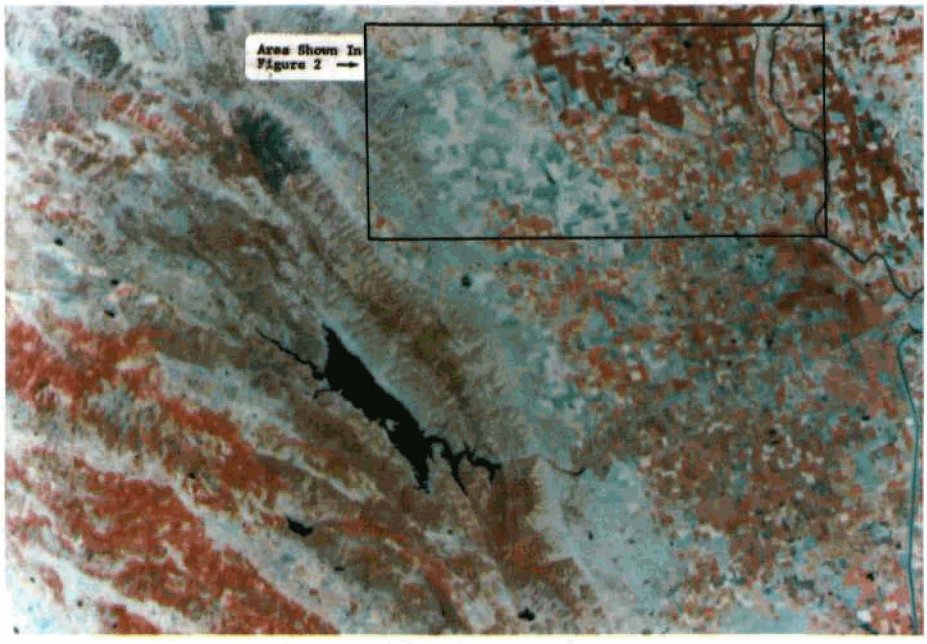

Figure XXVI-1. Enlargement of a portion of an ERTS color composite of the San Francisco area.

ENVIRONMENTAL RESEARCH INSTITUTE OF MICHIGAN
DIGITAL RECOGNITION MAP
OF SACRAMENTO VALLEY AGRICULTURE
ERTS FRAME 1003-18175, 25 July 1972

LEGEND

Color	Identification	Acreage	Color	Identification	Acreage
Dark Green	Rice	17105	Blue	Water	1755
Light Green	Other Green Crops	50974	Dark Red	Wet Bare Soil	4497
Gray	Safflowers	34293	Medium Red	Bare Soil	91280
Black	Truck Crops	8417	Light Red	Barley Stubble	37193
			White	Not Recognized	116

Figure XXVI-2. Computer generated color coded recognition map of the area shown in the inset in Figure XXVI-1.

THE ADVANTAGES OF SIDE-LAP STEREO INTERPRETATION OF ERTS-1 IMAGERY IN NORTHERN LATITUDES

Charles E. Poulton
Oregon State University

Since working with stereo interpretation of Apollo VI photography in southern Arizona, a number of us associated with that project and the SO65 Experiment were convinced that the parallax in space photography was great enough to justify serious consideration of its exploitation for human interpretation. Thus, one of the first things we examined upon receipt of both RBV and MSS imagery from ERTS-1 was the possible enhancement of interpretability of these new systems by exploiting binocular reinforcement and true or "apparent" stereo.

We found benefits significant although at this point we have not had time to experiment and determine the true information gain from stereo interpretation by human photo interpreters (PI's). The results are sufficiently encouraging, however, for us to urge NASA to continue to acquire all possible side-lap up to 50 to 60 percent and to urge that all participants who are in any way using the human PI approach to image analysis, fully exploit the stereo capability of the system to the extent that side-lap is provided at their latitudes.

In one of the EarthSat test sites, Sierra-Lahontan, between Latitude 38° and 40° N, the system initially gave us slightly over 50 percent side-lap. Subsequent to the 28 August orbit adjustment, we have been getting 46 percent side-lap at approximately 45° N in Oregon. This high percentage of side-lap is a tremendous asset if fully exploited in interpretation. Those working farther north should realize full stereo coverage. This capability is particularly important when interpreting natural vegetation, geological and landform features. In flat country, the advantage comes only from binocular reinforcement, but even this is significant. In strongly rolling to hilly relief, the gain in reinforcing the tone patterns is significant and in mountainous terrain it is very substantial.

Figure XXVII-1a shows a side-lap stereo model from ERTS-1 RBV in a moderately hilly to mountainous relief near the California-Nevada border south of Honey Lake. Figure XXVII-1b shows approximately the same area from the MSS-5 band also in side-lap stereo. You are urged to study these models first without stereo and subsequently with a stereoscope. You should be appreciative of the loss in reproduction, but note especially how the various tones representative of different vegetational types can be accurately related to landform and relief when viewed in stereo. This is exemplary of the information gain through associated evidence when interpretation is done from a stereo model. The following are my main conclusions at this time:

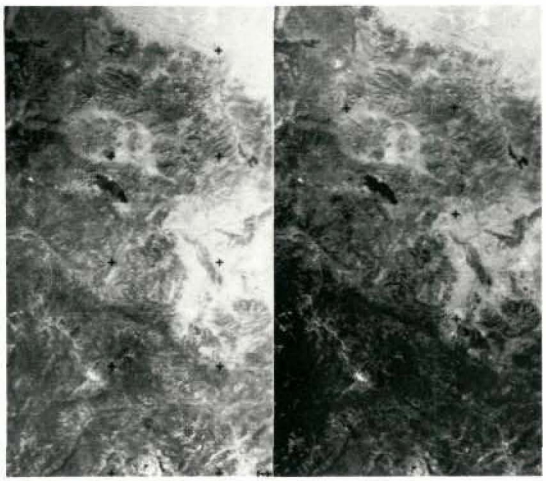

Figure XXVII-1a. An RBV Stereogram in a Mountainous Area. These lands are vegetated by coniferous forest, mountain brush types, sagebrush-grass types, bitterbrush types, and meadows with limited areas of lakes, barren rockland and agricultural cropping. Small areas of deciduous trees can be found in the mountains. Compare your perception of resource related information content of this imagery under monocular viewing and under stereo viewing. Note especially how vegetational features can be accurately related to landforms when viewed in stereo. Compare stereo perception between this RBV and the MSS in Figure XXVII-1b. The tone difference between the frames is exactly as it appeared in the original NASA product, a 9 x 9 positive print. Note also the comparative loss of information in the high density areas of the mountains.

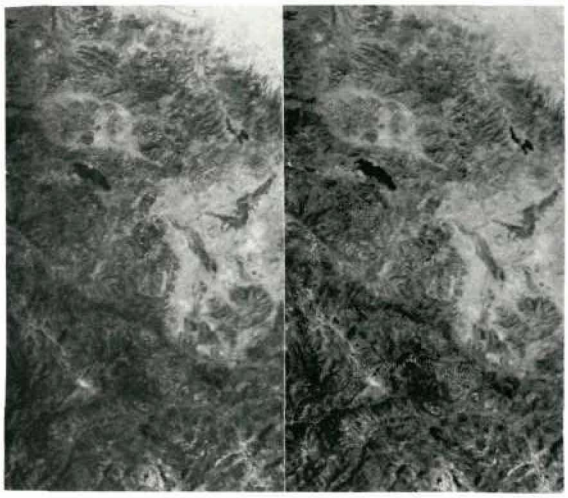

Figure XXVII-1b. An MSS-5 Stereogram of Essentially the Same Area as in Figure XXVII-1a. Note the higher radiometric fidelity and scene contrast as reflected in tone values between the two images from the MSS system as compared to the RBV. This difference holds true for all of the RBV imagery we have been able to examine. Some viewers have felt that stereo perception was better with the RBV than the MSS.

Figure XXVII-2. A Stereogram from Apollo VI Photography over southern Arizona. This is the San Pedro River area. Benson, Arizona is on the river almost in the middle of the stereogram. The snow-capped mountains are the Rincon Mountains. The southern mountain system is the Whetstone Mountains. The Tombstone Hills appear in the extreme lower right corner of the stereogram. We first became excited about the possibilities of stereo applications from space imagery as a result of having made intensive vegetation, landform and land-use interpretations from this photograph. On this unmanned mission, an outstanding strip of 60 percent forward-lap, stereo photography was taken virtually across the continent. Its information content has never been fully exploited. This imagery is somewhat suggestive of what might be done even better with a convergent imaging system from space.

- Side-lap registry from stereo viewing of bulk processed data is good. As you move about the model, some repositioning is required.

- For quick-look evaluation the red band is near ideal for evaluation of vegetational, soil, and landform features as we predicted. The 9x9 format is highly usable although some greater enlargement may be desirable.

- While we have not had the opportunity to examine color reconstitutions in stereo, we believe the combination will have tremendous possibilities for human interpretation.

- With stereo viewing, in mountainous and hilly relief, and even strongly rolling relief of arid areas, vegetational and/or soil differences and type boundaries are more easily seen, and one can capitalize on associated evidence of relief and landform relationships in identifying vegetational analogues, if of course one knows what to expect.

- With stereo, ground locations in all but flat relief are made much more quickly than when the often uncertain or "apparent" relief suggested by tone patterns is viewed monocularly. As one approaches minor drainages and the heads of major drainages, they can be traced with much greater reliability and accuracy with stereo viewing.

- Both end-lap and side-lap in the RBV provides stereo parallax, but the MSS provides true stereo parallax only in the side-lap area so that the only apparent advantage in the MSS end-lap area is from binocular reinforcement.

To provide a somewhat independent assessment of stereo viewing from space, I had a geologist friend of mine, who had never before tried to interpret space imagery, examine some of this same material with absolutely no prompting. He was given first a monocular view in the Sierra mountains and then the stereo over-lap for the same area. His almost immediate reaction was, "Give me side-lap imagery every time." After examining the stereo model for a few minutes he said, "I can see a real saving in time required for interpretation and a substantial increase in the potentially derivable information from the use of stereo space imagery."

On the basis of these limited observations, strongly supported from experience in depth with Apollo VI (Figure XXVII-2) and SO65 imagery, I would urge NASA to continue to provide up to 50 or 60 percent side-lap imagery at very opportunity; and I would urge investigators who are interpreting imagery with human interpreters to take advantage of this feature even if it is limited to only 10 or 15 percent side-lap. These limited over-lap areas provide a stereo sample far superior to none.

It is highly probable that interpretation by most of the initial operational users of ERTS-1 imagery will be done with a minimum of sophisticated instrumentation, perhaps nothing but a color combining device if that much. It is now obvious that stereo viewing and

binocular reinforcement hold just as much advantage for the interpretation of space imagery in the photographic mode as has long been recognized for conventional aerial photography.

ACKNOWLEDGEMENTS

This report is based on work done by the author and his graduate students on Apollo VI stereo photography, on the SO65 Experiment aboard Apollo IX, and on work done in the initial assessment of ERTS-1 imagery being evaluated in an Earth Satellite Corporation (EarthSat) project. In this latter investigation, the author with other colleagues in the company, is performing an experiment to determine the inter-regional repeatability of the signatures of vegetation analogues and to further develop and test a standard legend system devised by the author for the inventory and monitoring of natural vegetation, environmental complexes, and the cereal crop, rice, a key food crop of the world.

GLOSSARY*

A

Altitude – the distance from the nadir ground point to the spacecraft.

B

Band – A set of adjacent wavelengths in the electromagnetic spectrum with a common characteristic, such as the visible band. *See also* Sensor/Band Identification.

Bulk Processing Subsystem – *See* Initial Image Generating Subsystem.

C

Channel – there are 6 channels (scan-line detectors) per MSS spectral Bands 4, 5, 6, and 7; hence, the MSS is a 24-channel scanner on ERTS-1.

Color Composite Image – as associated with ERTS-1, a 9½ inch color negative, transparency, or print generated from Bulk or Precision black and white triplet sets, usually using MSS Bands 4, 5, and 7. The resulting colors are arbitrarily derived, hence the expression, "false color." Also called Color Additive Image and Color Infrared.

Contrast – the ratio of two adjacent scene radiances expressed as a number equal to or greater than one.

D

Densitometer – an instrument for the measurement of optical density (photographic transmission, photographic reflection, visual transmission, etc.) of a material, generally of a photographic image.

Digital Subsystem (formerly Special Processing Subsystem) – receives digitized image data from system correction and scene correction processing and produces digital image data in 7-track and 9-track computer-compatible, magnetic-tape format.

E

Electromagnetic Radiation – energy propagated through space or through material media in the form of an advancing disturbance in electric and magnetic fields existing in space or in the media. The term radiation, alone, is used commonly for this type of energy, although it actually has a broader meaning. Also called electromagnetic energy or simply radiation.

Electromagnetic Spectrum – the ordered array of known electromagnetic radiations, extending from the shortest cosmic rays, through gamma rays, X-rays, ultraviolet radiation, visible radiation, infrared radiation, and including microwave and all other wavelengths of radio energy.

*Compiled from the following sources:

William H. Allen, *Dictionary of Technical Terms for Aerospace Use*, National Aeronautics and Space Administration, SP 7, 1965.

Data Users Handbook, Earth Resources Technology Satellite, prepared by General Electric Space Division for NASA/ Goddard Space Flight Center, 1972.

John E. Estes and Leslie W. Senger, Editors, *An Introductory Reader in Remote Sensing,* University of California, Santa Barbara, 1972.

Emission – with respect to electromagnetic radiation, the process by which a body emits electromagnetic radiation as a consequence of its temperature only.

Enhancement – refers to various processes and techniques designed to render optical densities on imagery more susceptible to interpretation.

F

Format Center – the center of the RBV and MSS total image writing area in Bulk Processing. MSS Format Center is identical to RBV Format Center; defined as the intersection of the film registration mark diagonals. The image is corrected so that the geometric extension of the spacecraft axis to the earth's surface occurs at the Format Center.

G

Geometric Accuracy, of which there are four types: *Geographic (latitude-longitude)* – based on the standard earth-fixed coordinate reference system, which employs latitude and longitude. *Positional* – the ability to locate a point in an image with respect to a map. *Scene Registration* – the ability to superimpose the same point in two images of a scene taken at the same time (different spectral bands). *Temporal Registration* – the ability to superimpose a point in two images of the same scene taken at different times (same or different spectral bands).

Ground Control Point – any point that has a known location on the earth's surface which can be identified in ERTS imagery.

Ground Truth – information concerning the actual state of the ground at the time of a remote sensing overflight.

I

Image/Frame – that data from one spectral band of one sensor for a nominal framing area of the earth's surface.

Imagery – the visual representation of energy recorded by remote sensing instruments.

Infrared Radiation (IR) – electromagnetic radiation lying in the wavelength interval from about .70 microns to an indefinite upper boundary sometimes arbitrarily set at 1000 microns (0.01 centimeter). At the lower limit of this interval, the infrared radiation spectrum is bounded by visible radiation, whereas on its upper limit it is bounded by microwave radiation of the type important in radar technology. *See also* Electromagnetic Spectrum.

Initial Image Generating Subsystem (formerly Bulk Processing Subsystem) – converts all video data from RBV and MSS sensors to 55 by 55 (or 53) mm annotated and corrected images, on 70 mm film.

Image Processing Subsystem – receives video data, image annotation, and correction data to produce both film imagery and digital image data.

Infrared (IR) – infrared radiation or pertaining to infrared radiation, as an infrared absorber.

M

Master Image – the 70 mm film output from video data as originally processed in Bulk Processing; this image is held in archive.

Micrometer (μm) – *See* Nanometer.

Micron (μ) – a unit of length equal to one-millionth of a meter or one-thousandth of a millimeter. The micron is a convenient length unit for measuring wavelengths of infrared radiation, diameters of atmospheric particles, etc.

Multiband – the simultaneous use of two or more sensors to obtain imagery from different portions of the reflectance portion of the electromagnetic spectrum (most commonly used in connection with black and white photography).

Multispectral – the simultaneous use of two or more sensors to obtain imagery from different portions of the electromagnetic spectrum.

MSS (Multispectral Scanner Subsystem) – on ERTS 1 the MSS subsystem gathers data by imaging the surface of the earth in several

spectral bands simultaneously. It is a four band scanner operating in the solar reflected spectral band region from 0.5 to 1.1 micrometer wavelength. The object plane is scanned by means of an oscillating flat mirror between the scene and the double-reflector, telescope type of optical chain. The four bands are nominally referred to as Bands 4, 5, 6, and 7.

N

Nadir – the intersection with the earth's surface of a line from the spacecraft perpendicular to the nearest plane tangent to the earth ellipsoid.

Nanometer (μm) – a unit of measure equal to one millimicron or one millionth of a millimeter.

Near Infrared (B & W, color) – that portion of the electromagnetic spectrum between visible light and thermal infrared with wavelengths from .7 to 4 microns. B and W vs. color refers to the film type which is used to image in the portion of the spectrum from .7 to .9 microns.

Noise – any undesired sound; by extension, noise is any unwanted disturbance within a useful frequency band, such as undesired electric waves in a transmission channel or device.

O

Observation/Scene – the collection of the image data of one nominal framing area of the earth's surface; this includes all data from each spectral band of each sensor.

Optical density – photographic transmission density.

Orthophotograph – a photograph of the earth taken or rectified such that the optical axis of the taking camera is perpendicular to the plane tangent to the earth's surface at the nadir point; this photograph can then be used as a map with appropriate annotation.

P

Photographic Transmission Density – the common logarithm of opacity. Hence, film transmitting 100 percent of the light has a density of zero, transmitting 10 percent, a density of 1, etc. Density may be diffuse, specular, or intermediate. Conditions must be specified. Also called optical density.

Platform – a Data Collection System sensor package on the earth's surface.

Playback – the later transmission of data which was recorded locally at the time of occurrence.

Precision Processing Subsystem – *see* Scene Correcting Subsystem.

Principal Point – the intersection with the earth's surface of a line which is an extension of the optical axis of an RBV camera. This point differs from the format center by the boresight angle error from nominal alignment.

R

Radiation – the process by which electromagnetic energy is propagated through free space by virtue of joint undulatory variations in the electric and magnetic fields in space. This concept is to be distinguished from conduction and convection. Also, the process by which energy is propagated through any medium by virtue of the wave motion of that medium, as in the propagation of sound waves through the atmosphere, or ocean waves along the water surface. Also called radiant energy. Also called electromagnetic radiation, specifically, high-energy radiation such as gamma rays and X-rays. Radiation also refers to corpuscular emissions, such as α or β-radiation. Includes nuclear radiation and radioactivity.

Radiometric – concerned with the combined electronic and optical transmission of data.

RBV (Return Beam Vidicon Camera) – ERTS-1 the RBV camera subsystem contains three individual cameras operating in different nominal spectral bands, Camera 1: .475 - .575 (Blue/Green); Camera 2: .580 - .680 (Green/Yellow); and Camera 3: .698 - .830 (Red/IR). The three Bands are nominally referred to as Bands 1, 2, and 3.

Real Time – generally associated with data transmission at the time of occurrence, i.e., no delay.

Reflection – the process whereby a surface of discontinuity turns back a portion of the incident radiation into the medium through which the radiation approached.

Reflectivity – a measure of the fraction of radiation reflected by a given surface; defined as the ratio of the radiant energy reflected to the total that is incident upon that surface.

Registration Marks – locations on the film plane outside the image writing area of Bulk Processing; there are four marks, one outside each corner of the writing area, fixed in position such that their diagonals intersect at the format center, or center of the tick mark coordinate center.

Reseau – the rectangular grid pattern inscribed on the RBV faceplate to facilitate geographic identification.

Resolution – the ability of a remote sensing system to render a sharply defined image, and including the three following terms. *Ground Resolution* – the minimum distance between two or more adjacent features or the minimum size of a feature which can be detected; usually measured in conventional distance units, e.g., feet or inches. *Image Resolution* – resolution expressed in terms of lines per millimeter for a given photographic emulsion under specified situations. *Thermal Resolution* – image resolution expressed as a function of the minimum temperature difference between two objects or phenomena.

S

Saturation – the point at which additional input energy to the sensor results in no increase in sensor output.

Scene Correcting Subsystem (formerly Precision Processing Subsystem) – receives user-selected, system-correcting imagery and produces precision-located, scene-corrected imagery on 9-½ inch (241.3 mm) film.

Sensor – the component of an instrument that converts an input signal into a quantity which is measured by another part of the instrument. Also called sensing element.

Sensor/Band Identification – the RBV spectral bands are identified as Bands 1, 2, and 3; the MSS as Bands 4, 5, 6, and 7.

Shading – varying output across the RBV photoconductive surface when a uniform input energy exposes it.

Signature – the unique reflectance or emission response from a particular object or environmental association.

Sun Azimuth Angle – angle in degrees measured in the horizon plane from true north to a vertical circle passing through the sun.

Sun Elevation Angle – angle of the sun above the horizon measured in degrees.

W

Wavelength (symbol λ) – in general, the mean distance between maximums (or minimums) of a roughly periodic pattern. Specifically, the least distance between particles moving in the same phase of oscillation in a wave disturbance.